APPLICATION OF PENETRATION THEORY TO MASS TRANSFER ON A SIEVE TRAY

by

Raymond K. Smith

B. S. and M. S. in Chemical Engineering

Thesis submitted to the Graduate Faculty of the

Virginia Polytechnic Institute

in candidacy for the degree of

DOCTOR OF PHILOSOPHY

in

CHEMICAL ENGINEERING

1965

Blacksburg, Virginia

TABLE OF CONTENTS

LIST OF TABLES

LIST OF FIGURES

I. Introduction

A large volume of literature has been published in connection with the problems associated with the absorption of gases into liquids. In this literature two principal models have been used to describe mass transfer: the two-film theory of Whitman[18] and the penetration model developed by Higbie[11]. While there have been numerous experiments attempting to verify these theories, these experiments have been limited to systems of rather simple design such as wetted-wall columns and laminar liquid jets. Attempts to analyze more complicated systems, particularly those of industrial importance, have yielded negligible results.

One of the ultimate purposes for developing accurate mass transfer models was to facilitate the design of process equipment; however, in the design of gas absorption equipment exact theoretical analysis was complicated by the inability to completely describe the complex flow characteristics of such apparatus. For this reason most absorption theories have been principally used in the correlation of data, rather than for design of process equipment.

Models for predicting mass transfer rates generally involved such parameters as interfacial contact area and effective contact time. The latter referred to the time interval during which the fluid elements were in contact with the soluble gas. In industrial apparatus, such as sieve-trays or packed columns, these quantities

could only be roughly approximated. It was then, not the lack of an adequate absorption model, rather it was lack of knowledge describing the physical state of the system which prevented rigorous equipment design. This suggested that further improvement in basic design techniques depended upon better understanding of the physical behavior of apparatus.

The objective of this investigation was then to determine if existing absorption-with-reaction theory could be applied to a sieve-tray and obtain meaningful values of interfacial area and contact time. The method used in determing these characteristic parameters for a sieve-tray was to measure the rates of absorption for several different chemical systems and then force the theory to give results consistent with the observed absorption rates. If the theoretical parameters were found to depend only upon the physical parameters of the tray, it could then be concluded that the values determined were truly characteristic of the operation of the tray and hence could be used for "a priori" predictions of absorption.

II. LITERATURE REVIEW

The literature pertinent to this investigation was divided into two distinct areas - first that which dealt with mass transfer and secondly that which considered bubble mechanics. The section on mass transfer included summaries of the two-film and penetration theories of mass transfer. The summary of bubble behavior included sections on bubble size distribution and rate of rise of bubbles in froths and foams.

Mass Transfer

In reviewing the mechanisms for the transport of solutes from interfaces, the relatively straightforward theories for diffusion in stagnant fluids and diffusion in fluids moving in laminar flow were considered prior to the more complex problem of transport to mobile interfaces. This placed the theories in rough chronological order and also arranged them in order of decreasing importance which each theory assigned to molecular diffusion.

Theoretical Basis. The various theories of mass transfer which have been proposed to fit experimental data were based on Fick's laws for diffusional processes. Fick's first law, which was applicable for steady state conditions was expressed empirically as:

$$N_A = k (c_{A_s} - c) \qquad (1)$$

where;

N_A = molar flux of A with respect to fixed coordinate system, mole / cm^2 sec

k = mass transfer rate constant, cm / sec

c_{A_s} = saturation concentration of A, mole / cm^3

c = point concentration of A, mole / cm^3

The assumption implied in the use of the above concentration difference as the overall driving force was that a saturation concentration of the absorbing gas always existed at the interface. For high rates of mass transfer in which the interface concentration fell short of saturation the mean driving force would be substantially reduced.

Film Theory. The two film theory of Whitman[18] was the first significant attempt to interpret conditions which occurred when material was transferred from one fluid stream to another. Although the two-film theory did not represent the physical conditions which existed in most industrial equipment, it gave relatively simple expressions which could be used to interpret the available experimental data. For this reason the film theory has enjoyed wide use.

In this theory it was assumed that turbulence had completely diminished at the interface and that a laminar layer existed in each of the two fluids. Outside the laminar layer turbulent eddies supplemented the action caused by the random movement of the molecules; thus, the resistance to transfer in this region was assumed to be negligible. This theory was best applied to the

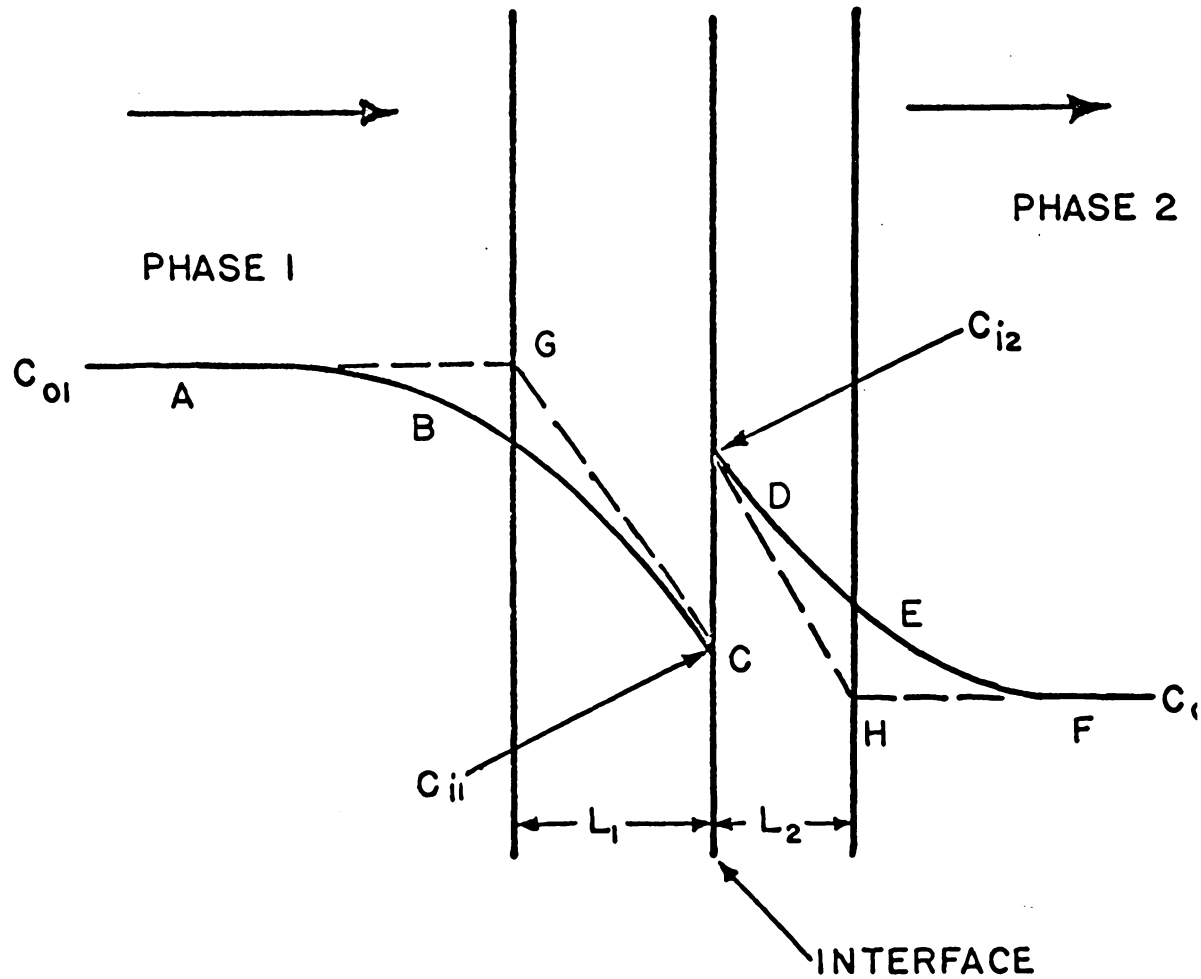

FIGURE 1 MODEL FOR TWO-FILM THEORY

specific case of equimolar counter diffusion in which the concentration gradient was essentially linear close to the interface and decreased to zero at a finite distance. This was represented in Figure 1 by the full lines ABC and DFE. The total resistance to mass transfer was considered to be concentrated in these two hypothetical films in which molecular diffusion controlled all mass transfer. The broken lines in Figure 1, AGC and DHF, indicated the hypothetical concentration distributions for the films of thickness L_1 and L_2. Since equilibrium was assumed to exist at the interface, the concentration at points C and D was determined by the equilibrium relationships for the phases. For this case Whitman[18] has shown that the flux may be expressed as:

$$N_A = \frac{D}{L} (c_{A_s} - c) \qquad (2)$$

where:

D = binary diffusion coefficient in phase i, cm / sec^2

L = film thickness in phase i, cm

With the possible exception of mass transfer from solids dissolving in a stagnant fluid, the film theory did not describe any physical situation. Thus the most serious deficiency of the film theory was its failure to predict the variation of absorption rate for transient contact times.

Penetration Theory. The work of Higbie[11] formulated the basis of the penetration theory for transient mass transfer between two phases. In this theory it was assumed that fresh fluid was brought to the phase boundary for each new contact time where it was

exposed to the second phase for a specific interval of time after which the surface element was remixed with the fluid bulk. In this manner fluid whose initial composition corresponded to the bulk fluid far from the interface was suddenly exposed to the second phase for a finite period of time. In this model it was assumed that equilibrium was attained immediately at the interface; that in the ensuing time a process of transient molecular diffusion occured; and that the element was remixed after a fixed interval of time. Inherently, it was assumed that the depth of liquid was infinite; this was justified as long as the time of exposure was sufficiently short so that only the surface layers were penetrated by the diffusing species. Additionally, the existance of velocity gradients within the fluids was ignored and thus the fluid at all depths was considered to be moving at the same velocity. For this model Higbie[11] has shown the average rate of mass transfer to be:

$$N_A = 2 (c_i - c_o) \sqrt{\frac{D}{\pi t_c}} \qquad (3)$$

where;

c_i = interface concentration of A, mole / cm^3

c_o = bulk fluid concentration of A, mole / cm^3

t_c = contact time, sec

Thus for a given concentration gradient, the shorter the contact time the greater the rate of mass transfer. At present a precise value can not be assigned to t_c in any type of industrial equipment; however, its value would clearly decrease as the amount of turbulence was increased. If it were assumed that each fluid element resided

at the surface for the same contact time, t_c; equation 3 gave the overall rate of mass transfer. It should also be noted that the mass transfer rate was predicted to be a linear function of the concentration gradient - as was the case in the two-film theory. However, in the penetration theory, the flux was proportional to the square root of the diffusivity and inversely proportional to the square root of the time of contact.

Surface Renewal Theory. In a modification of Higbie's work Danckwerts[4] suggested that each element of the liquid was not exposed to the gas phase for the same time, but that a Poisson Distribution of ages existed. He assumed that the probability of any element of surface becoming destroyed through mixing with the bulk of the fluid was independent of the age of the element. Danckwerts' modification yielded the following equation:

$$N_A = (c_i - c_o)\sqrt{D\,s} \qquad (4)$$

where:

s = fractional rate of surface renewal, sec^{-1}

Here again it was seen that the mass transfer rate was proportional to the concentration gradient and to the square root of the diffusivity. A numerical value of the fractional rate of surface renewal, s, was extremely difficult to estimate for any sort of gas contactor; however, s would clearly be a direct, increasing function of the degree of turbulence.

Penetration-Film Theory. Toor and Marchello[16] have developed a theory of mass transfer which incorporated the principals of both the two-film and penetration theories. In their model all of the resistance to transfer was regarded as lying within a laminar film at the interface, as in the two-film theory, but the mass transfer taking place was considered to be a transient process in that material which traversed the film was instantaneously mixed with the bulk of fluid. It was assumed that fresh surface was formed at intervals from fluid which was transported from the bulk of the fluid to the interface by the action of turbulent eddies. Mass transfer was then assumed to take place as in the penetration theory, except that the resistance to mass transfer was confined to a finite film next to the interface. For short contact times, when none of the material had reached the far side of the layer, the model was identical to that postulated in the penetration theory. For long periods of exposure, when a steady concentration gradient had developed, the model approached the two-film theory in form. The final form of the Toor-Marchello model was:

$$N_A = (c_i - c_o)\sqrt{\frac{D}{\pi t_c}}\left[1 + 2\exp(-L^2 / Dt_c)\right] \qquad (5)$$

As before the difficulty in applying equation 5 was that not all parameters, i.e., the contact time and the film thickness were known quantities. Toor and Marchello also showed that equation 5 was a a simplification of the boundary layer theory of mass transfer.

Other Theories of Mass Transfer. Kishinevshij[13] has suggested a model for mass transfer across interfaces in which there was no contribution due to molecular diffusion. He assumed that fresh material was continuously supplied to the interface as a result of turbulence within the fluid and that, after exposure to the second phase, the fluid element attained equilibrium with the second phase and then became mixed again with the bulk fluid. This model thus proposed surface renewal without penetration and therefore the effect of molecular diffusion should be negligible. However, there was no data available to substantiate this theory.

Bakowski[1] has also considered the rate of mass transfer from a turbulent gas to a liquid interface. He proposed that the transfer rate would be a function of the number of molecules of the diffusing component in the gas in contact with the liquid. The absorption of molecules by the liquid was assumed to be very fast so that the rate of replacement of the component in the surface layer was the rate controlling factor. Thus, the velocity of the gas stream over the surface directly influenced the mass transfer rate in that it affected the transfer of the gas molecules to the surface layer.

Mass Transfer Coefficients. In each of the theories discussed the rate of mass transfer in the absence of bulk flow was directly proportional to the driving force expressed as a difference in molar concentration. Thus for the general case the following equation was obtained:

$$N_A = k'(c_i - c_o) \qquad (6)$$

where:

k' = general mass transfer coefficient, cm / sec

In the two-film theory k' was directly proportional to the diffusivity and inversely proportional to the film thickness. The penetration theory predicted that k' varied as the square root of the diffusivity and, when all elements were exposed for the same period of time, k' was inversely proportional to the square root of the time of exposure. For surface renewal theory, k' was a simple function of square root of the diffusivity and rate of surface renewal. In the film-penetration theory, the mass transfer coefficient was a complex function of the diffusivity, the film thickness, and the time of exposure. For the majority of applications the mass transfer coefficient could not be evaluated from first principles- this was, for the most part, due to lack of adequate knowledge of the physical parameters describing the system in question.

Variation of Mass Transfer Coefficient. For the absorption of carbon dioxide in water Gibbs[9] has shown that the total resistance to mass transfer lay within the liquid phase, i.e., the total mass transfer coefficient, k', was identical with the liquid phase mass transfer coefficient. The variation of the liquid phase mass transfer coeficient, k_L, with the physical parameters of the syster has been the subject of several investigations. Davies[8] has shown that k_L, for bubbles smaller than 0.20 cm in diameter, was independent of the degree of agitation and bubble size. Davies also showed that for these bubbles k_L was proportional to the two-thirds power of the molecular diffusivity; this variation was very close to the square root relationship predicted by the

penetration theory. For larger bubbles Toor[16] has also shown that k_L was independent of size and degree of mechanical agitation.

Chemically speaking both the penetration theory and the two-film theory predicted that the overall mass transfer coefficient would vary as a function of the diffusivity. However, the variation of the diffusion coefficient with ionic strength was not satisfactorily predicted by theory. Hence, the variation of k_L with concentration had to be experimentally determined.

Rates of Absorption of Carbon Dioxide. Danckwerts and Kennedy[5] have measured the transient rate of absorption of carbon dioxide into pure water and various aqueous solutions. Their data for absorption into pure water and dilute sodium hydroxide were quite pertinent to this investigation. Figures 2 and 3 show the transient rate of absorption of carbon dioxide into water and 0.085 M aqueous sodium hydroxide solutions. For the carbon dioxide water system Danckwerts and Kennedy showed that the diffusivities of all ions were 10-20 percent less in a solution 2.3 molar in sodium ions than in pure water. This decrease in diffusivity was found to be roughly linear with ionic strength. Thus, the correction required for diffusivities in a 0.085 M caustic solution was negligible.

Interfacial Concentration of Carbon Dioxide. Harned and Davis[10] have studied the solubility of carbon dioxide into aqueous solutions. The results of this investigation were summarized in Figure 4. In this figure the solubility of carbon dioxide into

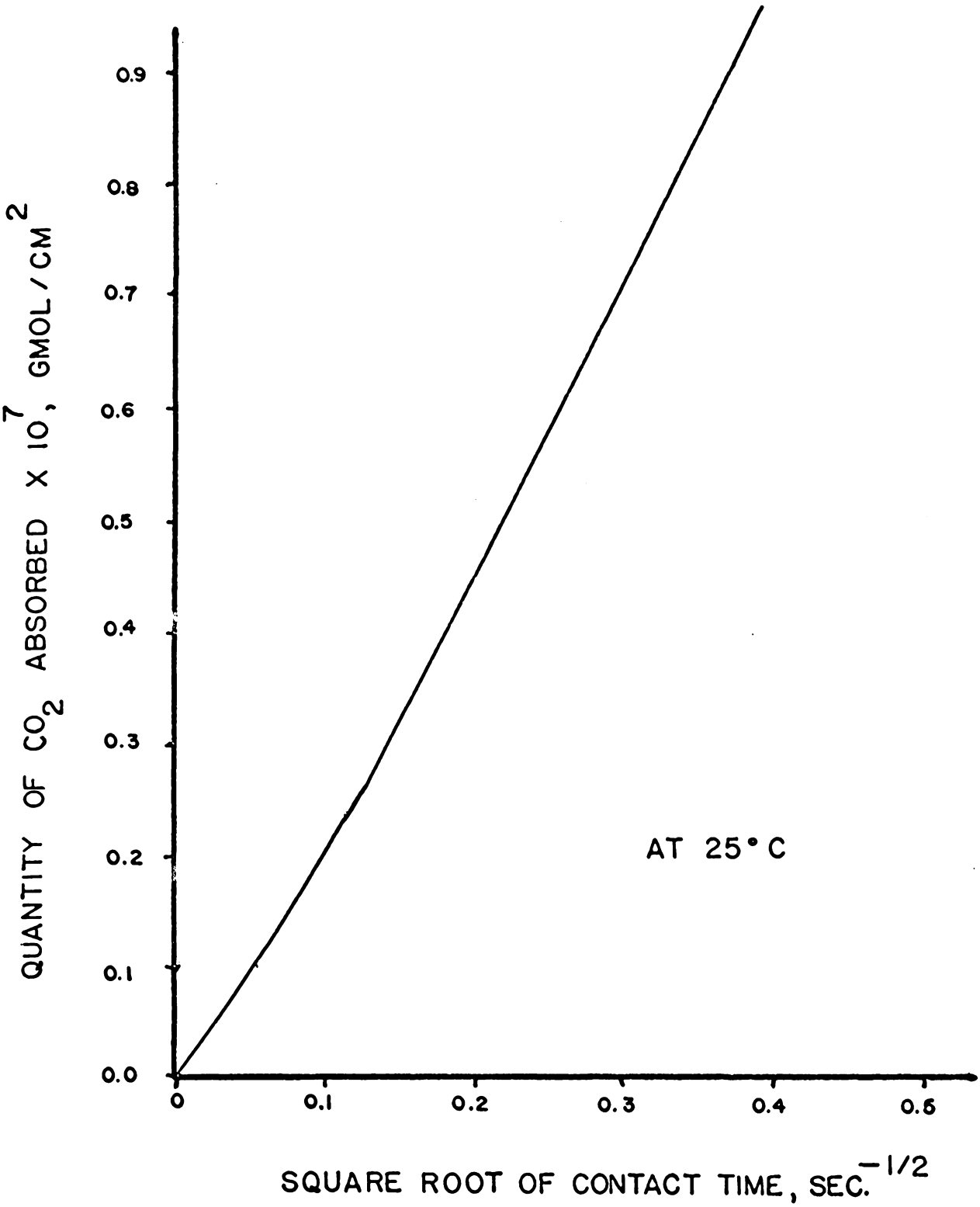

FIGURE 2. TRANSIENT RATE OF ABSORPTION OF CO_2 INTO 0.085 M AQUEOUS SODIUM HYDROXIDE SOLUTION

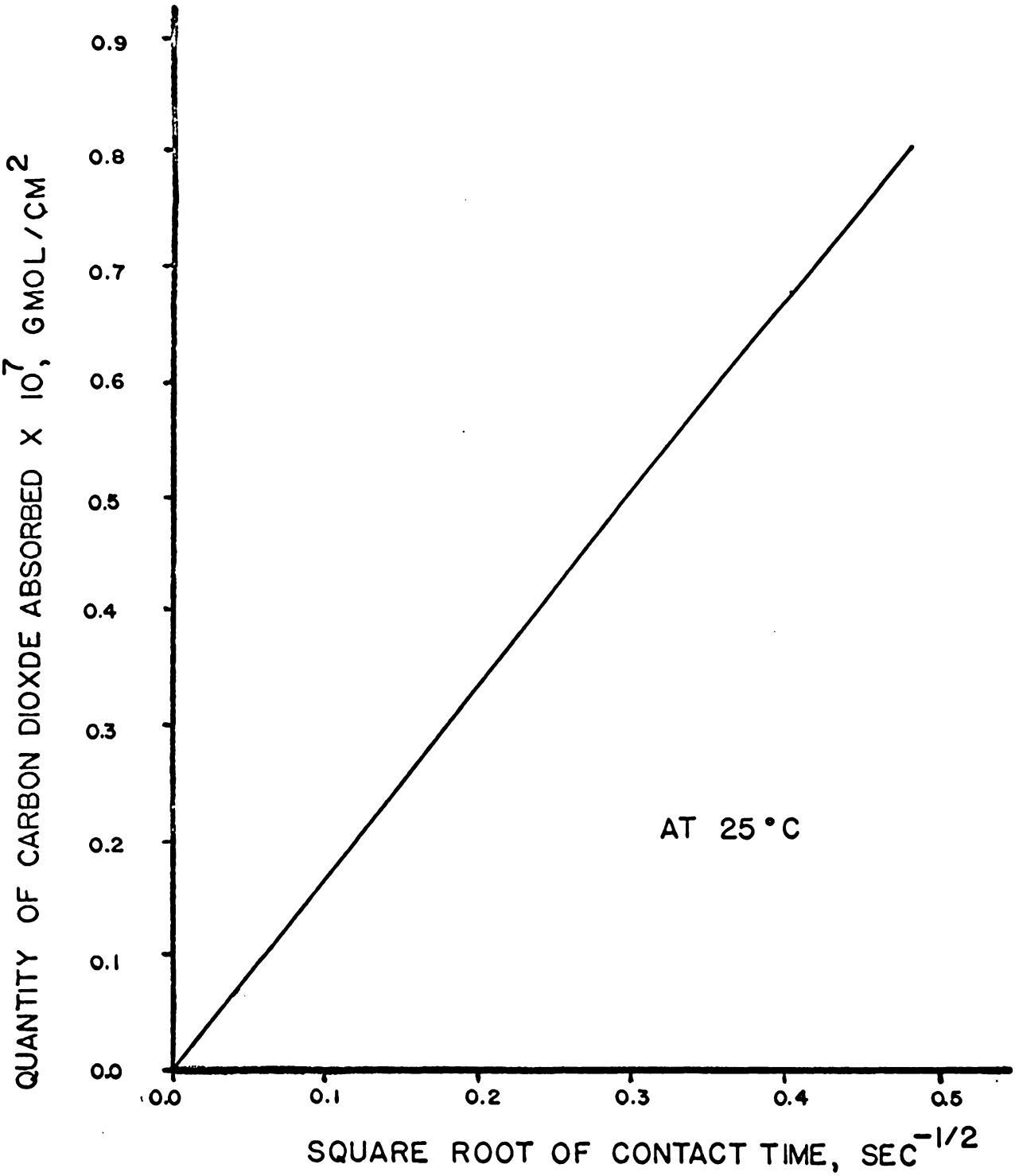

FIGURE 3. TRANSIENT RATE OF ABSORPTION OF CARBON DIOXIDE INTO WATER

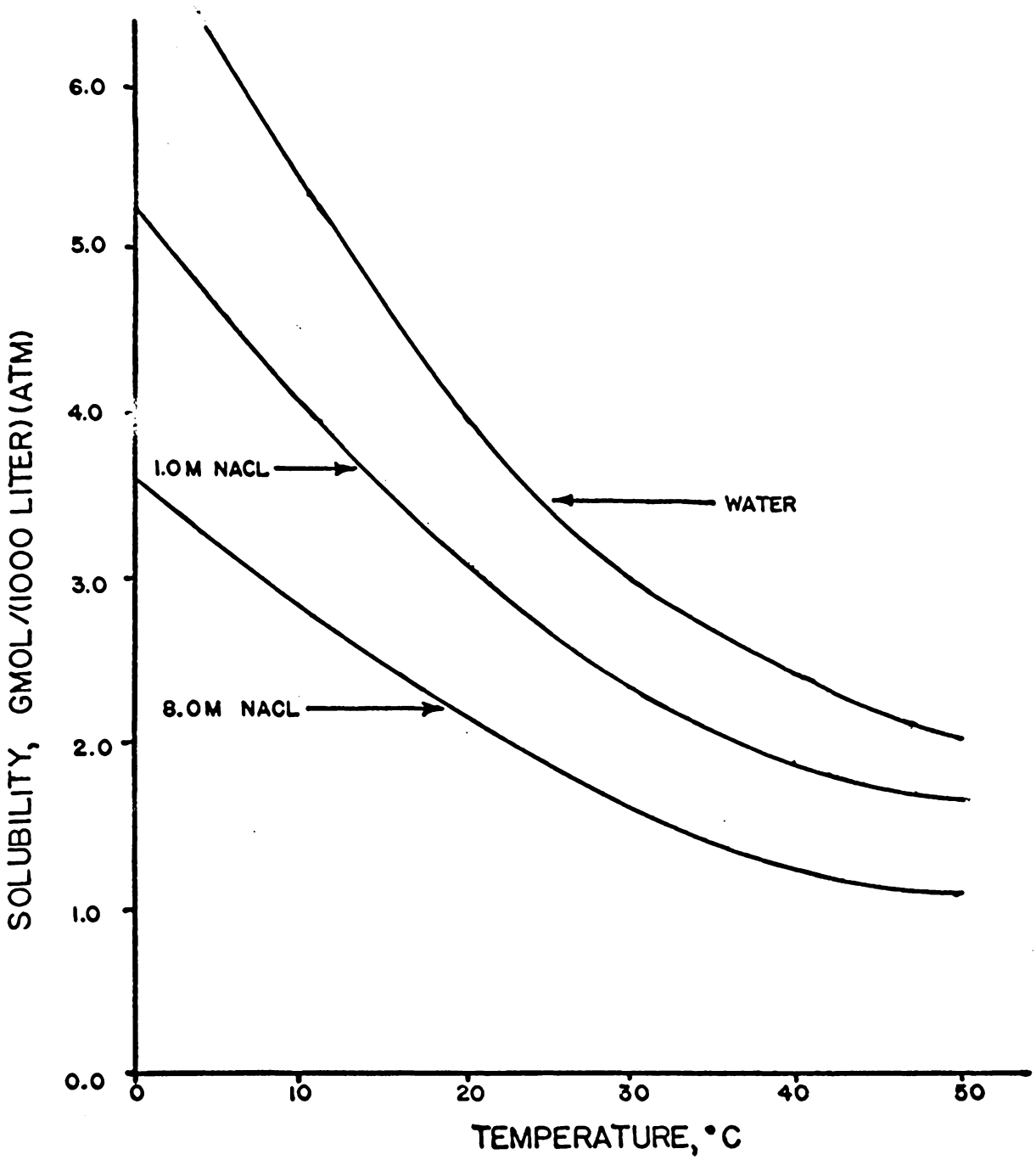

FIGURE 4. SOLUBILITY OF CO_2 IN WATER AND IN SODIUM CHLORIDE SOLUTIONS

various solutions of sodium chloride was plotted against temperature. This figure showed that solubility decreased with ionic strength; later investigations by these two authors showed that for dilute solutions of strong electrolytes the solubility was dependent only upon total ionic strength.

Bubble Mechanics

The mechanics of bubble formation from an orifice has been the object of many studies. The parts of this literature which were pertinent to this investigation were summarized in the following section.

Bubble Frequency. There have been two distinct regions of bubble formation defined in the literature. One region occurred at low gas flow rates where the bubble volume was approximately constant and could be predicted roughly by equating the buoyant force to the surface tension force holding the bubble on the orifice. Therefore, in this region the frequency was directly proportional to the flow rate. The second region occurred at higher gas throughput where the frequency approached a constant value and the volume thus became flow dependent.

Numerous investigators have noted that the size of the chamber located immediately upstream from the orifice had a marked effect on bubble frequency. Hughes[12] postulated an electrical analogue to describe this phenomena in which the electromotive force and

current were the equivalent of gas pressure and flow rate respectively. The chamber volume was interpreted as a capacitance effect and from these results he formulated the following dimensionless group:

$$N_c = \frac{4 g \Delta V}{D_o^2 \rho_G c^2} \tag{7}$$

where:

N_c = capacitance number, dimensionless

g = local acceleration of gravity, cm / sec^2

$\Delta = \rho_L - \rho_G$, gm / cm^3

ρ_L = density of liquid, gm / cm^3

ρ_G = density of gas, gm / cm^3

V = volume of gas chamber, cm^3

D_o = diameter of orifice, cm

c = velocity of sound in the gas, cm / sec

Hughes found experimentally that when N_c was approximately equal to unity, the chamber volume, V, had its most marked influence. Robinson[19] has proposed that the bubble frequency was related to the resonant frequency which has been observed in all chamber-orifice systems. His theory predicted the bubble frequency to be proportional to the square root of the chamber volume. Large chamber volumes, particularly with small orifices, produced the phenomenon known as "intermittant bubbling" or pairing in which bubbles were generated in groups followed by brief pauses. (This

was distinct from "merging" which was the term applied to the coalescence of two bubbles in the immediate vicinity of the orifice.) Siemes[15] and Davidson[7] have treated this separately and both came to the same conclusion: that the first bubble did not form until some critical pressure was reached in the chamber below the orifice and that the suction created when the first bubble left the orifice was sufficient to drag the second bubble through the orifice. However, the same authors also observed that if the chamber volume were sufficiently large, or if the volume of the bubble formed was very small, the formation of the first bubble did not reduce the chamber pressure below the value required to generate a second bubble.

Bubble Velocity. The literature pertaining to the velocity of rise of bubbles received a thorough review by Bowman and Johnson[2]. They noted that much of the available data were applicable only for single bubbles formed at low frequencies and thus the data were not applicable for the rather high frequencies encountered in most mass transfer equipment. A number of investigators[12,15] have studied velocities in the medium frequency range; but, as of yet, no systematic observations have been reported. However, it was possible to state that in general:

a. the velocity for single rising bubbles did not change with increasing bubble size.

b. for very small bubbles the frequency had a marked effect on the velocity.

Bowman and Johnson[2] have shown that the velocity of rise of carbon dioxide bubbles in water was a direct function of the seal depth; this is shown in Figure 5.

Bubble Shape. Many workers[2,11,17] studying mass transfer in a bubble column have made the assumption that the bubbles studied were spheres or so close to being spheres that calculation of interfacial area on this basis was a good approximation. Indeed, until a sphere has flattened to an axis ratio of 2 to 1 the surface area did not increase by more than ten percent.

Siemes and Gunther[16] studied the bubble size distribution which resulted from the break-up of the bubble jet which occurred at high gas rates; they catagorized the bubbles which formed from this break-up into three groups:

a. spheres - volume less than 0.05 cc

b. oblate spheriods - volume 0.05 to 0.78 cc

c. flat bottom domes - volume greater than 0.78 cc

Rennie and Evans[14] have studied this same break-up on a sieve plate in which they studied the gas hold-up and the average bubble diameter. The average bubble diameter was based on the assumption that the bubbles were spheres. The results of this investigation were presented in Figures 6 and 7.

Interfacial Area. Chu et al[3] have studied interfacial area and contact time for bubbles formed at single vertical slots in aqueous solutions. While this work was intended to be applied to mass transfer in a bubble-cap system, the results could only

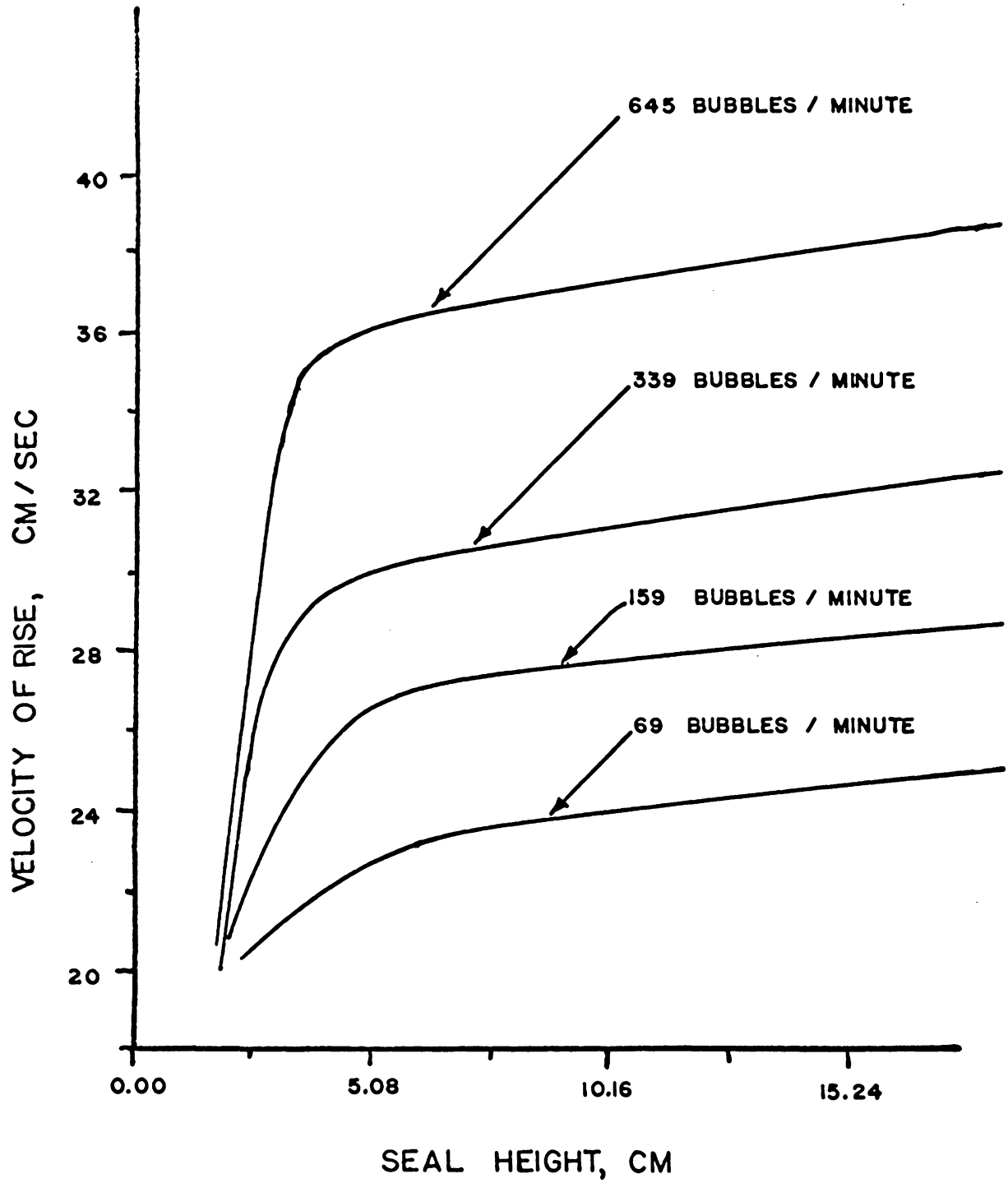

FIGURE 5. EFFECT OF SEAL HEIGHT ON VELOCITY OF RISE OF CO_2 BUBBLES IN WATER AT CONSTANT VOLUME

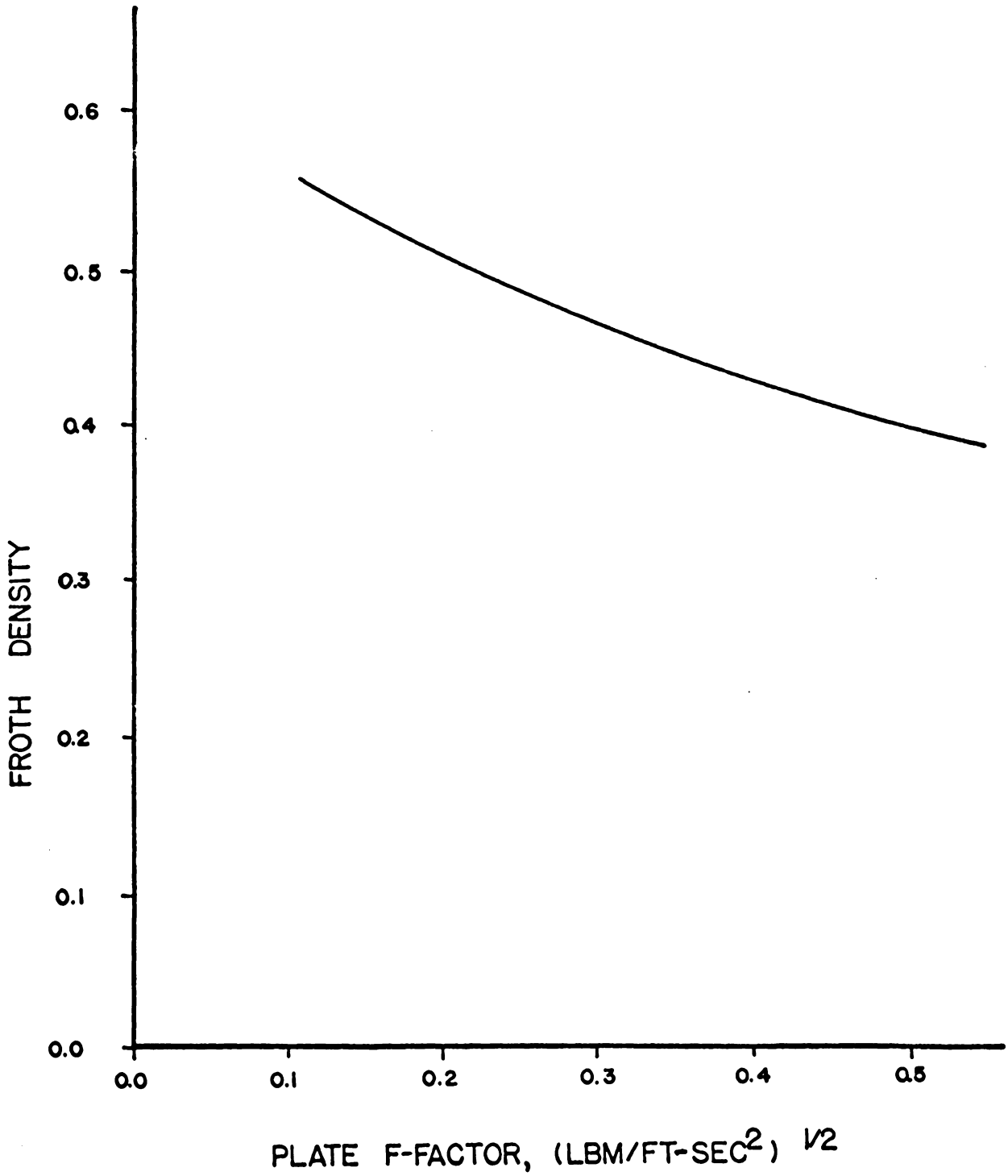

FIGURE 6. FROTH DENSITY VERSUS PLATE F-FACTOR

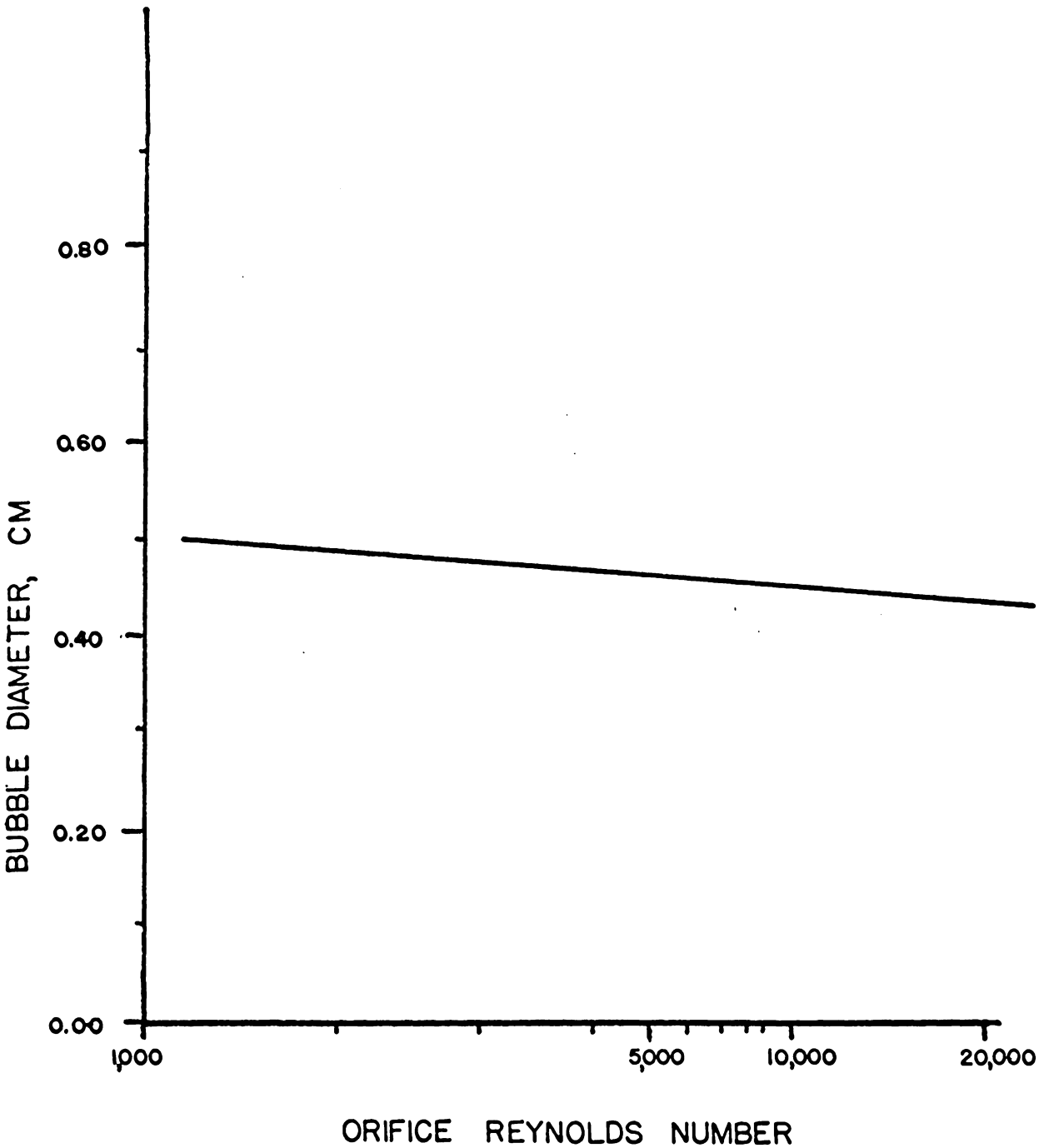

FIGURE 7. BUBBLE DIAMETER VERSUS ORIFICE REYNOLDS NUMBER

be qualitatively applied to this investigation. The plot of static slot submergence versus interfacial area per volume of vapor for various slot velocities was shown in Figure 8. In this plot it was seen that the interfacial area per volume of vapor, a, was essentially constant for static submergences of greater than 2.0 inches and increased rapidly for slot submergence of less than 2.0 inches. Figure 9 showed the influence of liquid viscosity on a; this figure demonstrated that a increased with increasing viscosity and that doubling the viscosity could increase a by as much as an order of magnitude. Chu also demonstrated that smaller holes produced smaller bubbles and hence a larger value of the interfacial area; this was consistent with previously reported data.

Choice of Data. The data presented in Figures 2 through 7 was chosen for its internal consistency and reproducibility. In addition the data in Figure 6 was determined for a column of quite similar design to the one used in this investigation.

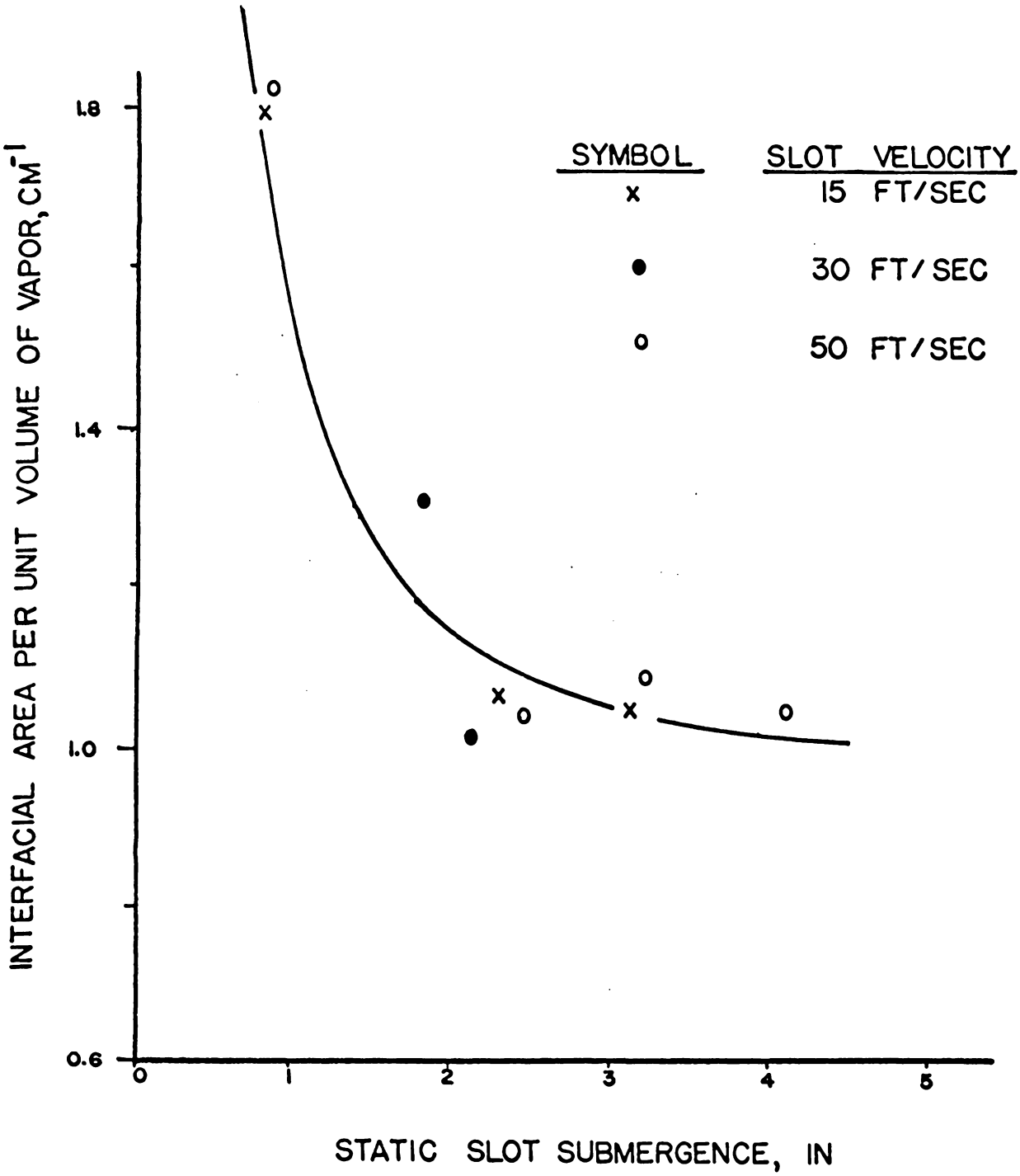

FIGURE 8. INTERFACIAL AREA PER VOLUME OF VAPOR VERSUS STATIC SLOT SUBMERGENCE

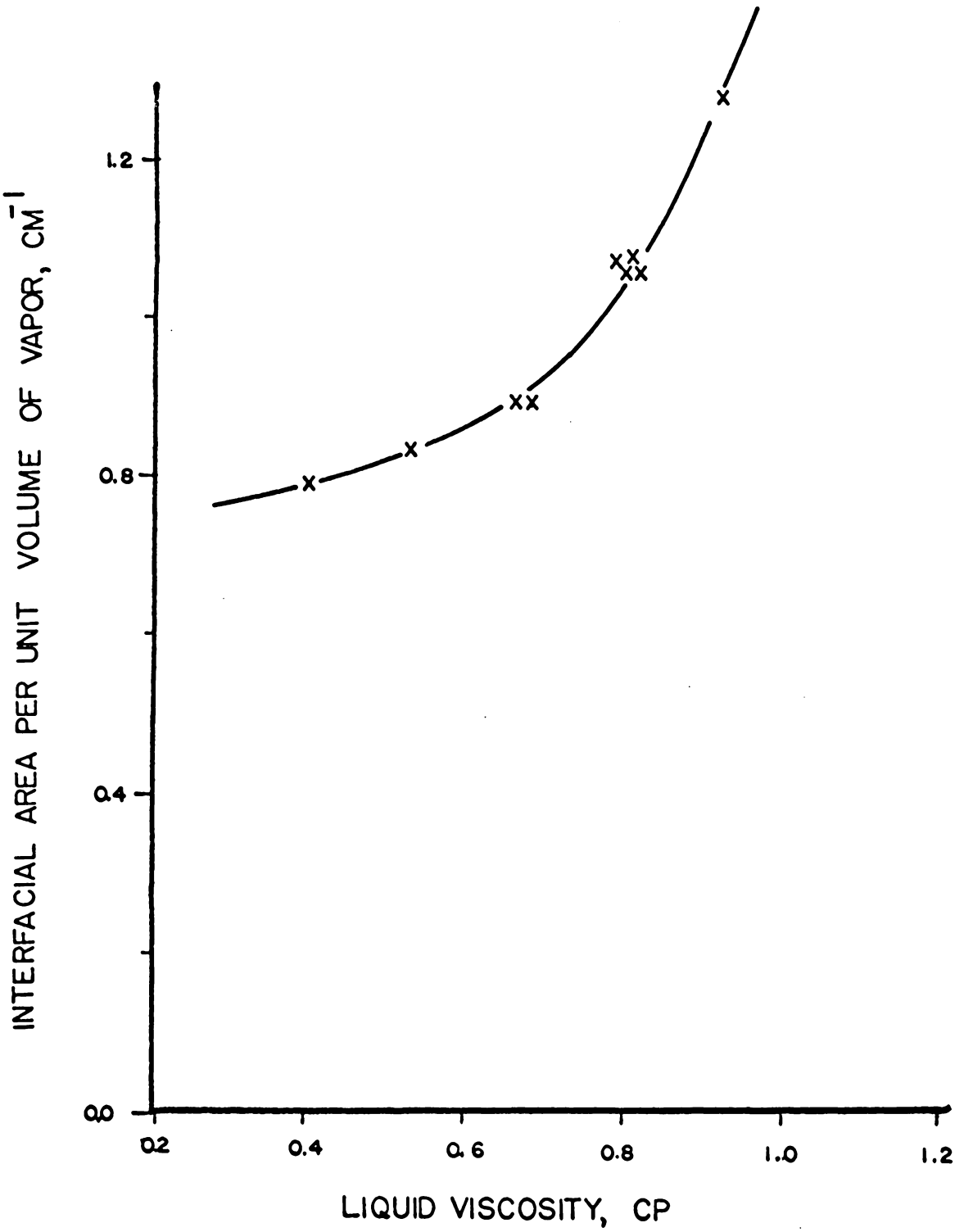

FIGURE 9. EFFECT OF LIQUID VISCOSITY ON INTERFACIA AREA FOR SLOT SUBMERGENCE GREATER THAN 2.5 I

III. EXPERIMENTAL

The plan of investigation, a list of materials and apparatus used, the procedures employed in operating the equipment and analyzing the data obtained, the data and results obtained, and the sample calculations were included in the following section.

Plan of Investigation

The plan of investigation consisted of a literature review, development of a method of interpreting the data, construction of the apparatus, measurement of rates of absorption, and evaluation of the experimental data.

Literature Review. The literature review for this investigation included a review of the fundamental models for gas absorption accompanied by chemical reaction as well as a general review of transient rate of absorption data. In addition, since a sieve-plate was used for the gas-liquid contacting, a search was made concerning the mechanics of gas bubbles in a liquid.

Method of Interpretating Data. From previous measurements[4] of transient absorption rates on simple devices, a general method was developed to measure the effective contact time for transient absorption on complex apparatus. The interfacial area was also determined from these same measurements.

Construction of Apparatus. A single sieve-plate, gas absorption tower with the auxillary equipment necessary to give data consistent with the literature was constructed.

Measurement of Rates of Absorption. The measurement of the rate of absorption was determined by acid-base titration. The end point of each titration, a pH of 7.0, was determined by a pH meter.

Evaluation of Data. The data obtained from the experiments were compared to estimates of the contact time and interfacial area made by previous investigators[2,3,14].

Materials

The materials used in this investigation were listed in the following section.

Carbon Dioxide. Technical grade. Obtained from Air Reduction Compressed Gas Co., Lynchburg, Virginia. Used as a reactant gas for the rate tests.

Hydrochloric Acid. Reagent grade, lot no. 23,933. Obtained from the Industrial and Biochemicals Department of E. I. DuPont and Company, Chicago, Illinois. Used in titrations of reacting liquid.

Nitrous Oxide. Technical grade. Obtained from Air Reduction Compressed Gas Co., Lynchburg, Virginia. Used as a reactant gas for the rate tests.

Phenolphthalein. Reagent grade, lot no. 11244. Manufactured and distributed by J. T. Baker Chemical Company, Phillipsburg, New Jersey. Used as an indicator in titrations.

Sodium Hydroxide. Reagent grade, lot no. 19,335. Obtained from Fischer Scientific Company, Silver Spring, Maryland. Used to make aqueous solutions for reaction on a sieve-plate and for titration.

Water. Distilled. Obtained from the water still in the Department of Chemical Engineering of Virginia Polytechnic Institute, Blacksburg, Virginia. Used to make aqueous reaction solutions and titration solutions.

Apparatus

The apparatus used in this investigation were listed and described in the following section.

Balance. Analytical, dampered, 0 to 500 grams, 0.001 increments, "Chainomatic". Manufactured by Seedner-Kohlbush Company, Jersey City, New Jersey. Used to weigh reagents for titrating solutions.

Blower. High speed, model NHP, serial no. 101164, 110 v, ac. Manufactured by Clements Cadillac Corp., Jersey City, New Jersey. Used to provide continuous circulation of carbon dioxide.

Buret. Titration, 50 ml, 0.10-ml graduations. Obtained from the stockroom of the Department of Chemical Engineering of Virginia Polytechnic Institute, Blacksburg, Virginia. Used to hold and measure titrating solutions.

Buret Stand. Dual stand. Obtained from the stockroom of the Department of Chemical Engineering of Virginia Polytechnic Institute, Blacksburg, Virginia. Used to support the titration burets.

Column Stand. Cast iron and plywood construction. Made by the Department of Chemical Engineering of Virginia Polytechnic Institute, Blacksburg, Virginia. Used to support reaction tower and its auxillary apparatus.

Flanges. Aluminum, catalog no. 441B014, 4 inch Diameter. Manufactured by Fischer and Porter Co., Hatboro, Pennsylvania. Used to join glass pipe.

Flasks. Round bottom, glass 125 ml. Obtained from the stockroom of the Department of Chemical Engineering of Virginia Polytechnic Institute, Blacksburg, Virginia. Used in titrating solutions.

Pipe. Kimax glass, 4 inch diameter, two 12 inch sections, two 24 inch sections. Manufactured by the Fischer and Porter Co., Hatboro, Pennsylvania. Used to make the reaction column and the water saturation columns.

Pump. Centrifugal, model D11, type 100, serial no. C4B0339. Manufactured by Eastern Industries Inc., Hamden, Connecticut. Used to pump water from saturation column through constant temperature bath.

Pump. Positive displacement, model 1106, type 1258, serial no. AD56089. Manufactured by Proportioneer Inc., Providence R. I. Used to pump reaction solution from constant temperature bath to the reaction column.

Rotameter. Float, serial no. P4-1100/1, tube no. B4A-25. Manufactured by Fischer and Ported Co., Hatboro, Pennsylvania. Used to measure flow of aqueous solutions from constant temperature bath to reaction column.

Sieve-Plate. Stainless steel, shown in Figure 11. Obtained from Whitehead Metal Products, Philadelphia, Pennsylvania. Used to contact gas and liquid.

Tank. Stainless steel, 50 gal. Obtained from Alsop Engineering Corp., Milldale, Connecticut. Used to hold aqueous solution of sodium hydroxide and provide a constant temperature bath.

Tank. Stainless steel, 100 gal. Obtained from Celanese Corp., Narrows, Virginia. Used as a surge tank for carbon dioxide.

Tubing. Copper, 3/8 inch and 3/4 inch inside diameter. Obtained from shop of Department of Chemical Engineering, Virginia Polytechnic Institute, Blacksburg, Virginia. Used to provide piping for carbon dioxide and aqueous sodium hydroxide solution.

Valve. Brass gate valves for 3/8 inch tubing. Obtained from shop of Department of Chemical Engineering, Virginia Polytechnic Institute, Blacksburg, Virginia. Used to control flow of aqueous solutions.

Valve. Brass gate valve for 2 inch pipe. Obtained from shop of Department of Chemical Engineering, Virginia Polytechnic Institute, Blacksburg, Virginia. Used to control gas flow.

Procedure

The procedure employed in this investigation consisted of assembly of equipment, preliminary tests and calibrations, operation tests, and derivation of method to analyze the data.

Assembly of Equipment. The reaction column, schematic diagram in Figure 10, was fabricated from two twelve-inch sections of four-inch diameter, Kimax, double strength, flanged glass pipe with a sieve-plate placed between the two sections of glass pipe. The top and bottom of the column were blanked with quarter-inch steel plate. The liquid lines running to and from the column were fabricated from three eights-inch, stainless-steel tubing. The gas lines were constructed from one-inch, thin wall copper tubing.

The water saturation column, schematic diagram in Figure 10, was constructed from two two-foot sections of four-inch diameter, Kimax, double strength, flanged, glass pipe. The top and bottom of the column were blanked with quarter-inch, stainless-steel plate. The gas and liquid lines to and from the column were constructed in the same manner as for the reaction column.

The feed tank was constructed from 16 gauge stainless-steel and mounted on a stand constructed from angle iron. The tank was thirty-inches high and twenty-inches in diameter.

The surge tank was fabricated from quarter-inch stainless-steel and mounted on a stand constructed from angle iron. The tank was fifty-inches long and thirty-inches in diameter. The gas lines to and from the tank were constructed from one-inch diameter copper tubing. A high speed, variable output blower was placed in the gas line and attached to the side of this tank.

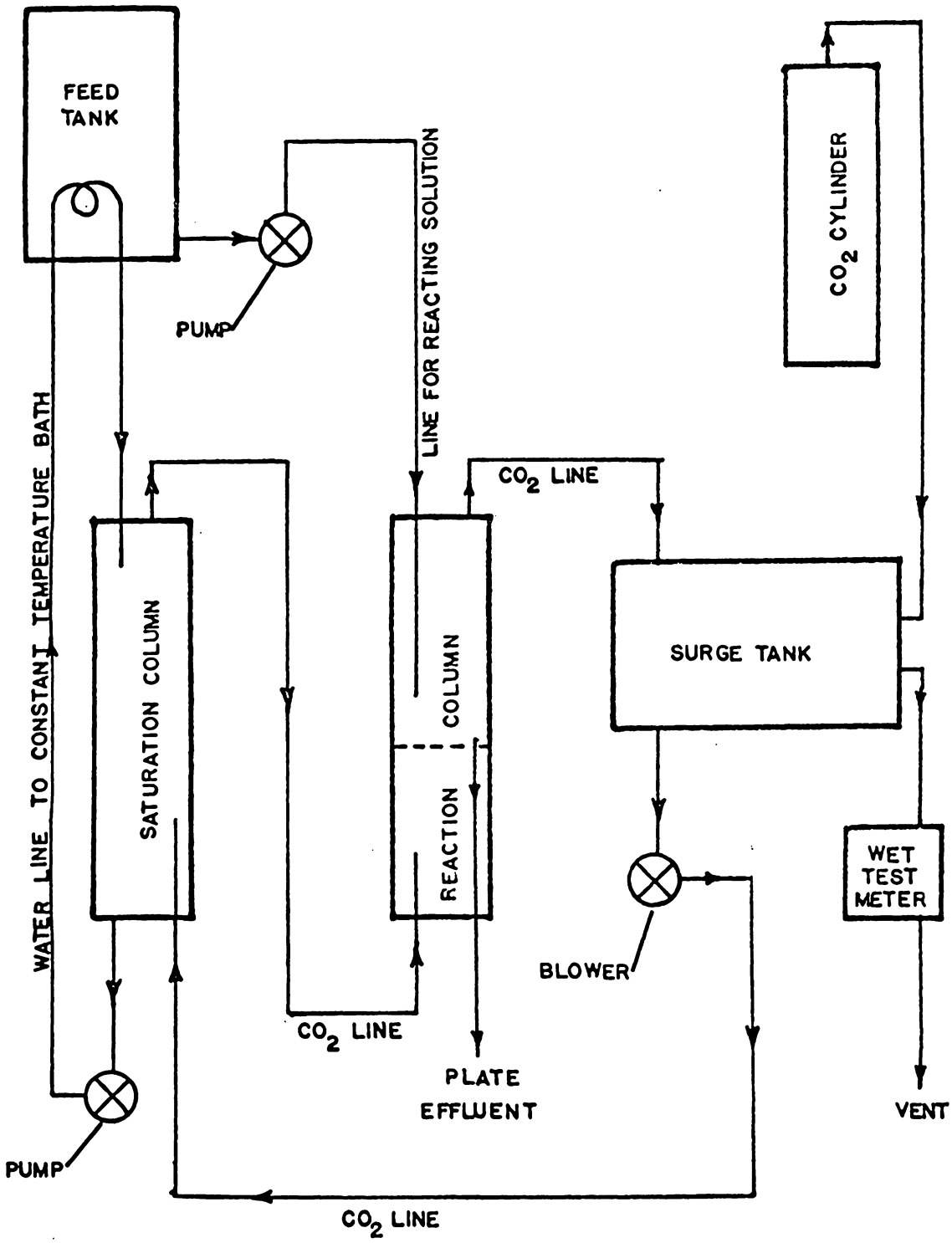

FIGURE 10. SCHEMATIC DIAGRAM OF APPARATUS

All glass pipe was joined with standard aluminum pipe flanges and fastened with six three-inch long quarter-inch diameter machine bolts. Teflon gaskets were used between the sections of glass pipe; neoprene gaskets were used between the flanges and glass pipe.

The columns were mounted on a specially prepared display stand which was constructed from one-inch plywood and angle iron. The liquid circulation pumps, rotameters, and manometers were also attached to this display panel.

Sieve-plates for the various tests were constructed from stainless-steel. A detailed diagram of a sieve plate was shown in Figure 11.

Caribration of Gas Orifice. The gas orifice was calibrated with pure carbon dioxide saturated with water. The test was performed with a wet test meter and checked with a bubble column. The results of these tests were presented on Table I and Figure 12.

Calibration of Feed Rotameter. The calibration of the feed rotameter was made with pure water and 0.085 M aqueous solution of sodium hydroxide. The results of this calibration were shown in Table II and Figure 13.

Calibration of Pressure Drop Across Dry Sieve-Plate. The pressure drop for gas flow across several dry sieve-plates used in this investigation was determined by using water saturated carbon dioxide as the gas. The results of these tests were presented in Table III and Figure 14.

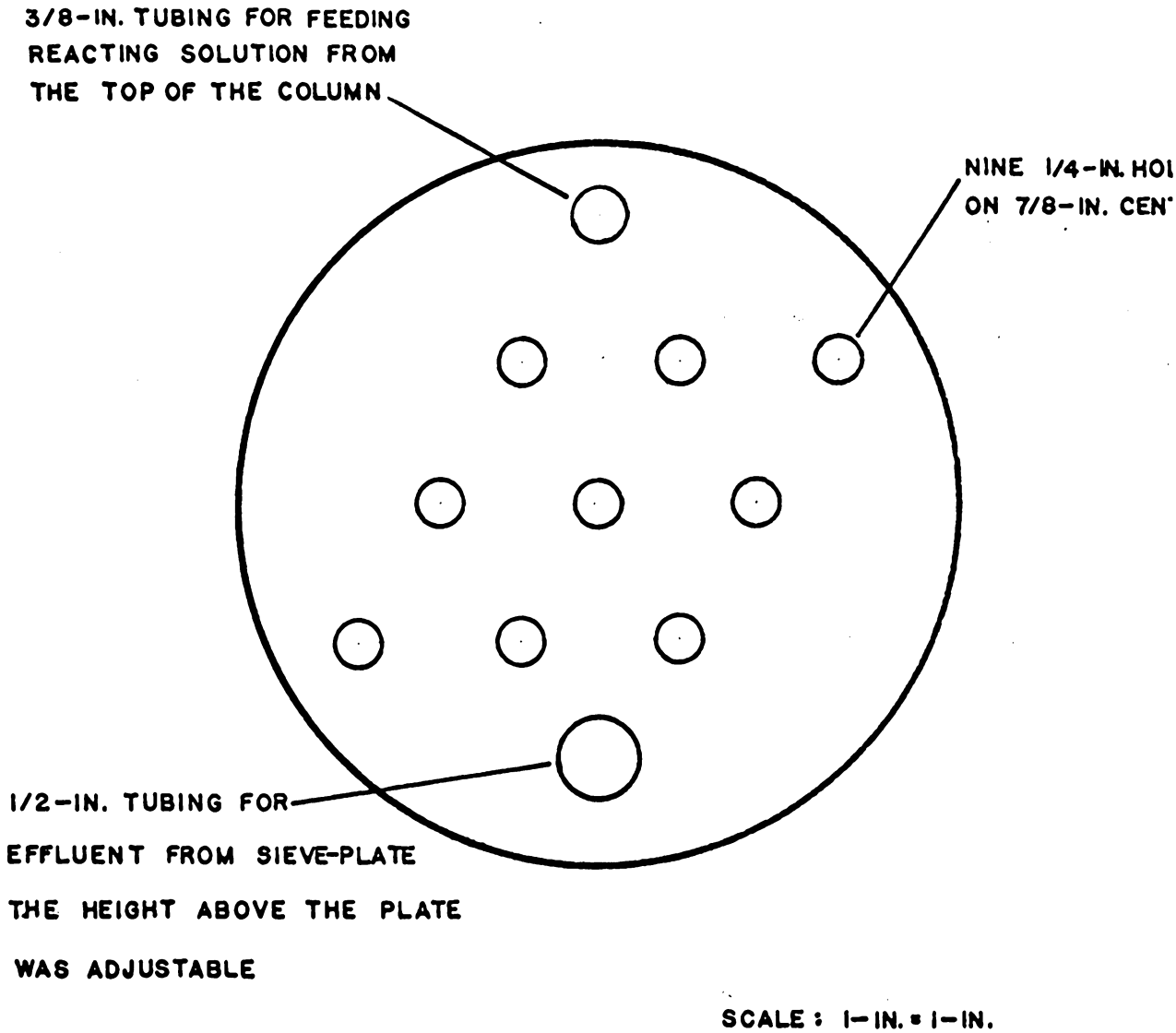

FIGURE II. TOP VIEW OF A SIEVE-PLATE WITH NINE 1/4-IN. DIAMETER HOLES

TABLE I

Calibration[a] of Orifice for Vapor Flow

Pressure Drop Across Orifice, in H_2O	Flow of CO_2, ft^3	Time of Flow min : sec	Velocity of CO_2 through Column ft/sec
1.10	6.50	1:43	0.650
2.25	10.00	1:50	0.935
2.50	10.00	1:43	1.003
3.00	10.00	1:40	1.030
4.15	10.00	1:22	1.255
4.60	10.00	1:19	1.305
8.10	10.00	0:55	1.875

[a] Temperature of calibration was 25 °C.

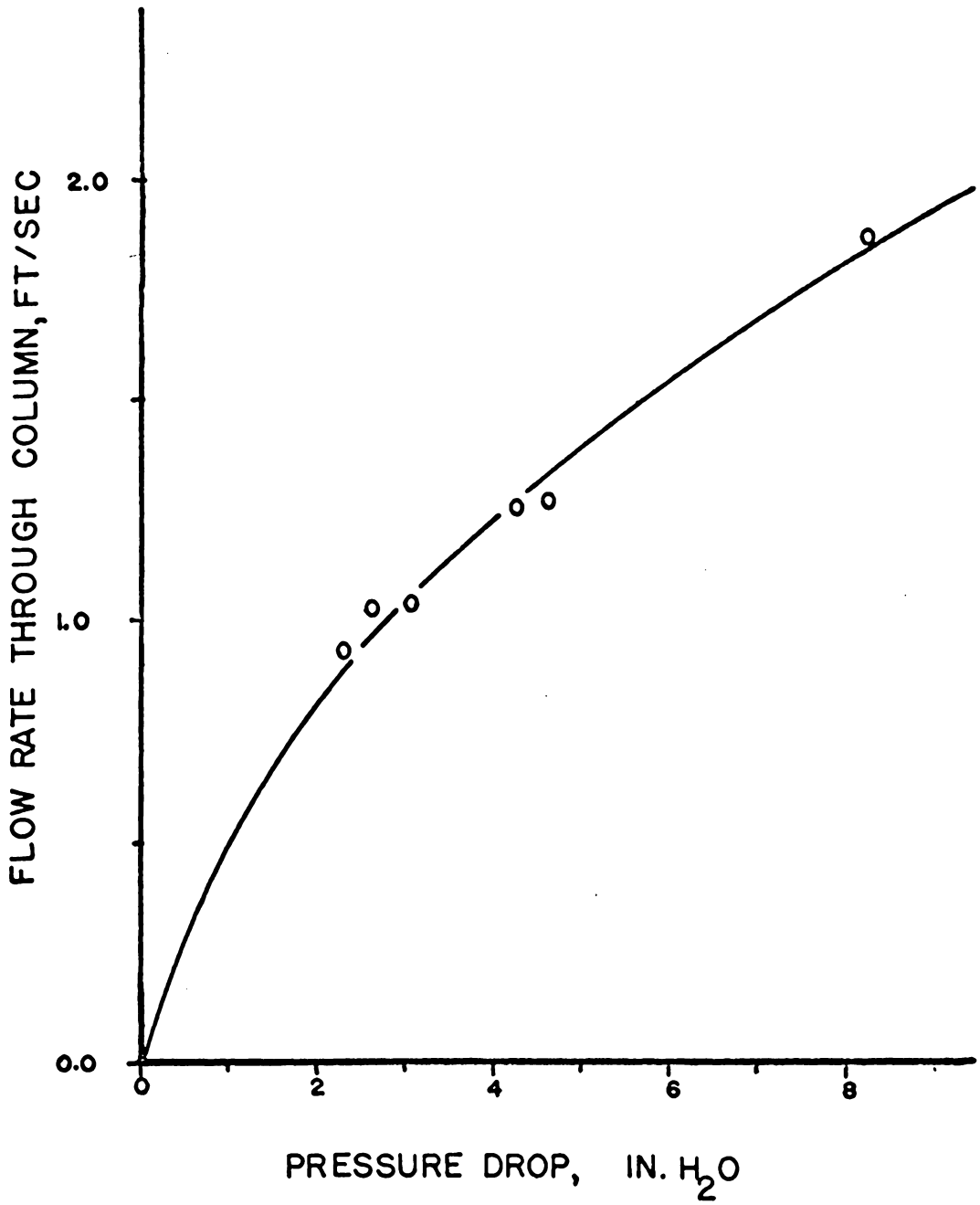

FIGURE 12. ORIFICE PRESSURE DROP VERSUS FLOW THROUGH COLUMN

TABLE II

Calibration[a] of Liquid Feed Rotameter

Rotameter Reading	Time of Flow, sec	Quantity[a] of Flow, cc	Rate of Flow cc / sec
0.135	100.0	940.0	9.49
0.275	60.0	1060.0	17.80
0.285	60.0	1110.0	18.50
0.350	50.0	1100.0	22.00
0.410	50.0	1203.0	24.10
0.440	45.0	1116.0	24.80
0.535	35.0	1170.0	33.50
0.660	30.0	1185.0	39.40
0.660	30.0	1150.0	38.80
0.740	25.0	1092.0	43.70
0.770	25.0	1137.0	45.50

[a] Rotameter was calibrated with distilled water at 25 °C.

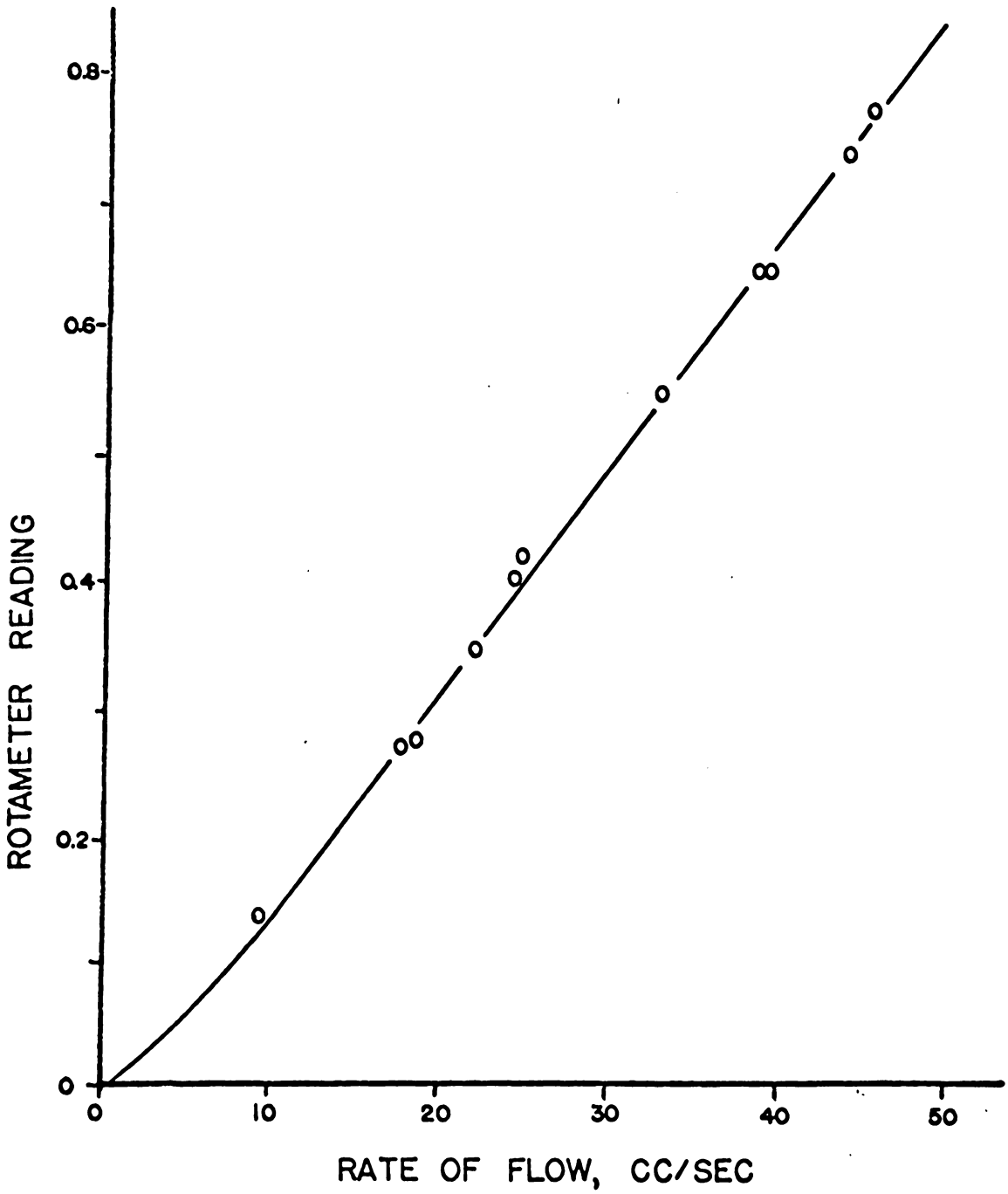

FIGURE 13. CALIBRATION CURVE FOR LIQUID FEED ROTAMETER

TABLE III

Determination of Pressure Drop Across Dry Sieve-Plate

Flow Rate Through the Column ft/sec	Pressure Drop Across Plate A[a] in H_2O	Pressure Drop Across Plate B[b] in H_2O	Pressure Drop Across Plate C[c] in H_2O
0.797	0.35	0.30	0.28
0.675	0.25	0.23	0.20
0.505	0.15	0.13	0.12
1.000	0.40	0.35	0.32
1.575	0.80	0.70	0.65
1.600	0.75	0.67	0.62
1.255	0.55	0.48	0.45
0.985	0.40	0.35	0.33
0.727	0.30	0.27	0.25
0.685	0.25	0.22	0.20
1.389	0.60	0.53	0.50
1.089	0.50	0.45	0.40
0.915	0.45	0.40	0.37

[a] Plate A is 1/8-inch thick with thirty-six 1/8-inch diameter holes.

[b] Plate B is 1/8-inch thick with nine 1/4-inch diameter holes.

[c] Plate C is 1/8-inch thick with four 3/8-inch diameter holes.

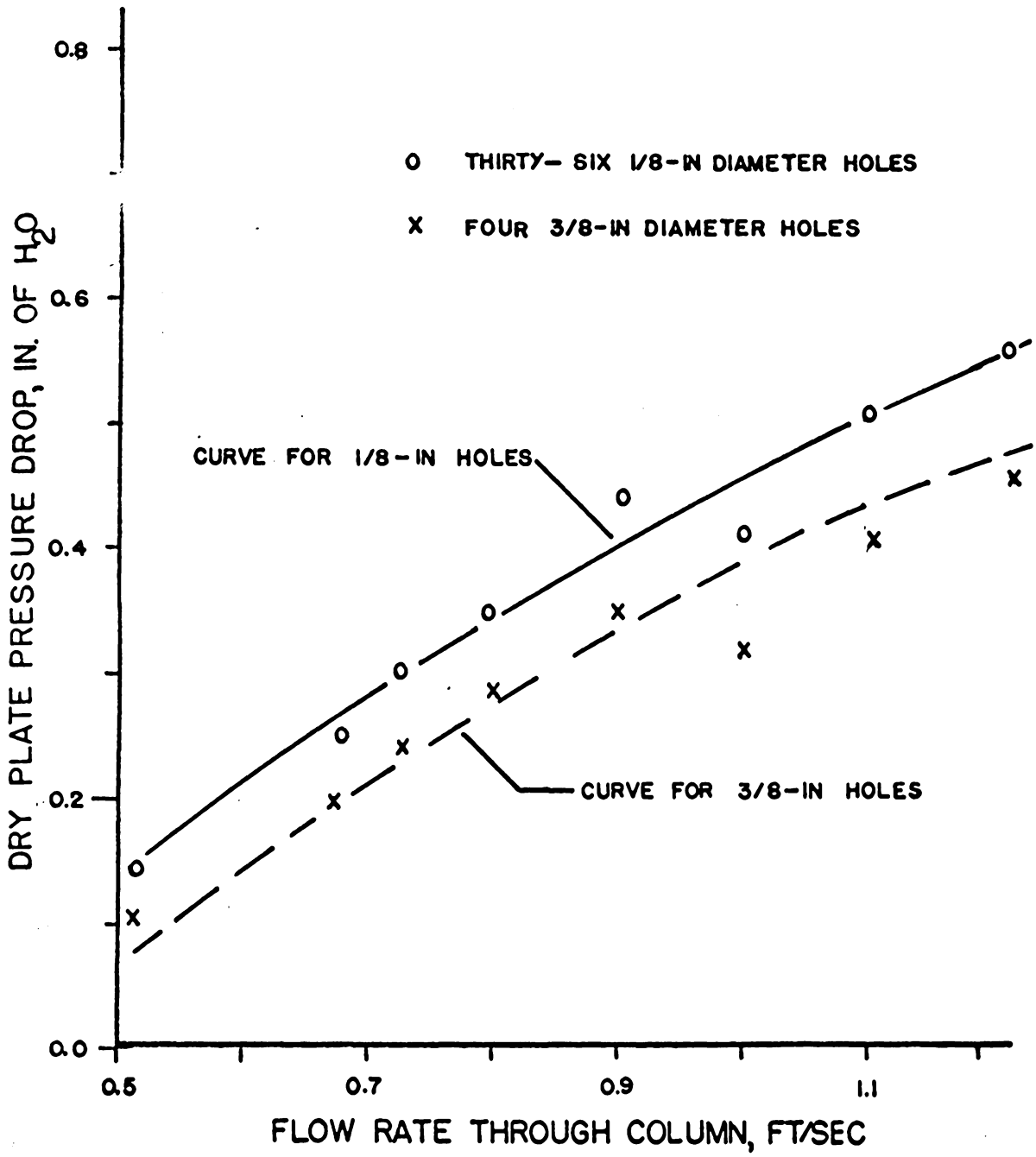

FIGURE 14. DRY PLATE PRESSURE DROP VERSUS WATER SATURATED CO_2 FLOW RATE

Calibration of Positive Displacement Pump. The results for the calibration of the positive displacement pump were presented in Table IV and Figure 15.

Operational Test. The procedures outlined in this section refer to Figure 10. It was assumed that the system was completely empty.

Testing was started by turning on the carbon dioxide cylinder and adjusting the flow so that the flow of carbon dioxide from the vent was sufficient to extinguish a match held six inches away from the vent. Next the water circulating pump on the saturation column was started. This circulated water from the saturation column through the constant temperature reservoir, the feed tank, and back into the saturation column. After this the feed solution, at 25.0 $^{o}C \pm 0.1\ ^{o}C$, was placed in the feed tank. At this point the gas blower was turned on and the vent was rechecked to insure that carbon dioxide was still flowing out of the vent. When this check was completed, the pump from the feed tank was started and the feed flow rate was adjusted to the desired value. Next the gas flow rate was adjusted to the value desired for the test. At this point the sampling procedure was begun.

Sampling Procedure. After all flow conditions had been set at the desired values, a period of ten minutes was allowed for the system to come to steady state. Then the effulent from the sieve-plate was collected for a period of ten minutes. The samples to be titrated, 25 ml aliquots, were taken from the ten minute composite sample. Feed samples were taken directly from the feed tank.

TABLE IV

Calibration of "Proportioneer" Pump

Pump Setting	Time, sec	Flow[a] cc	Flow Rate cc/min
100	600.0	500.3	50.0
90	600.1	450.0	45.0
80	600.0	400.8	40.0
70	600.3	349.9	35.0
60	600.0	300.1	30.0
50	600.0	250.7	25.0
40	600.2	200.2	20.0
30	600.1	150.6	15.0
20	600.2	100.9	10.0
10	600.0	53.1	5.3

[a] Flow is cc of water at 25 °C.

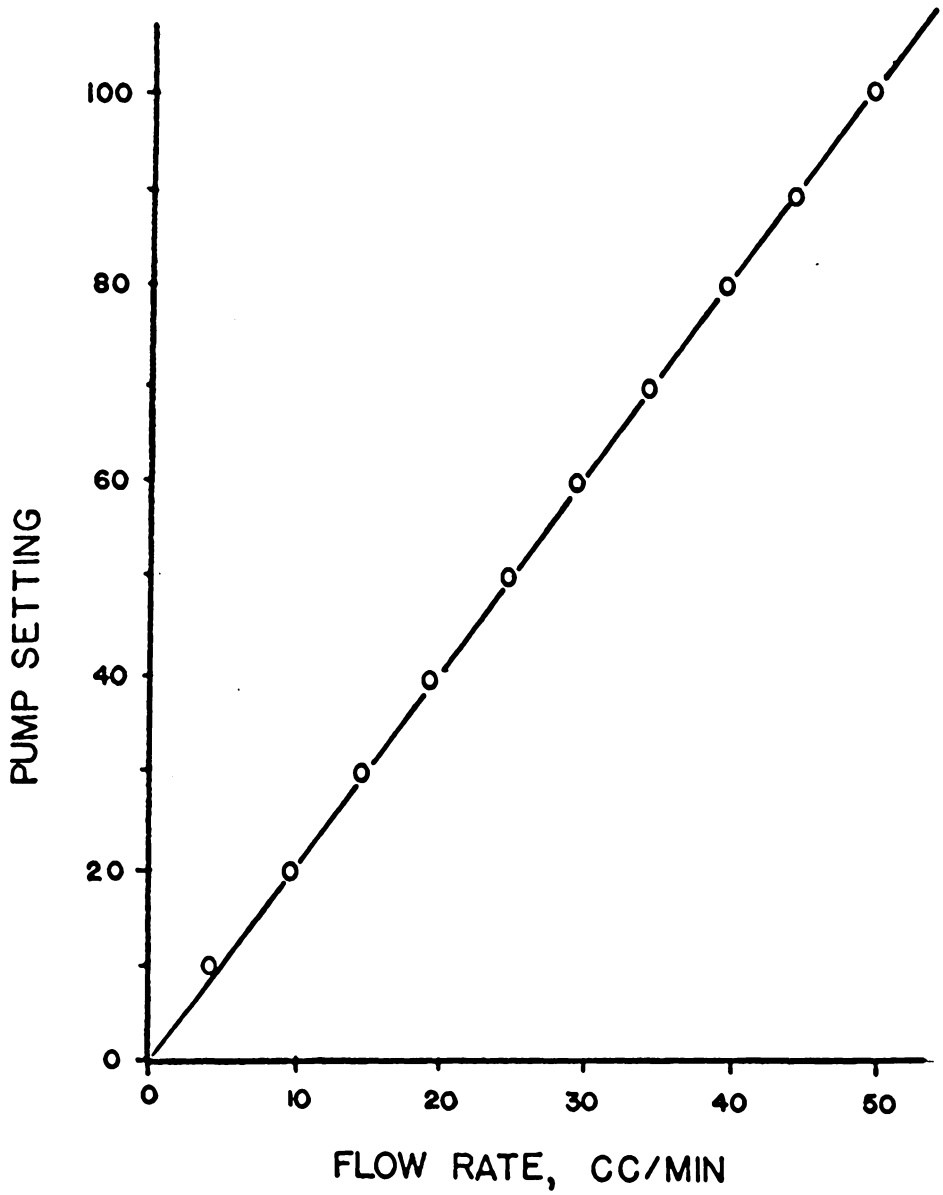

FIGURE 15. CALIBRATION CURVE FOR THE "PROPORTIONEER" PUMP

Analytical Procedures. The 20 ml aliquots, taken with pipets, were placed in sample bottles in a constant temperature bath maintained at 25 °C. The samples were removed from the constant temperature bath and titrated with suitable titrating solutions - either 0.0340 M caustic or 0.0340 M hydrochloric acid solutions. The end point of the titrations, a pH of 7.00, was measured with a pH meter.

Development of a Method for Analysis of Data. From the data of Danckwerts[5] in Figures 2 and 3 it was observed that the rate of absorption of carbon dioxide into dilute caustic solutions was always greater than the rate of absorption into pure water. This difference in rates existed because the absorption into the dilute caustic involved a coupling of pure absorption and chemical reaction; whereas, the absorption into the water was a case of pure absorption. However, as the times of contact approached zero the rates of absorption into the two liquids approached the same limiting rate. Since the rates of absorption were equal at zero contact time and were greater for the absorption into the dilute caustic at finite contact times, it was apparent that the ratio of the rate of absorption of carbon dioxide into a dilute caustic solution to the rate of absorption into water was a function of contact time. Figure 16 on page 45 shows a plot of this ratio for the absorption of carbon dioxide into a 0.085 M caustic solution and pure water.

Multiplying Equation 3 through by the interfacial area, a, yielded the following equation:

$$Q_A = 2\,a\,(c_i - c_o)\sqrt{\frac{D}{\pi\, t_c}} \qquad (8)$$

where:

Q_A = quanity of A absorbed, mol / sec

a = total interfacial area, cm^2

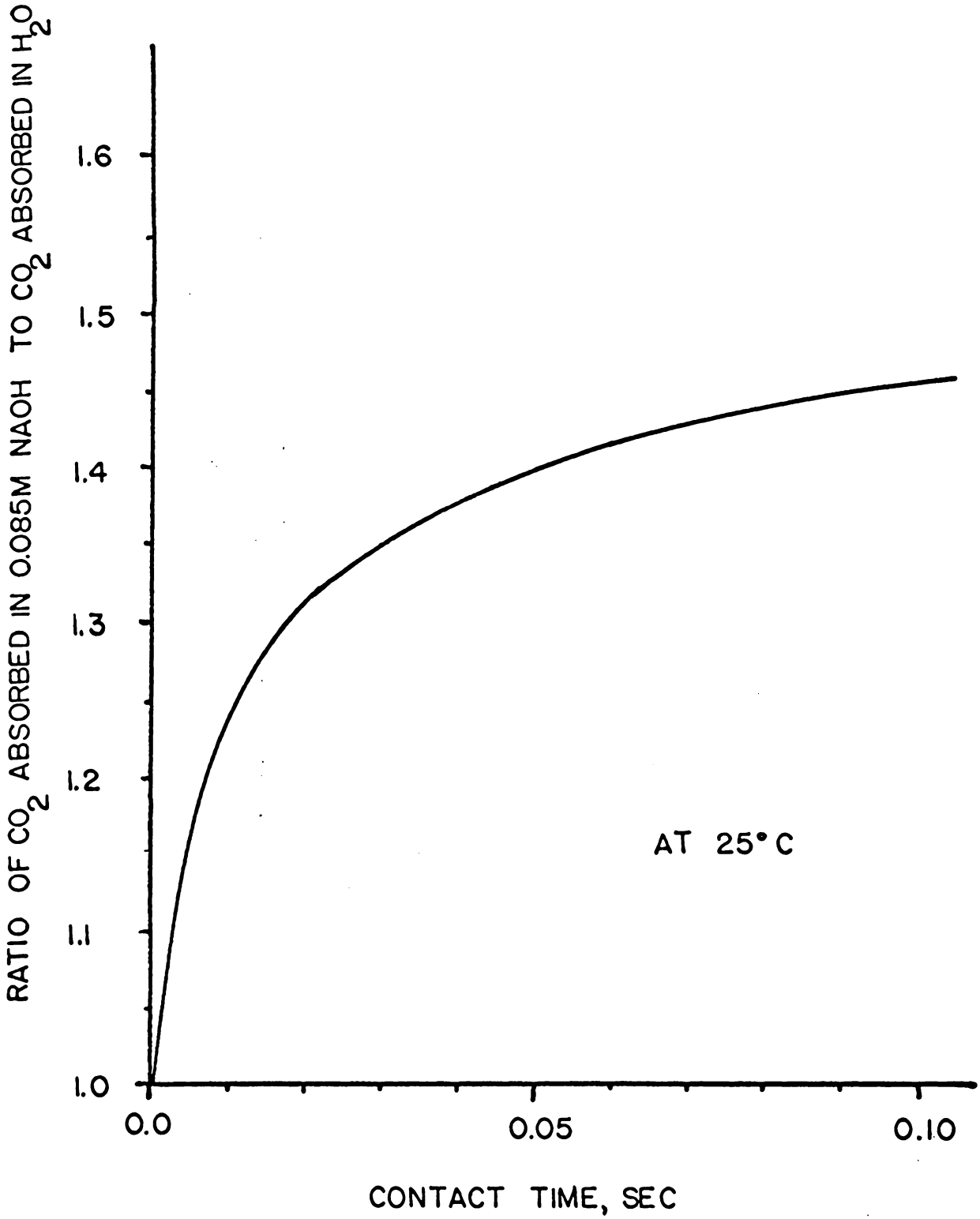

FIGURE 16. CONTACT TIME VERSUS RATIO OF CO_2 ABSORBED IN 0.085 M NAOH TO CO_2 ABSORBED IN H_2O

From Equation 8 the ratio of the amount of carbon dioxide absorbed in dilute caustic to the carbon dioxide absorbed in pure water would be:

$$R = \frac{Q'_{AC}}{Q_{AW}} = \frac{2\,a'\,(c'_i - c'_o)\sqrt{\dfrac{D'_{eff.}}{\pi\, t'_c}}}{2\,a\,(c_i - c_o)\sqrt{\dfrac{D}{\pi\, t_c}}}$$

where the primed values refer to the caustic solution and:

R = the point value of the ratio of carbon dioxide absorbed in dilute caustic to carbon dioxide absorbed in water

Q'_{AC} = rate of absorption into caustic, mol / sec

Q_{AW} = rate of carbon dioxide absorption into water, mol / sec

$D'_{eff.}$ = effective diffusion coefficient for the absorption and chemical reaction of carbon dioxide into caustic solution; a complex function of the time of contact, reaction rate constant and binary diffusion coefficient; cm^2 / sec

Since the physical parameters describing the flow characteristics on the sieve-tray were the same for each of the two cases the interfacial areas and contact times canceled leaving the following equation:

$$R = \frac{(c'_i - c'_o)}{(c_i - c_o)}\sqrt{\frac{D'_{eff.}}{D}} \qquad (8b)$$

For the case plotted in Figure 16, page 45, in which the two liquids were exposed for only one contact time the concentration differences also canceled leaving the ratio as a simple function of the two diffusivities. The diffusivity of carbon dioxide in water has been measured by many investigators[5,6] and was readily determined for the conditions employed in this investigation. The effective diffusivity of carbon dioxide in dilute

caustic solutions could be evaluated from the data of Danckwerts[5].

For given liquid concentrations of carbon dioxide and a given ratio of carbon dioxide absorbed in caustic to carbon dioxide absorbed in water the contact time could be evaluated from Equation 8b. However, the evaluation of contact times from Equation 8b was not straightforward since the effective diffusivity of the carbon dioxide in the caustic was a very complex function of the time of contact. In this investigation times of contact were evaluated from Figure 16 thus eliminating the difficult solution of Equation 8b. Because the data in Figure 16 was based upon single contact times, extreme care had to be exercised to insure that the liquid effluent from the tray (bulk concentration on the tray) corresponded to pure water or 0.085 M caustic which had been exposed for a single contact time. This necessitated a trial and error solution in which a contact time was assumed and a test made using this assumed contact time; the results of the first trial were used to evaluate a second approximation to the contact time from Figure 16. This method was continued until sucessive approximations yielded the same contact times.

The experimental value of the interfacial area can be estimated from Equation 8. The interfacial area per unit volume, a', could be evaluated independently[14] from the following equation:

$$a' = \frac{3(1-V)}{r} \qquad (9)$$

where:

a' = interfacial area per unit volume of froth, cm^{-1}

V = froth density, gm / cm^3

r = mean radius of bubbles, cm

Data and Results

The following section contains the data and results obtained during this investigation. As a check of reproducibility and to insure accuracy ten samples were taken under each set of operating conditions. However, this additional sampling proved superfluous since the maxium variation of experimentally determined parameters, the interfacial area and contact time, was less than one percent about the test mean. In view of the extremely small variation of the experimentally determined parameters about the test mean and the large number of observations it was felt that the data could be presented more concisely through the use of the averages of the ten samples. Therefore the data taken during this investigation were summarized and presented in Tables V through XV on pages 50 through 60.

Effect of Liquid Rate. The effect of the liquid feed rate on time of penetration (contact) and interfacial area was presented in Figures 17 and 18 pages 61 and 62. The data for these figures were taken from Tables V, VIII, and IX on pages 50, 53, and 54.

Effect of Hole Size. The effect of hole size on the time of penetration (contact) and interfacial area was presented in Figures 19, 20, 21, and 22 on pages 63, 64, 65, and 66. The data for these figures were taken from Tables V, VI, VII, X, and XI on pages 50, 51, 52, 55, and 56.

Effect of Free Area. The effect of free area, the ratio of the area of holes to the total plate area, on the time of penetration (contact)

and interfacial area was presented in Figures 22, 23, 24, 25, 26, and 27 on pages 66, 67, 68, 69, 70, and 71. The data for these figures were taken from Tables X, XI, XII, and VIII on pages 55, 56, 57, and 58.

Effect of Plate Thickness. The effect of plate thickness on the time of penetration (contact) and interfacial area was shown in Figures 28, 29, 30, 31, 32, 33, 34, and 35 on pages 72, 73, 74, 75, 76, 77, 78, and 79. The data for these figures were taken from Tables VI, XIV, and XV on pages 51, 59, 60.

Effect of Slot Velocity and Depth of Unaerated Liquid on Tray. The effect of slot velocity and depth of unaerated liquid on the tray, the major independent variables in this investigation, on the time of penetration (contact) and interfacial area was shown in Figures 17 through 35 on pages 61 through 79. The data for these plots came from Tables V through XV on pages 50 through 60.

TABLE V

Absorption of Carbon Dioxide into Water and Caustic Solution on a 1/8 - inch Thick Sieve-Tray with Nine 1/4 - inch Holes

Run No.	Liq. Feed Rate ml/sec	Column Gas Vel. ft/sec	Slot Gas Vel. ft/sec	Depth of Liq Unair. in H_2O	Titre[a] of CO_2 Abs in Water ml	Titre[a] of CO_2 Abs in Caustic ml	Ratio	Time of Penet. t_c sec	Expt. Area a' cm^{-1}	Calc Area a' cm^{-1}
1	20.0	0.625	22.0	1.00	95.80	138.15	1.442	0.080	7.3	7.0
2	20.0	0.625	22.0	2.00	197.00	284.45	1.428	0.069	7.1	7.0
3	20.0	0.625	22.0	3.00	271.55	386.95	1.425	0.067	6.3	7.0
4	20.0	0.739	26.0	1.00	112.30	160.25	1.427	0.068	7.9	7.4
5	20.0	0.739	26.0	2.00	225.10	317.85	1.412	0.058	7.6	7.4
6	20.0	0.739	26.0	3.00	312.10	440.05	1.410	0.057	6.9	7.4
7	20.0	0.853	30.0	1.00	131.55	185.75	1.412	0.058	8.5	7.6
8	20.0	0.853	30.0	2.00	266.35	372.90	1.400	0.051	8.1	7.6
9	20.0	0.853	30.0	3.00	393.00	548.70	1.396	0.049	7.8	7.6
10	20.0	0.966	34.0	1.00	151.75	212.90	1.403	0.052	9.3	7.8
11	20.0	0.966	34.0	2.00	324.00	449.85	1.388	0.045	9.1	7.8
12	20.0	0.966	34.0	3.00	466.50	645.25	1.383	0.043	8.7	7.8

[a] Titre is ml of 0.0340 M caustic necessary to titrate a 20 ml aliquot effluent.

TABLE VI

Absorption of Carbon Dioxide into Water and Caustic Solutions on a 1/8 - inch Thick Sieve-Tray with Thirty-six 1/8 - inch Holes

Run No.	Liq. Feed Rate ml/sec	Column Gas Vel. ft/sec	Slot Gas Vel. ft/sec	Depth of Liq Unair. in H_2O	Titre[a] of CO_2 abs in Water ml	Titre[a] of CO_2 Abs in Caustic ml	Ratio	Time of Penet. t_c sec	Expt. Area a' cm^{-1}	Calc Area a' cm^{-1}
13	20.0	0.625	22.0	1.00	95.75	138.05	1.442	0.080	7.3	7.0
14	20.0	0.625	22.0	2.00	199.25	284.55	1.428	0.069	7.1	7.0
15	20.0	0.625	22.0	3.00	271.60	387.05	1.425	0.067	6.3	7.0
16	20.0	0.739	26.0	1.00	112.40	160.40	1.427	0.068	7.9	7.4
17	20.0	0.739	26.0	2.00	225.05	317.75	1.412	0.058	7.3	7.4
18	20.0	0.739	26.0	3.00	312.15	440.15	1.410	0.057	6.7	7.4
19	20.0	0.853	30.0	1.00	131.65	185.90	1.412	0.058	8.5	7.6
20	20.0	0.853	30.0	2.00	266.45	373.05	1.400	0.051	8.1	7.6
21	20.0	0.853	30.0	3.00	393.05	548.70	1.396	0.049	7.8	7.6
22	20.0	0.966	34.0	1.00	151.70	212.85	1.403	0.052	9.3	7.8
23	20.0	0.966	34.0	2.00	324.10	449.85	1.388	0.045	9.1	7.8
24	20.0	0.966	34.0	3.00	466.45	645.10	1.383	0.043	8.7	7.8

[a] Titre is ml of 0.0340 M caustic necessary to titrate a 20 ml aliquot effluent.

TABLE VII

Absorption of Carbon Dioxide into Water and Caustic Solutions on a 1/8 - inch Thick Sieve-Tray with Four 3/8 - inch Holes

Run No.	Liq. Feed Rate ml/sec	Column Gas Vel. ft/sec	Slot Gas Vel. ft/sec	Depth of Liq Unair. in H_2O	Titre[a] of CO_2 Abs in Water ml	Titre[a] of CO_2 Abs in Caustic ml	Ratio	Time of Penet. t_c sec	Expt. Area a' cm^{-1}	Calc Area a' cm^{-1}
25	20.0	0.625	22.0	1.00	95.60	137.85	1.442	0.080	7.3	7.0
26	20.0	0.625	22.0	2.00	199.05	284.25	1.428	0.069	7.1	7.0
27	20.0	0.625	22.0	3.00	271.75	387.25	1.425	0.067	6.3	7.0
28	20.0	0.739	26.0	1.00	112.20	160.10	1.427	0.068	7.9	7.4
29	20.0	0.739	26.0	2.00	225.20	318.00	1.412	0.058	7.3	7.4
30	20.0	0.739	26.0	3.00	312.20	440.20	1.410	0.057	6.7	7.4
31	20.0	0.853	30.0	1.00	131.65	185.90	1.412	0.058	8.5	7.6
32	20.0	0.853	30.0	2.00	266.40	372.95	1.400	0.051	8.1	7.6
33	20.0	0.853	30.0	3.00	393.05	548.70	1.396	0.049	7.8	7.6
34	20.0	0.966	34.0	1.00	151.70	212.85	1.403	0.052	9.3	7.8
35	20.0	0.966	34.0	2.00	323.90	449.55	1.388	0.045	9.1	7.8
36	20.0	0.966	34.0	3.00	466.45	645.10	1.383	0.043	8.7	7.8

[a] Titre is ml of 0.0340 M caustic necessary to titrate a 20 ml aliquot effluent.

TABLE VIII

Absorption of Carbon Dioxide into Water and Caustic Solutions on a 1/8 - inch Thick Sieve-Tray with Nine 1/4 - inch Holes

Run No.	Liq. Feed Rate ml/sec	Column Gas Vel. ft/sec	Slot Gas Vel. ft/sec	Depth of Liq Unair. in H_2O	Titre[a] of CO_2 Abs in Water ml	Titre[a] of CO_2 Abs in Caustic ml	Ratio	Time of Pennet. t_c sec	Expt. Area a' cm^{-1}	Calc Area a' cm^{-1}
37	10.0	0.625	22.0	1.00	95.85	138.20	1.442	0.080	7.3	7.0
38	10.0	0.625	22.0	2.00	199.30	284.60	1.428	0.069	7.1	7.0
39	10.0	0.625	22.0	3.00	271.55	386.95	1.425	0.067	6.3	7.0
40	10.0	0.739	26.0	1.00	112.25	159.95	1.425	0.067	7.9	7.4
41	10.0	0.739	26.0	2.00	225.15	317.45	1.410	0.057	7.6	7.4
42	10.0	0.739	26.0	3.00	312.20	440.20	1.410	0.057	6.9	7.4
43	10.0	0.853	30.0	1.00	131.45	185.35	1.410	0.057	8.5	7.6
44	10.0	0.853	30.0	2.00	266.35	372.90	1.400	0.051	8.1	7.6
45	10.0	0.853	30.0	3.00	393.05	548.70	1.396	0.049	7.8	7.6
46	10.0	0.966	34.0	1.00	151.80	212.95	1.403	0.052	9.3	7.8
47	10.0	0.966	34.0	2.00	324.05	449.80	1.388	0.045	9.1	7.8
48	10.0	0.966	34.0	3.00	466.50	645.15	1.383	0.043	8.7	7.8

[a] Titre is ml of 0.0340 M caustic necessary to titrate a 20 ml aliquot effluent.

TABLE IX

Absorption of Carbon Dioxide into Water and Caustic Solutions on a 1/8 - inch Thick Sieve-Tray with Nine 1/4 - inch Holes

Run No.	Liq. Feed Rate ml/sec	Column Gas Vel. ft/sec	Slot Gas Vel. ft/sec	Depth of Liq Unair. in H_2O	Titre[a] of CO_2 Abs in Water ml	Titre[a] of CO_2 Abs in Caustic ml	Ratio	Time of Penet. t_c sec	Expt. Area a'^{-1} cm^{-1}	Calc Area a'^{-1} cm^{-1}
49	30.0	0.625	22.0	1.00	95.75	137.90	1.440	0.079	7.3	7.0
50	30.0	0.625	22.0	2.00	199.15	284.40	1.428	0.069	7.1	7.0
51	30.0	0.625	22.0	3.00	271.60	387.55	1.427	0.068	6.3	7.0
52	30.0	0,739	26.0	1.00	112.35	160.30	1.427	0.068	7.9	7.4
53	30.0	0.739	26.0	2.00	225.15	317.90	1.412	0.058	7.6	7.4
54	30.0	0.739	26.0	3.00	312.10	439.90	1.410	0.057	6.9	7.4
55	30.0	0.853	30.0	1.00	131.55	185.75	1.412	0.058	8.5	7.6
56	30.0	0.853	30.0	2.00	266.40	372.95	1.400	0.051	8.1	7.6
57	30.0	0.853	30.0	3.00	392.95	548.55	1.396	0.049	7.8	7.6
58	30.0	0.966	34.0	1.00	151.80	213.00	1.403	0.052	9.3	7.8
59	30.0	0.966	34.0	2.00	323.95	449.65	1.388	0.045	9.1	7.8
60	30.0	0.966	34.0	3.00	466.45	646.50	1.386	0.044	8.7	7.8

[a] Titre is ml of 0.0340 M caustic necessary to titrate a 20 ml aliquot effluent.

TABLE X

Absorption of Carbon Dioxide into Water and Caustic Solutions on a 1/8 - inch Thick Sieve-Tray with Eight 3/8 - inch Holes

Run No.	Liq. Feed Rate ml/sec	Column Gas Vel. ft/sec	Slot Gas Vel. ft/sec	Depth of Liq Unair. in H_2O	Titre[a] of CO_2 Abs in Water ml	Titre[a] of CO_2 Abs in Caustic ml	Ratio	Time of Penet. t_c sec	Expt. Area a' cm^{-1}	Calc Area a' cm^{-1}
61	20.0	1.250	22.0	1.00	115.45	166.25	1.440	0.079	8.8	8.2
62	20.0	1.250	22.0	2.00	248.20	354.45	1.428	0.069	8.6	8.2
63	20.0	1.250	22.0	3.00	336.25	479.85	1.427	0.068	7.8	8.2
64	20.0	1.478	26.0	1.00	133.70	190.80	1.427	0.068	9.4	8.4
65	20.0	1.478	26.0	2.00	271.40	383.20	1.412	0.058	8.8	8.4
66	20.0	1.478	26.0	3.00	381.95	538.55	1.410	0.057	8.2	8.4
67	20.0	1.706	30.0	1.00	154.70	218.15	1.410	0.057	10.0	8.6
68	20.0	1.706	30.0	2.00	315.70	442.00	1.400	0.051	9.6	8.6
69	20.0	1.706	30.0	3.00	468.50	654.05	1.396	0.049	9.3	8.6
70	20.0	1.932	34.0	1.00	176.25	247.30	1.403	0.052	10.8	8.8
71	20.0	1.932	34.0	2.00	377.05	523.35	1.388	0.045	10.6	8.8
72	20.0	1.932	34.0	3.00	546.65	756.00	1.383	0.043	10.2	8.8

[a] Titre is ml of 0.0340 M caustic necessary to titrate a 20 ml aliquot effluent.

TABLE XI

Absorption of Carbon Dioxide into Water and Caustic Solutions on a 1/8 - inch Thick Sieve-Tray with Eighteen 1/4 - inch Holes

Run No.	Liq. Feed Rate ml/sec	Column Gas Vel. ft/sec	Slot Gas Vel. ft/sec	Depth of Liq Unair. in H_2O	Titre[a] of CO_2 Abs in Water ml	Titre[a] of CO_2 Abs in Caustic ml	Ratio	Time of Penet. t_c sec	Expt. Area a'^{-1} cm	Calc Area a'^{-1} cm
73	20.0	1.250	22.0	1.00	115.40	166.40	1.442	0.080	8.8	8.2
74	20.0	1.250	22.0	2.00	248.25	354.50	1.428	0.069	8.6	8.2
75	20.0	1.250	22.0	3.00	336.25	479.15	1.425	0.067	7.8	8.2
76	20.0	1.478	26.0	1.00	133.75	190.85	1.427	0.068	9.4	8.4
77	20.0	1.478	26.0	2.00	271.45	383.30	1.412	0.058	8.8	8.4
78	20.0	1.478	26.0	3.00	381.90	538.50	1.410	0.057	8.2	8.4
79	20.0	1.706	30.0	1.00	154.75	218.20	1.410	0.057	10.0	8.6
80	20.0	1.706	30.0	2.00	315.70	442.00	1.400	0.051	9.6	8.6
81	20.0	1.706	30.0	3.00	468.55	654.10	1.396	0.049	9.3	8.6
82	20.0	1.932	34.0	1.00	176.30	247.35	1.403	0.052	10.8	8.8
83	20.0	1.932	34.0	2.00	377.05	523.35	1.388	0.045	10.6	8.8
84	20.0	1.932	34.0	3.00	546.65	757.65	1.386	0.044	10.2	8.8

[a] Titre is ml of 0.0340 M caustic necessary to titrate a 20 ml aliquot effluent.

TABLE XII

Absorption of Carbon Dioxide into Water and Caustic Solutions on a 1/8 - inch Thick Sieve-Tray with Four 1/4 - inch Holes

Run No.	Liq. Feed Rate ml/sec	Column Gas Vel. ft/sec	Slot Gas Vel. ft/sec	Depth of Liq Unair. in H_2O	Titre[a] of CO_2 Abs in Water ml	Titre[a] of CO_2 Abs in Caustic ml	Ratio	Time of Penet. t_c sec	Expt. Area a'^{-1} cm	Calc Area a'^{-1} cm
85	20.0	0.278	22.0	1.00	81.35	117.15	1.440	0.079	6.2	6.1
86	20.0	0.278	22.0	2.00	168.30	240.35	1.428	0.069	6.0	6.1
87	20.0	0.278	22.0	3.00	219.80	313.65	1.427	0.068	5.1	6.1
88	20.0	0.328	26.0	1.00	96.65	137.90	1.427	0.068	6.8	6.3
89	20.0	0.328	26.0	2.00	188.10	265.60	1.421	0.058	6.1	6.3
90	20.0	0.328	26.0	3.00	256.20	361.25	1.410	0.057	5.5	6.3
91	20.0	0.379	30.0	1.00	113.00	159.55	1.412	0.058	7.3	6.5
92	20.0	0.379	30.0	2.00	230.20	322.30	1.400	0.051	7.0	6.5
93	20.0	0.379	30.0	3.00	332.55	464.25	1.396	0.049	6.6	6.5
94	20.0	0.429	34.0	1.00	133.80	187.70	1.403	0.052	8.2	6.7
95	20.0	0.429	34.0	2.00	284.85	395.40	1.388	0.045	8.0	6.7
96	20.0	0.429	34.0	3.00	407.50	564.80	1.386	0.044	7.6	6.7

[a] Titre is ml of 0.0340 M caustic necessary to titrate a 20 ml aliquot effluent.

TABLE XIII

Absorption of Carbon Dioxide into Water and Caustic Solutions on a 1/8 - inch Thick Sieve-Trav with Sixteen 1/8 - inch Holes

Run No.	Liq. Feed Rate ml/sec	Column Gas Vel. ft/sec	Slot Gas Vel. ft/sec	Depth of Liq. Unair. in H_2O	Titre[a] of CO_2 Abs in Water ml	Titre[a] of CO_2 Abs in Caustic ml	Ratio	Time of Penet. a'^{-1} cm	Expt. Area a'^{-1} cm^{-1}	Calc Area a'^{-1} cm^{-1}
97	20.0	0.278	22.0	1.00	81.40	117.40	1.442	0.080	6.2	6.1
98	20.0	0.278	22.0	2.00	168.35	240.40	1.428	0.069	6.0	6.1
99	20.0	0.278	22.0	3.00	219.85	313.75	1.427	0.068	5.1	6.1
100	20.0	0.328	26.0	1.00	96.70	138.00	1.427	0.068	6.8	6.3
101	20.0	0.328	26.0	2.00	188.15	265.70	1.412	0.058	6.1	6.3
102	20.0	0.328	26.0	3.00	256.25	361.30	1.410	0.057	5.5	6.3
103	20.0	0.379	30.0	1.00	113.00	159.35	1.410	0.057	7.3	6.5
104	20.0	0.379	30.0	2.00	230.25	322.35	1.400	0.051	7.0	6.5
105	20.0	0.379	30.0	3.00	332.60	464.30	1.396	0.049	6.6	6.5
106	20.0	0.429	34.0	1.00	133.85	187.80	1.403	0.052	8.2	6.7
107	20.0	0.429	34.0	2.00	284.80	395.30	1.388	0.045	8.0	6.7
108	20.0	0.429	34.0	3.00	407.55	564.85	1.386	0.044	7.6	6.7

[a] Titre is ml of 0.0340 M caustic necessary to titrate a 20 ml aliquot effluent.

TABLE XIV

Absorption of Carbon Dioxide into Water and Caustic Solutions on a 1/16 - inch Thick Sieve-Tray with Thirty-six 1/8 - inch Holes

Run No.	Liq. Feed Rate ml/sec	Column Gas Vel. ft/sec	Slot Gas Vel. ft/sec	Depth of Liq Unair. in H_2O	Titre[a] of CO_2 Abs in Water ml	Titre[a] of CO_2 Abs in Caustic ml	Ratio	Time of Penet. t_c sec	Expt. Area a' cm^{-1}	Calc Area a' cm^{-1}
109	20.0	0.625	22.0	1.00	95.75	138.25	1.444	0.081	7.3	7.0
110	20.0	0.625	22.0	2.00	199.15	284.80	1.430	0.070	7.1	7.0
111	20.0	0.625	22.0	3.00	271.50	387.70	1.428	0.069	6.3	7.0
112	20.0	0.739	26.0	1.00	112.35	160.30	1.427	0.068	7.9	7.4
113	20.0	0.739	26.0	2.00	225.15	318.15	1.414	0.059	7.3	7.4
114	20.0	0.739	26.0	3.00	312.20	440.85	1.412	0.058	6.7	7.4
115	20.0	0.853	30.0	1.00	131.60	185.80	1.412	0.058	8.5	7.6
116	20.0	0.853	30.0	2.00	266.45	373.05	1.400	0.051	8.1	7.6
117	20.0	0.853	30.0	3.00	393.05	550.25	1.400	0.051	7.8	7.6
118	20.0	0.966	34.0	1.00	151.75	212.90	1.403	0.052	9.3	7.8
119	20.0	0.966	34.0	2.00	324.00	450.35	1.390	0.046	9.1	7.8
120	20.0	0.966	34.0	3.00	466.50	646.10	1.385	0.044	8.7	7.8

[a] Titre is ml of 0.0340 M caustic necessary to titrate a 20 ml aliquot of effluent.

TABLE XV

Absorption of Carbon Dioxide into Water and Caustic Solutions on a 1/2 - inch Thick Sieve-Tray with Thirty-six 1/8 - inch Holes

Run No.	Liq. Feed Rate ml/sec	Column Gas Vel. ft/sec	Slot Gas Vel. ft/sec	Depth of Liq Unair. in H_2O	Titre[a] of CO_2 Abs in Water ml	Titre[a] of CO_2 Abs in Caustic ml	Ratio	Time of Penet. t_c sec	Expt. Area a' cm^{-1}	Calc Area a' cm^{-1}
121	20.0	0.625	22.0	1.00	92.90	133.05	1.432	0.072	6.7	7.0
122	20.0	0.625	22.0	2.00	187.55	266.35	1.420	0.063	6.4	7.0
123	20.0	0.625	22.0	3.00	363.95	515.70	1.417	0.062	5.6	7.0
124	20.0	0.739	26.0	1.00	107.20	151.70	1.415	0.061	7.1	7.4
125	20.0	0.739	26.0	2.00	213.05	299.10	1.404	0.053	6.6	7.4
126	20.0	0.739	26.0	3.00	296.55	416.05	1.403	0.052	6.0	7.4
127	20.0	0.853	30.0	1.00	124.95	175.30	1.403	0.052	7.4	7.8
128	20.0	0.853	30.0	2.00	253.10	351.80	1.390	0.046	7.3	7.6
129	20.0	0.853	30.0	3.00	373.75	519.50	1.390	0.046	7.0	7.6
130	20.0	0.966	34.0	1.00	144.05	200.65	1.393	0.047	8.4	7.8
131	20.0	0.966	34.0	2.00	307.95	424.95	1.380	0.041	8.2	7.8
132	20.0	0.966	34.0	3.00	442.35	609.10	1.377	0.040	7.8	7.8

[a] Titre is ml of 0.0340 M caustic necessary to titrate a 20 ml aliquot effluent.

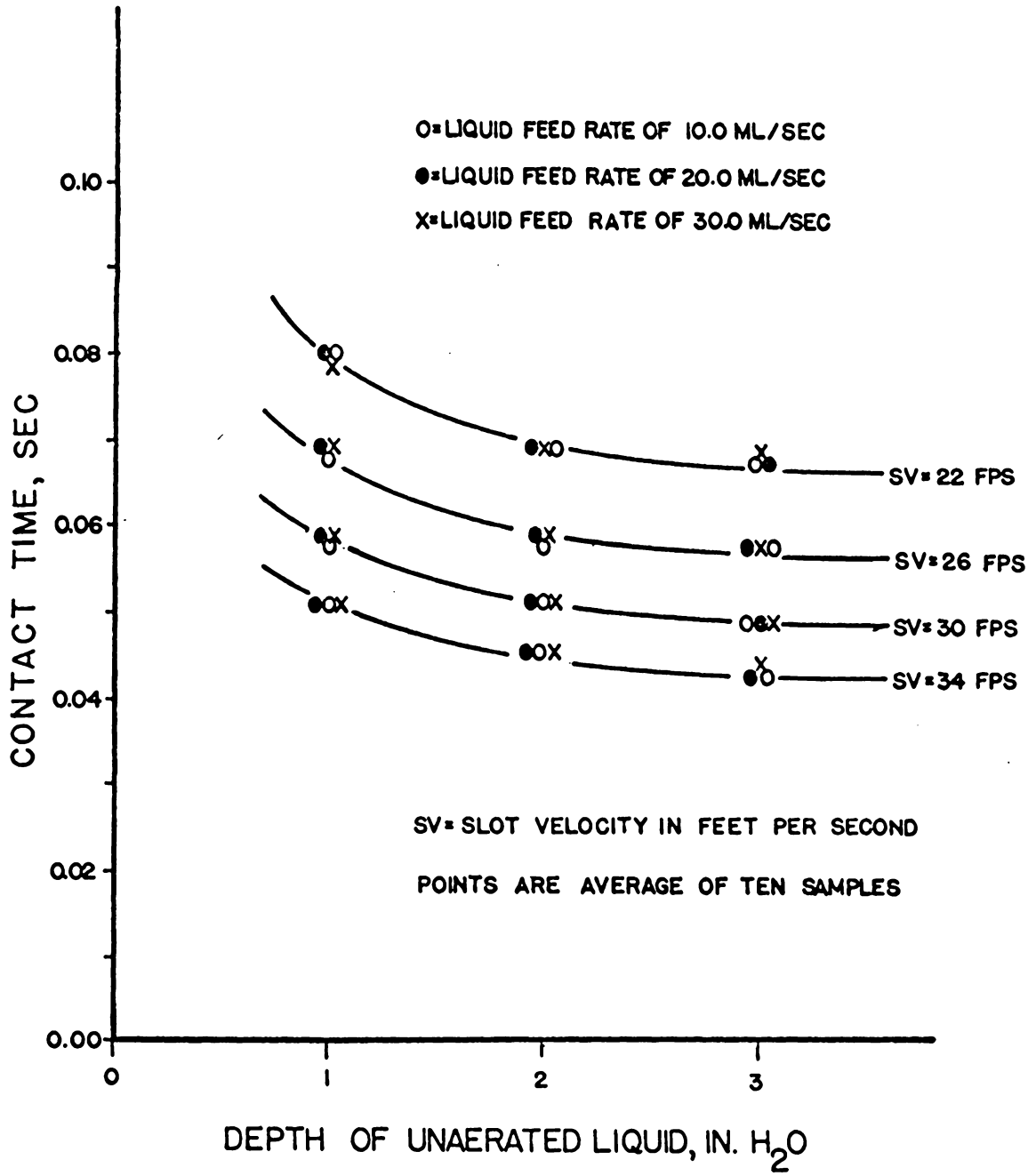

FIGURE 17. EFFECT OF LIQUID FLOW RATE, SLOT VELOCITY, AND DEPTH OF UNAERATED LIQUID ON TRAY AS A FUNCTION OF CONTACT TIME FOR 1/8-IN. THICK PLATE, NINE 1/4-IN. HOLES

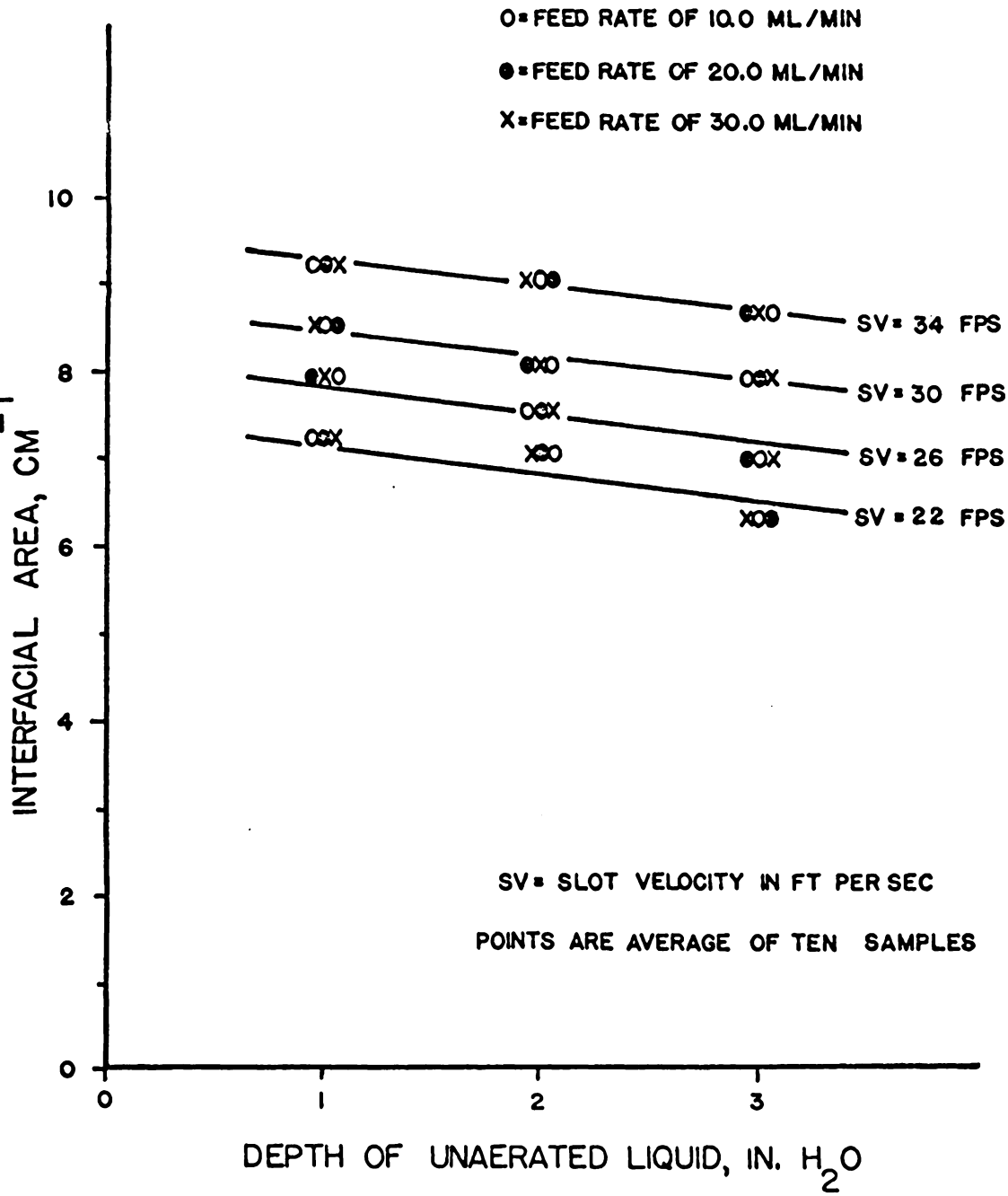

FIGURE 18. EFFECT OF LIQUID FLOW RATE, DEPTH OF UNAERATED LIQUID ON SIEVE-TRAY, AND SLOT VELOCITY AS A FUNCTION OF INTERFACIAL AREA FOR 1/8-IN THICK PLATE, NINE 1/4-IN HOLES

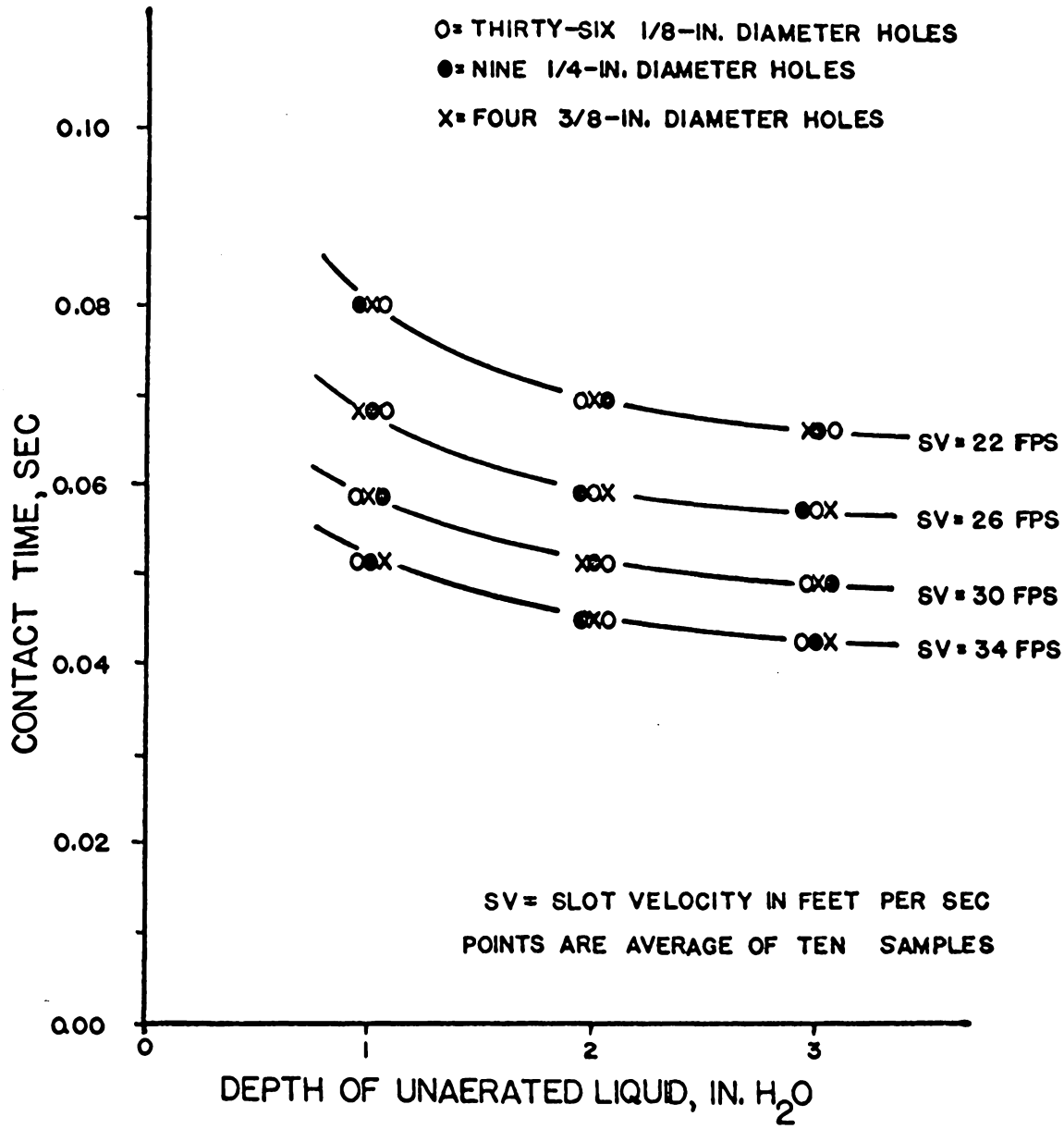

FIGURE 19. EFFECT OF HOLE DIAMETER, DEPTH OF UNAERATED LIQUID ON TRAY, AND SLOT VELOCITY ON CONTACT TIME FOR A FREE AREA OF 3.52 % AND PLATE THICKNESS OF 1/8-IN.

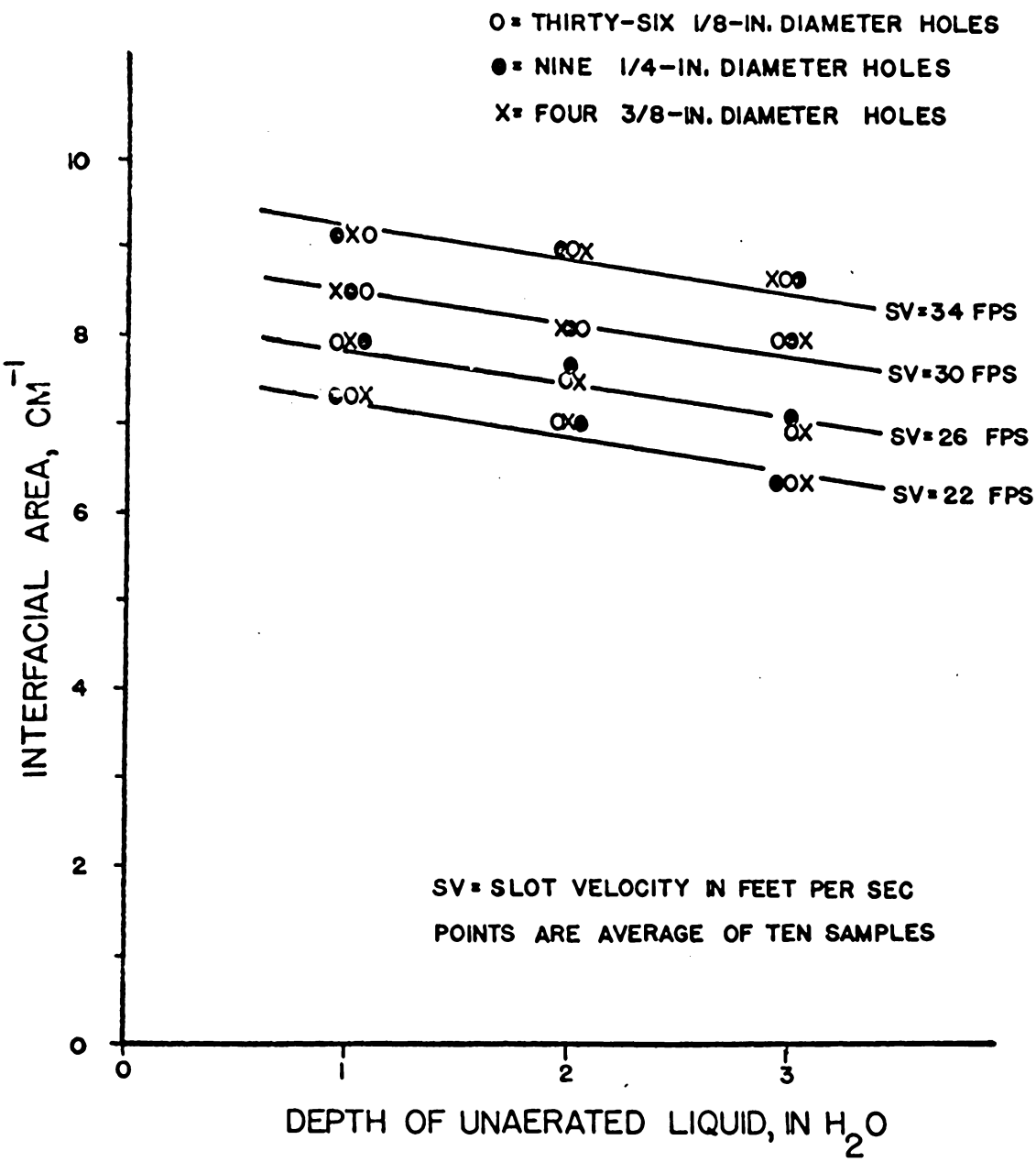

FIGURE 20. EFFECT OF HOLE SIZE, DEPTH OF UNAERATED LIQUID, AND SLOT VELOCITY ON THE INTERFACIAL AREA FOR A 1/8-IN. THICK PLATE WITH 3.52 % FREE AREA

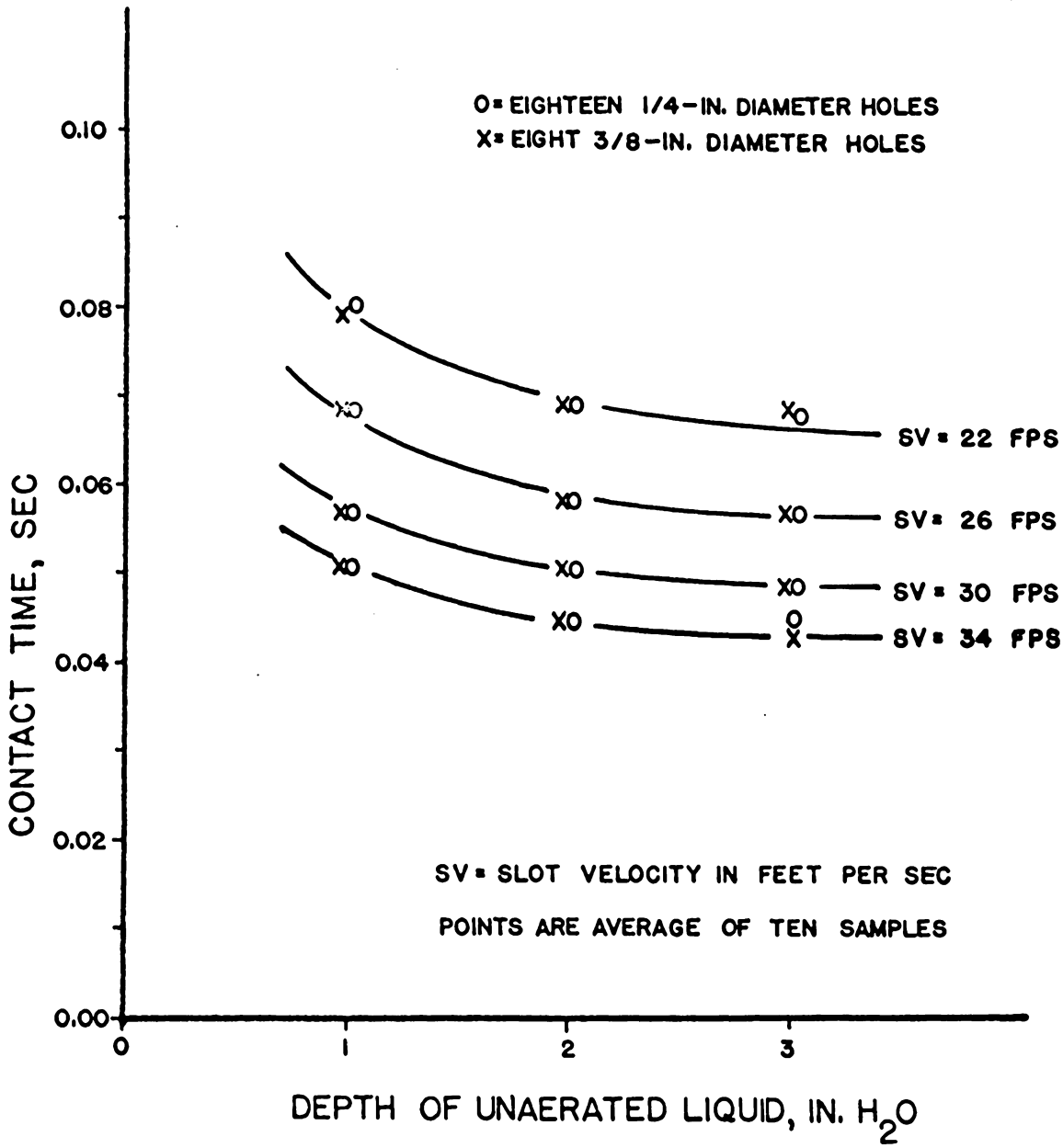

FIGURE 21. EFFECT OF HOLE SIZE, DEPTH OF LIQUID ON PLATE, AND SLOT VELOCITY ON CONTACT TIME FOR A 1/8-IN. THICK PLATE WITH A 7.04 % FREE AREA

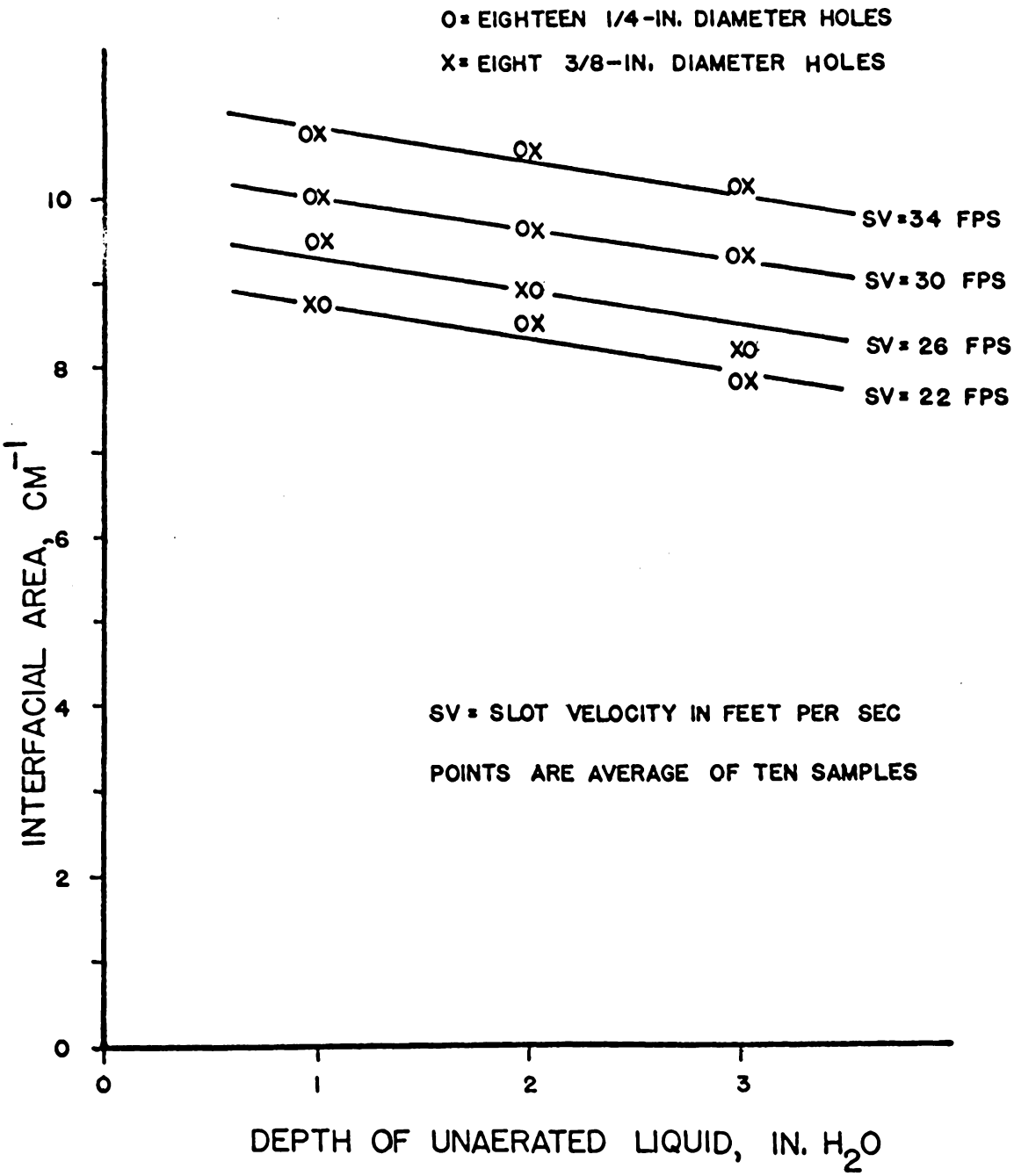

FIGURE 22. EFFECT OF HOLE SIZE, SLOT VELOCITY, AND DEPTH OF UNAERATED LIQUID ON TRAY ON THE INTERFACIAL AREA FOR A 1/8-IN. THICK PLATE WITH A 7.04% FREE AREA

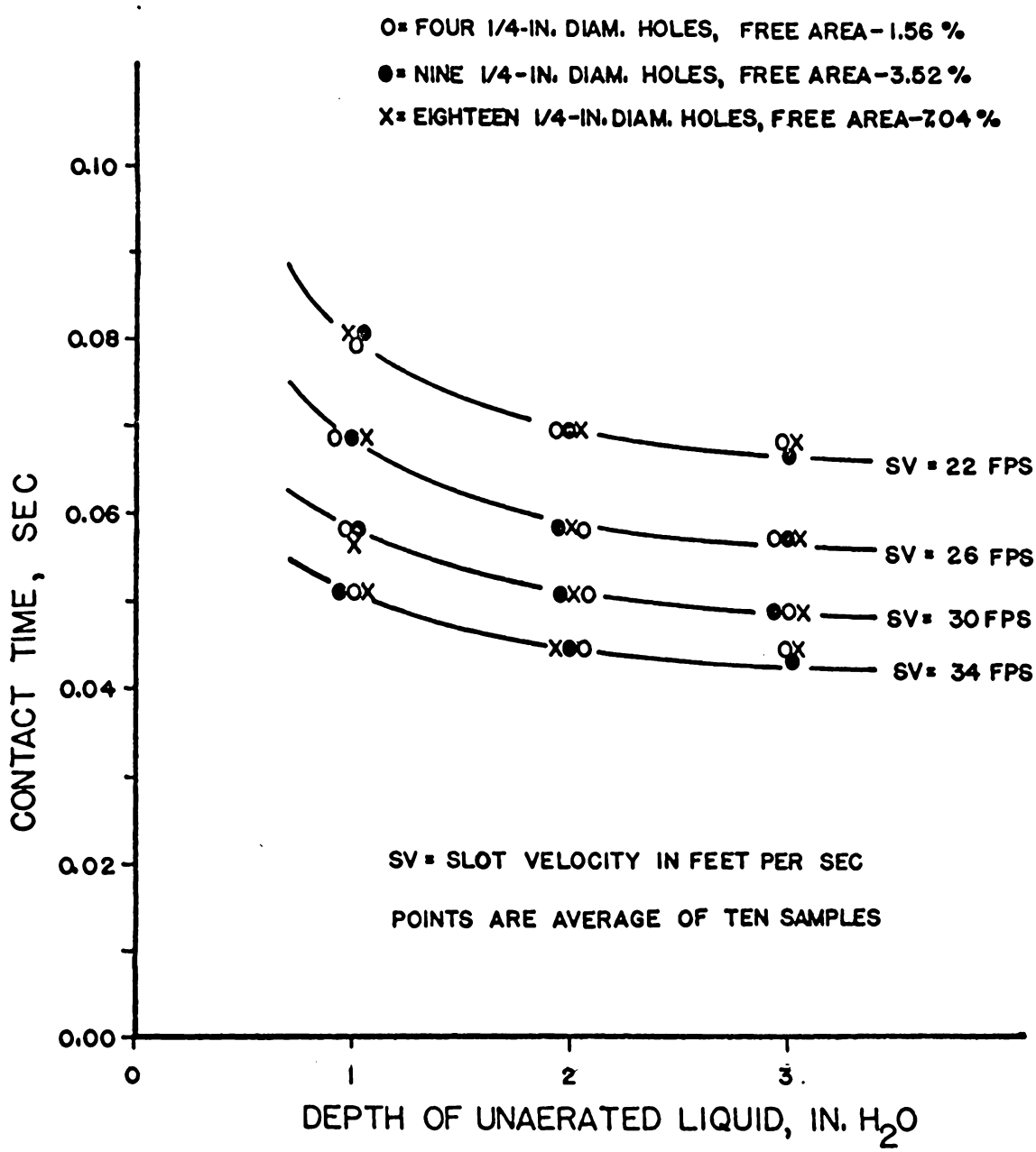

FIGURE 23. EFFECT OF FREE AREA, SLOT VELOCITY, AND DEPTH OF UNAERATED LIQUID ON TRAY ON THE CONTACT TIME FOR 1/4-IN. DIAMETER HOLES IN A 1/8-IN. THICK PLATE

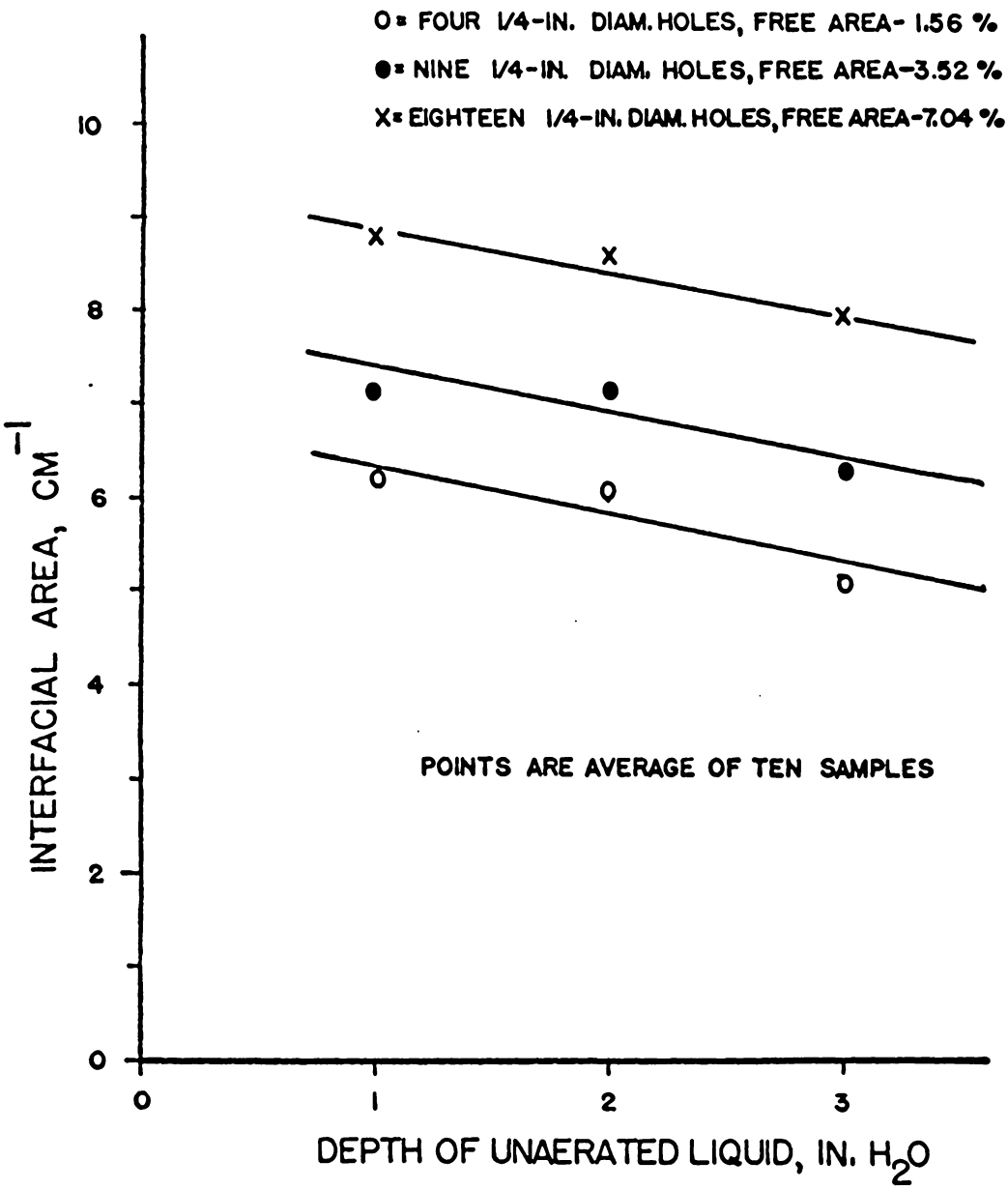

FIGURE 24. EFFECT OF FREE AREA AND DEPTH OF UNAERATED LIQUID ON TRAY ON INTERFACIAL AREA AT A SLOT VELOCITY OF 22 FEET PER SEC FOR 1/4-IN. DIAMETER HOLES IN A 1/8-IN. THICK PLATE

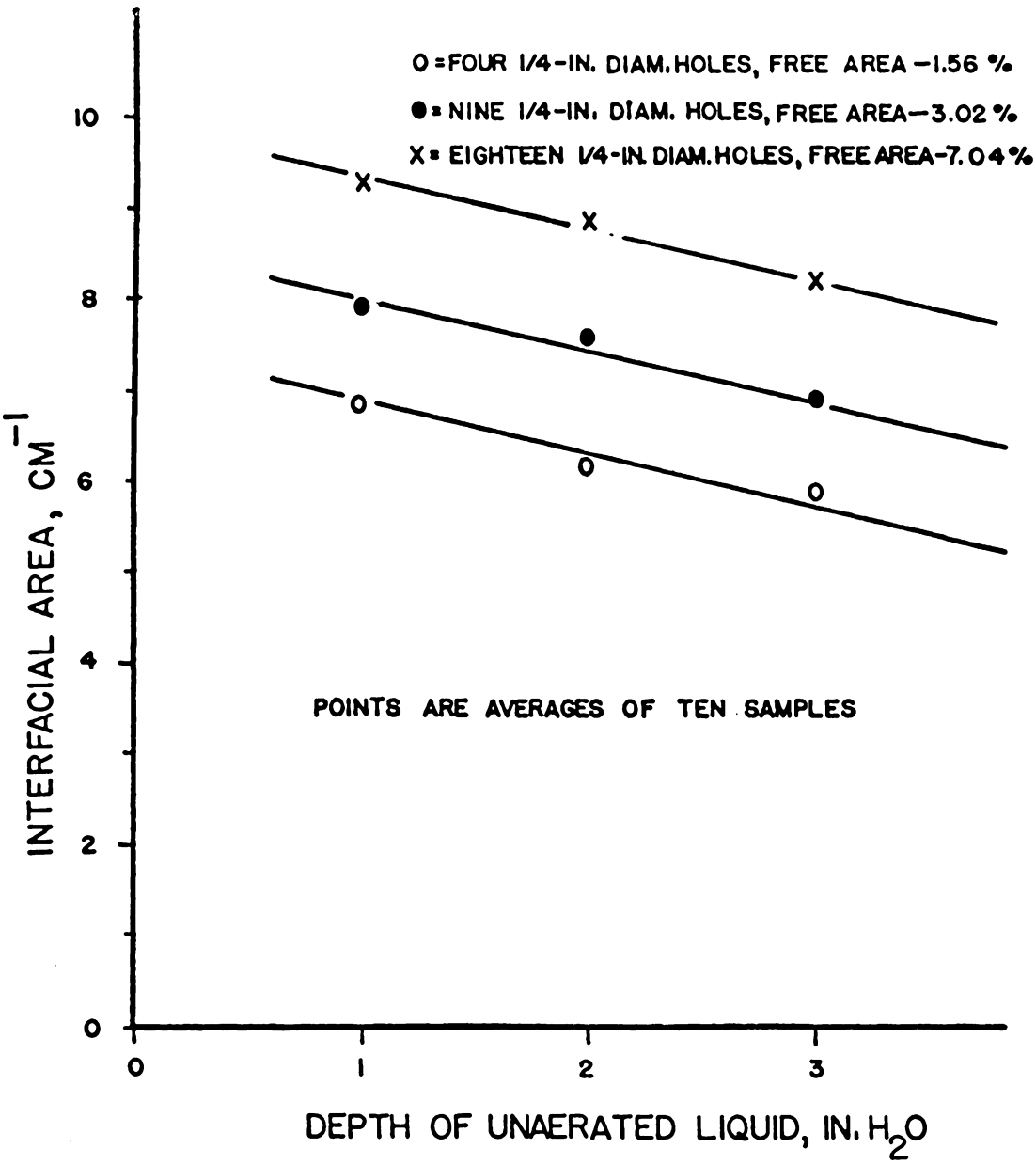

FIGURE 25. EFFECT OF FREE AREA AND DEPTH OF UNAERATED LIQUID ON TRAY ON THE INTERFACIAL AREA FOR 1/4-IN. DIAMETER HOLES IN A 1/8-IN. THICK PLATE WITH A SLOT VELOCITY OF 26 FEET PER SECOND

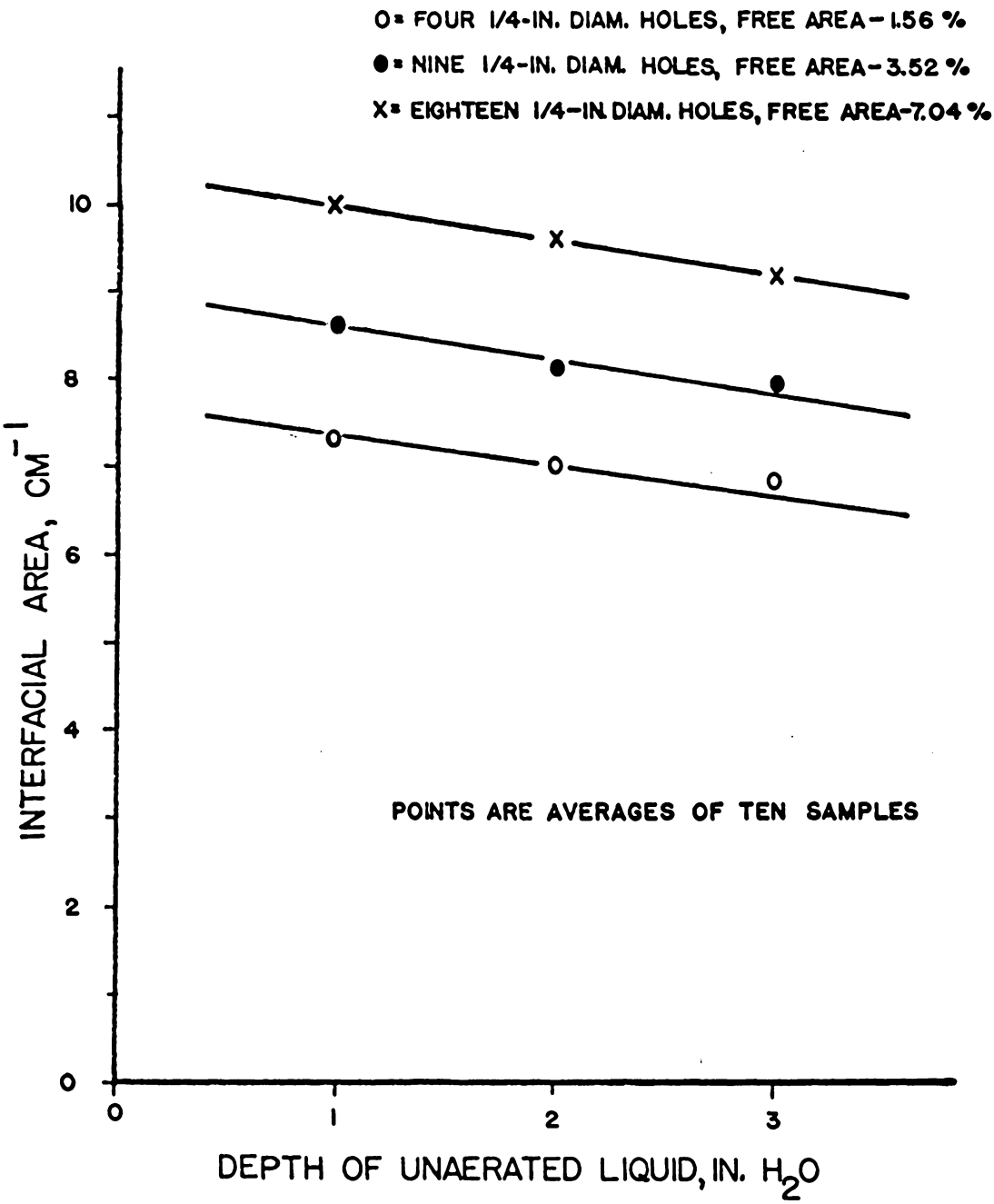

FIGURE 26. EFFECT OF FREE AREA AND DEPTH OF UNAERATED LIQUID ON TRAY ON THE INTERFACIAL AREA FOR 1/4-IN. DIAMETER HOLES IN A 1/8-IN. THICK PLATE WITH A SLOT VELOCITY OF 30 FEET PER SECOND

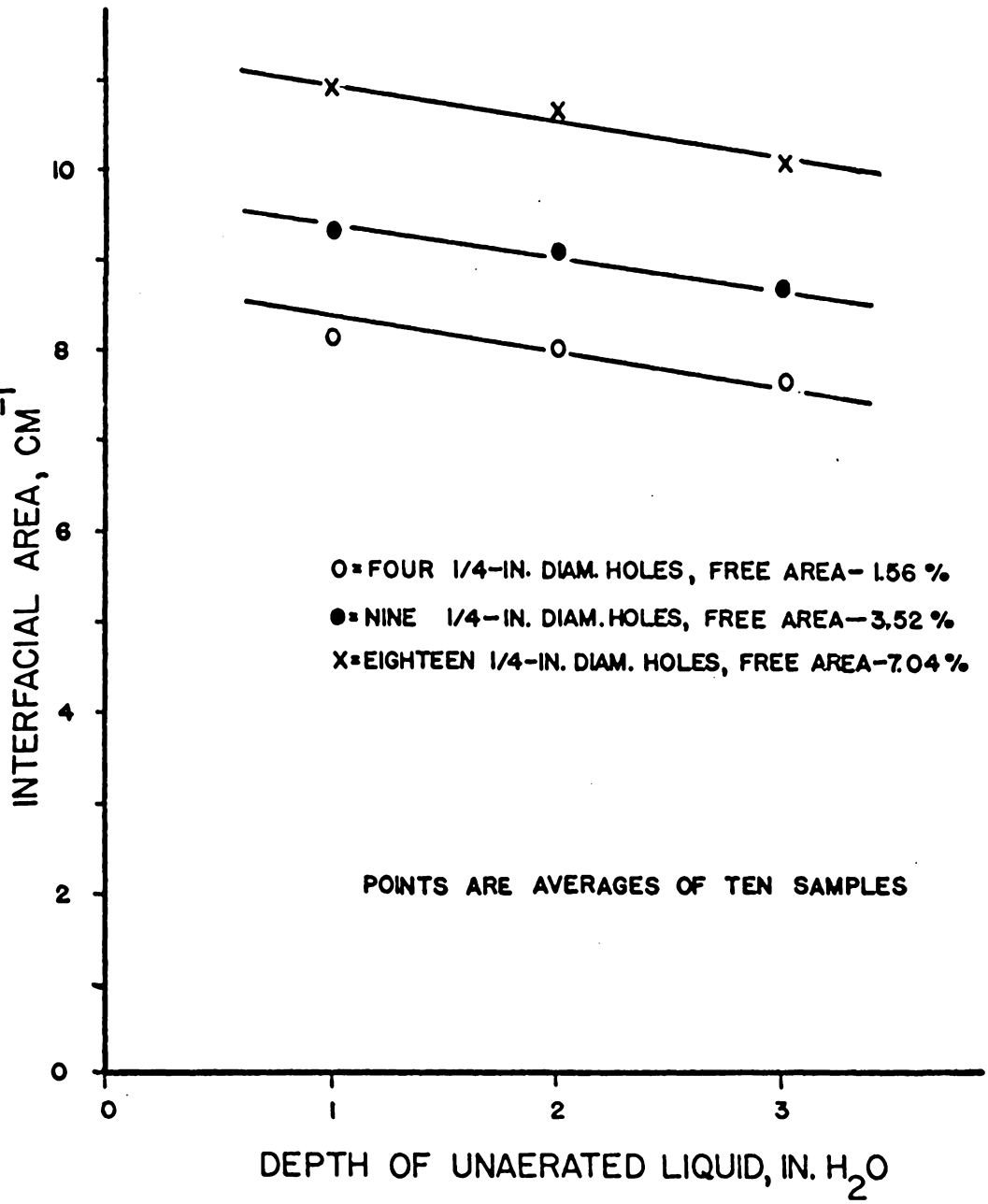

FIGURE 27. EFFECT OF FREE AREA AND DEPTH OF UNAERATED LIQUID ON TRAY ON INTERFACIAL AREA FOR 1/4-IN. DIAMETER HOLES IN A 1/8-IN. THICK PLATE WITH SLOT VELOCITY OF 34 FEET PER SECOND

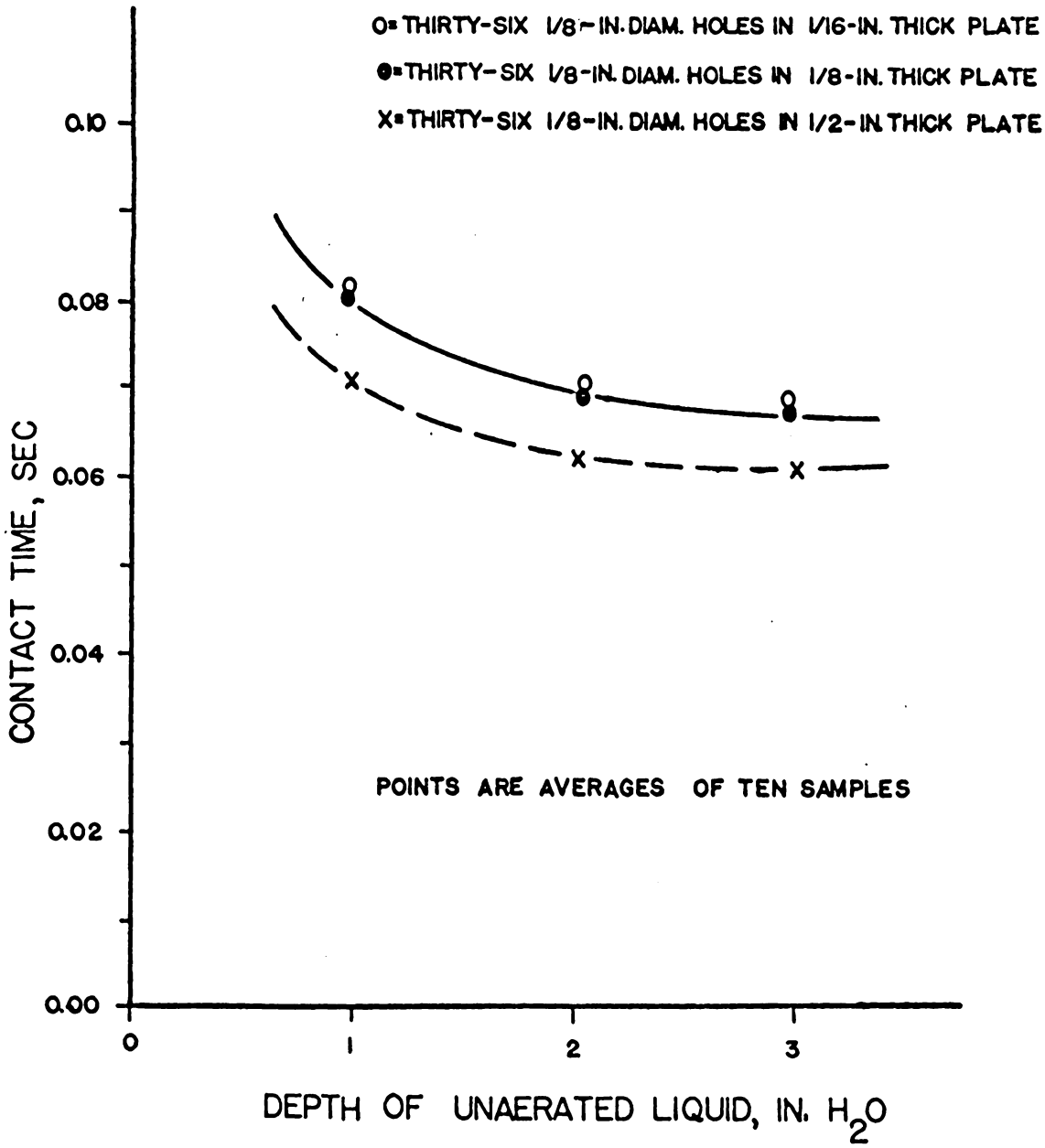

EIGURE 28. EFFECT OF PLATE THICKNESS AND DEPTH OF UNAERATED LIQUID ON TRAY ON THE CONTACT TIME FOR A SLOT VELOCITY OF 22 FEET PER SEC. AND 1/8-IN. DIAMETER HOLES

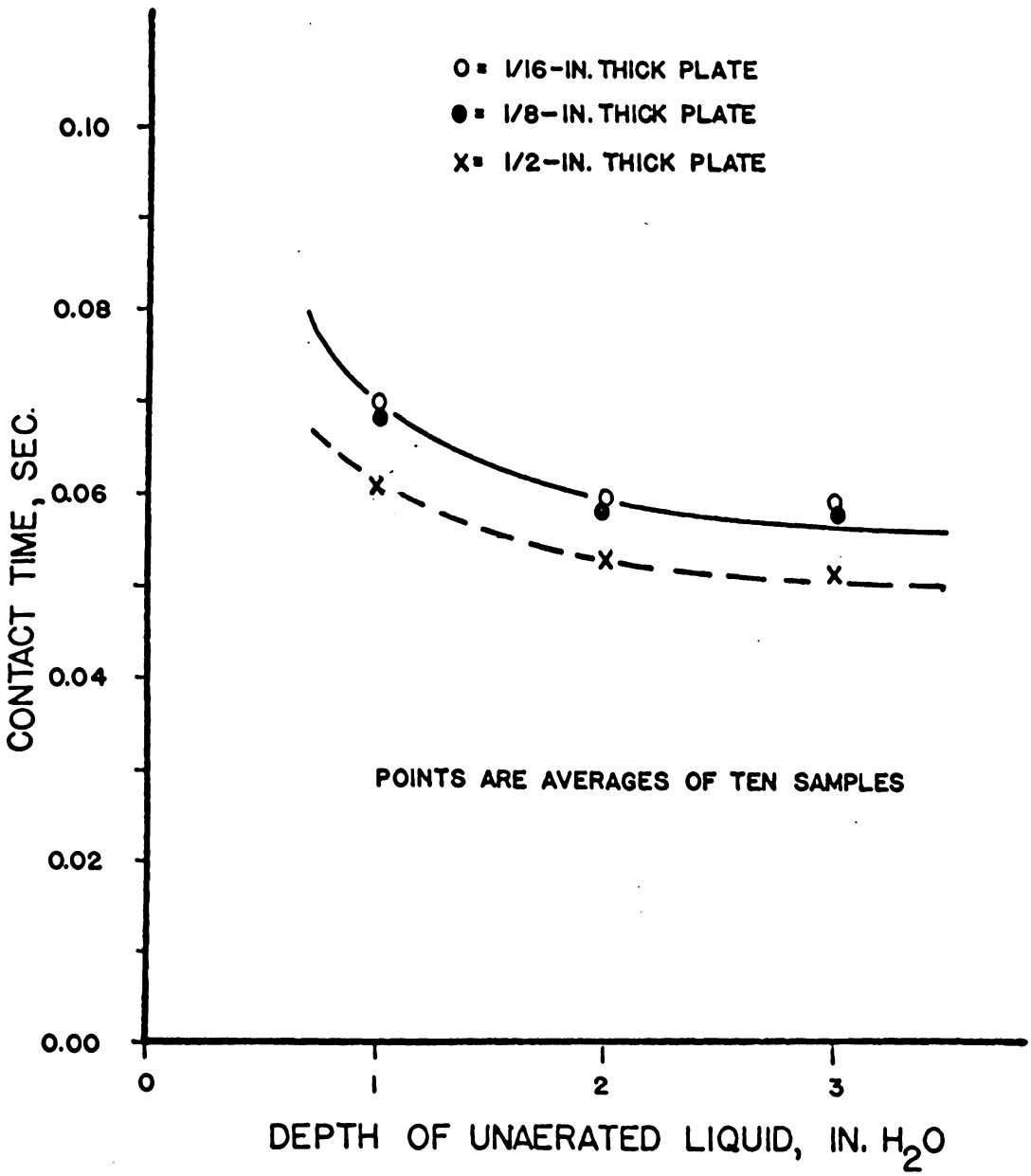

FIGURE 29. EFFECT OF PLATE THICKNESS AND DEPTH OF UNAERATED LIQUID ON THE CONTACT TIME FOR THIRTY-SIX, 1/8-IN. DIAMETER HOLES IN A SIEVE-PLATE WITH SLOT VELOCITY OF 26 FEET PER SEC

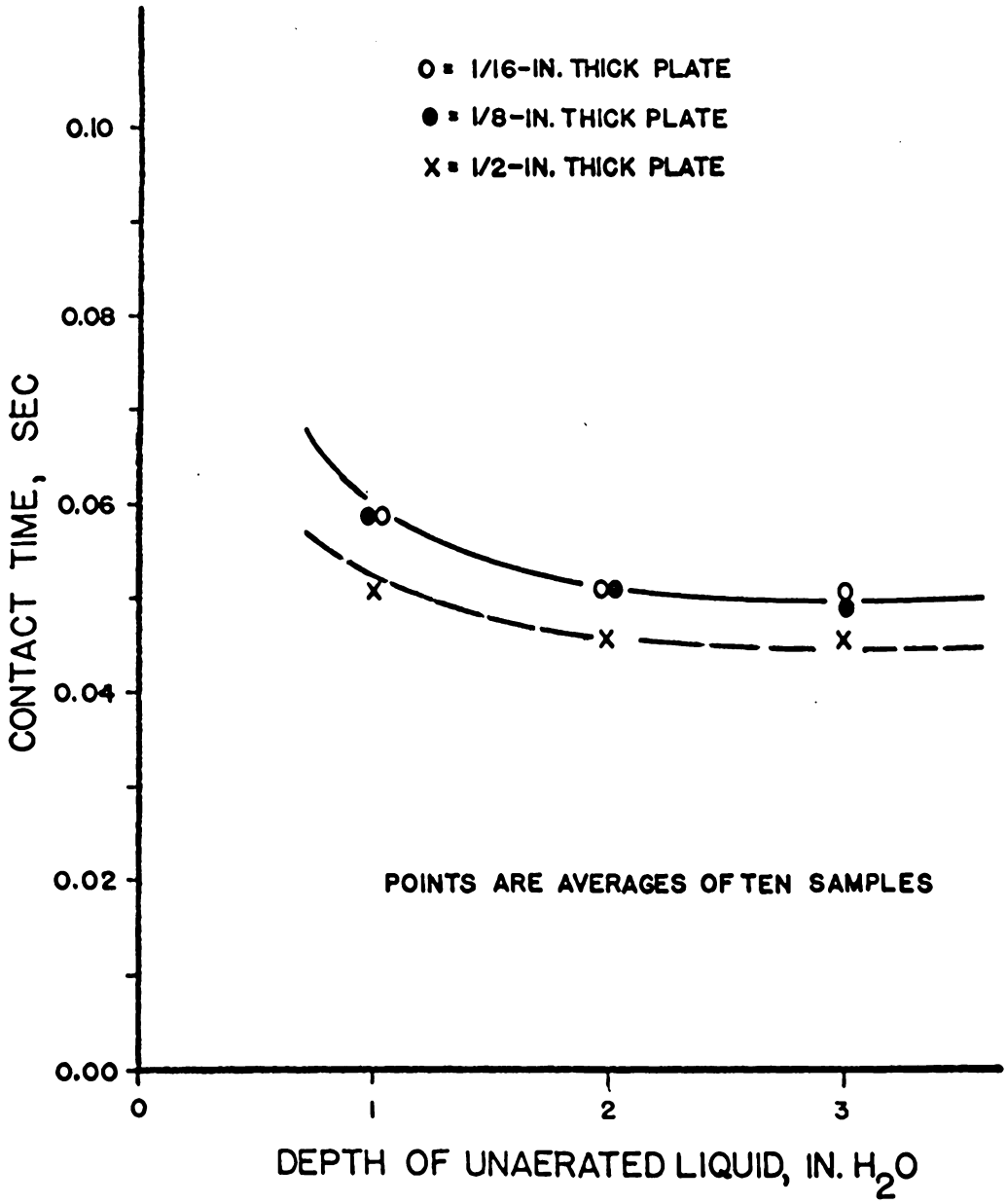

FIGURE 30. EFFECT OF PLATE THICKNESS AND DEPTH OF UNAERATED LIQUID ON TRAY ON CONTACT TIME FOR THIRTY-SIX, 1/8-IN. DIAMETER HOLES IN A SIEVE-TRAY WITH SLOT VELOCITY OF 30 FEET PER SEC.

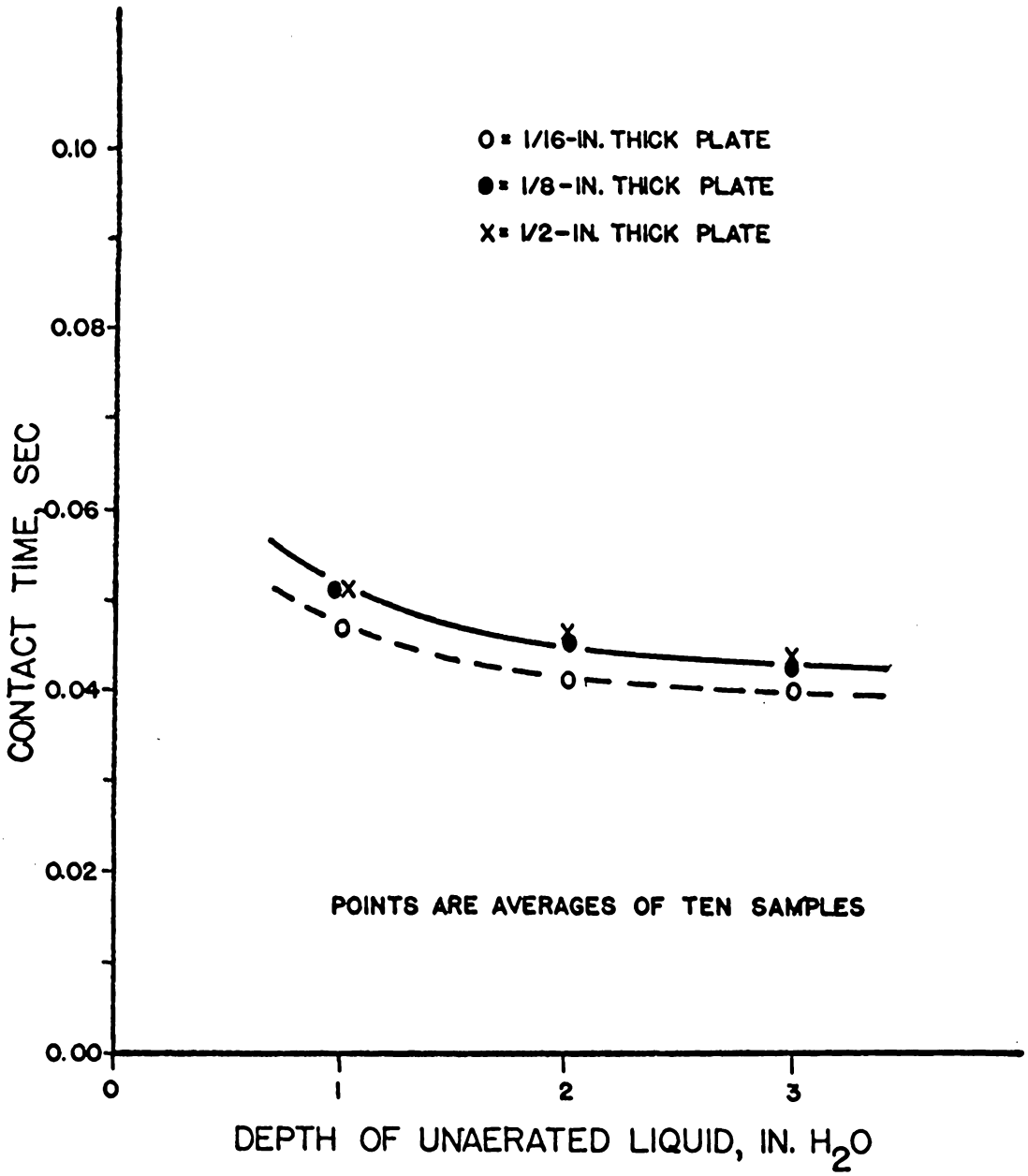

FIGURE 31. EFFECT PLATE THICKNESS AND DEPTH OF UNAERATED LIQUID ON TRAY ON CONTACT TIME FOR THIRTY-SIX 1/8-IN. DIAMETER HOLES IN A PLATE WITH A SLOT VELOCITY OF 34 FEET PER SECOND

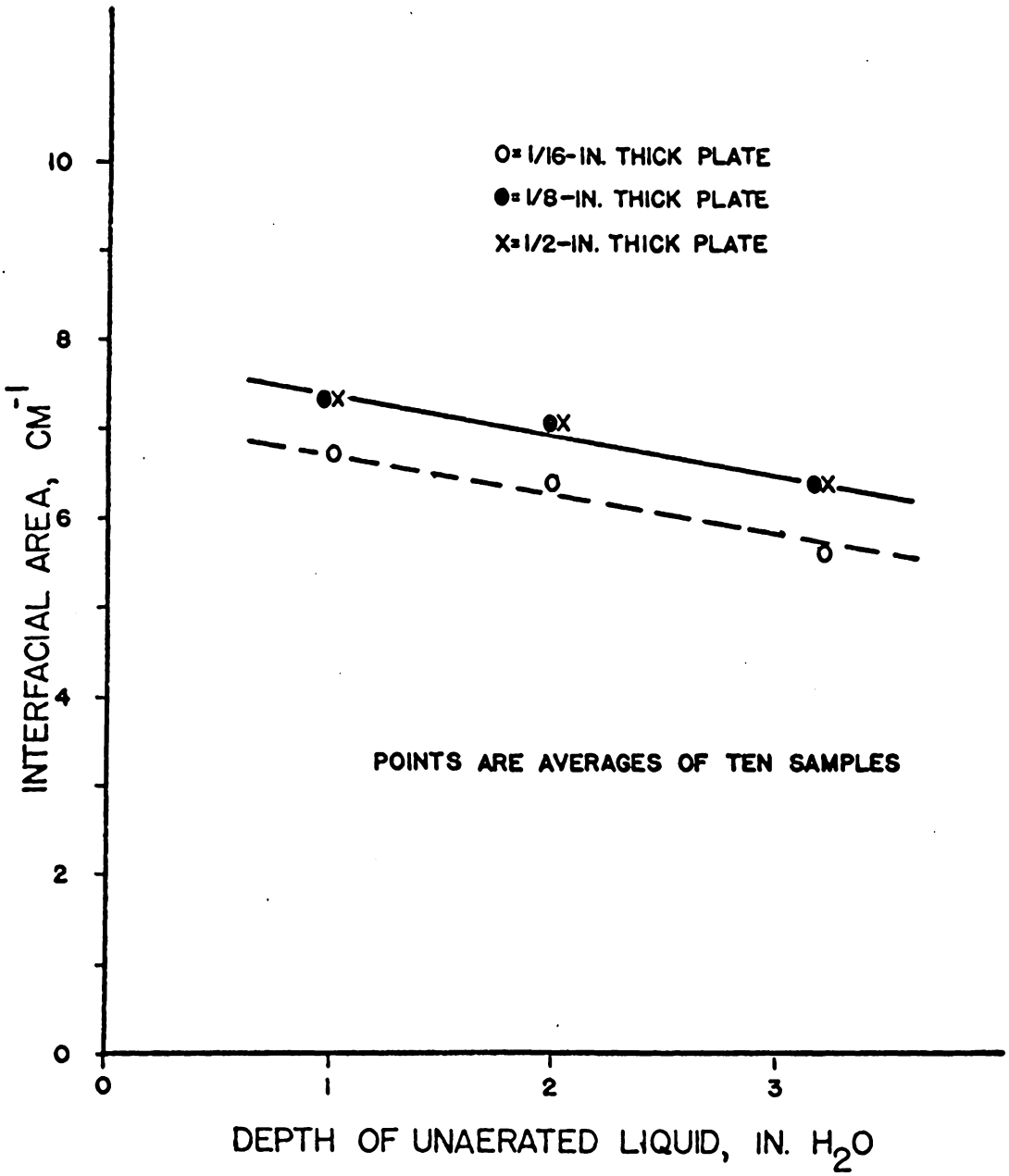

FIGURE 32. EFFECT OF PLATE THICKNESS AND DEPTH OF UNAERATED LIQUID ON TRAY ON THE INTERFACIAL AREA FOR THIRTY-SIX 1/8-IN. DIAMETER HOLES WITH A SLOT VELOCITY OF 22 FEET PER SECOND

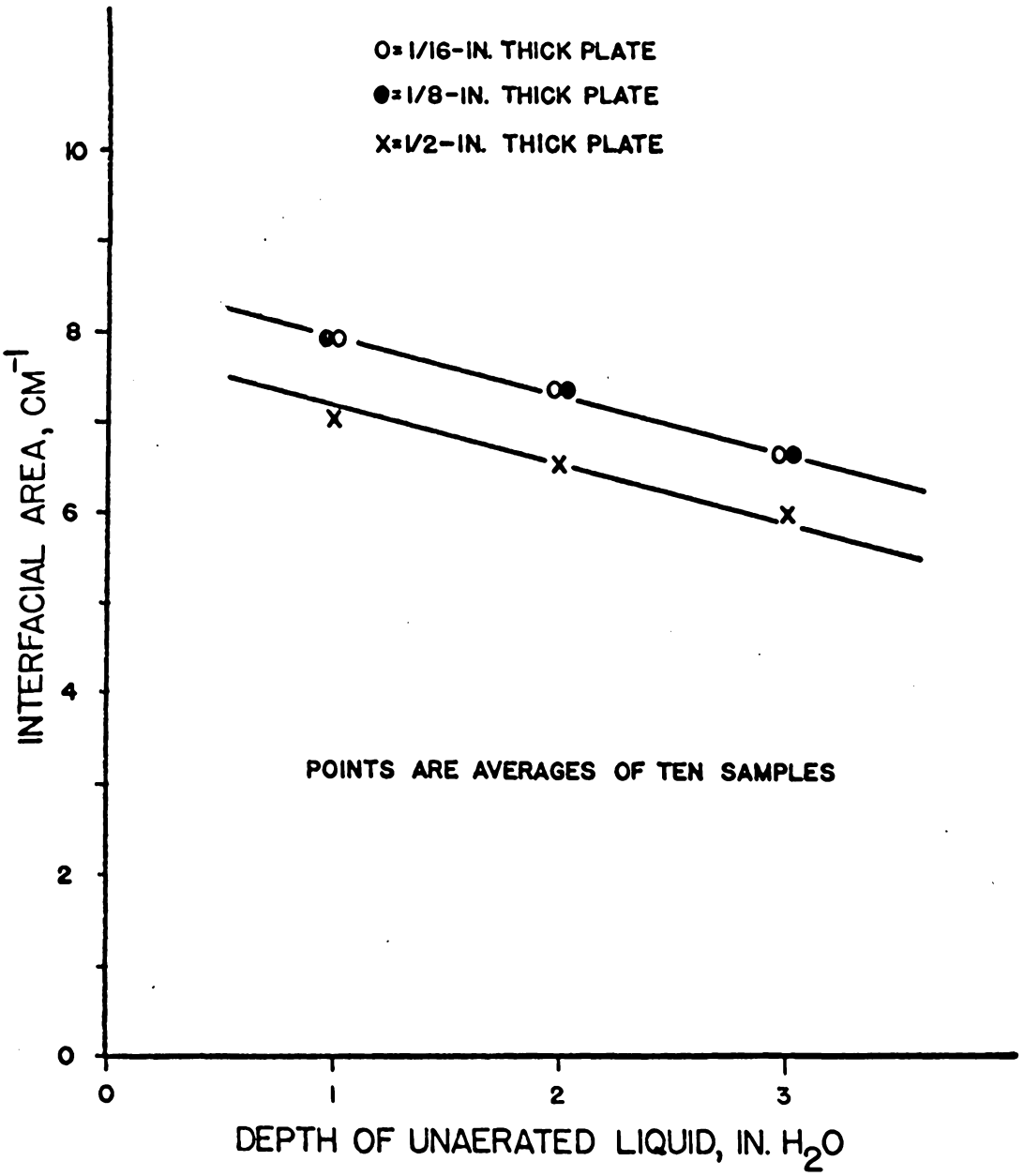

FIGURE 33. EFFECT OF PLATE THICKNESS AND DEPTH OF UNAERATED LIQUID ON TRAY ON THE INTERFACIAL AREA FOR THIRTY-SIX 1/8-IN. DIAMETER HOLES IN A PLATE WITH A SLOT VELOCITY OF 26 FEET PER SEC

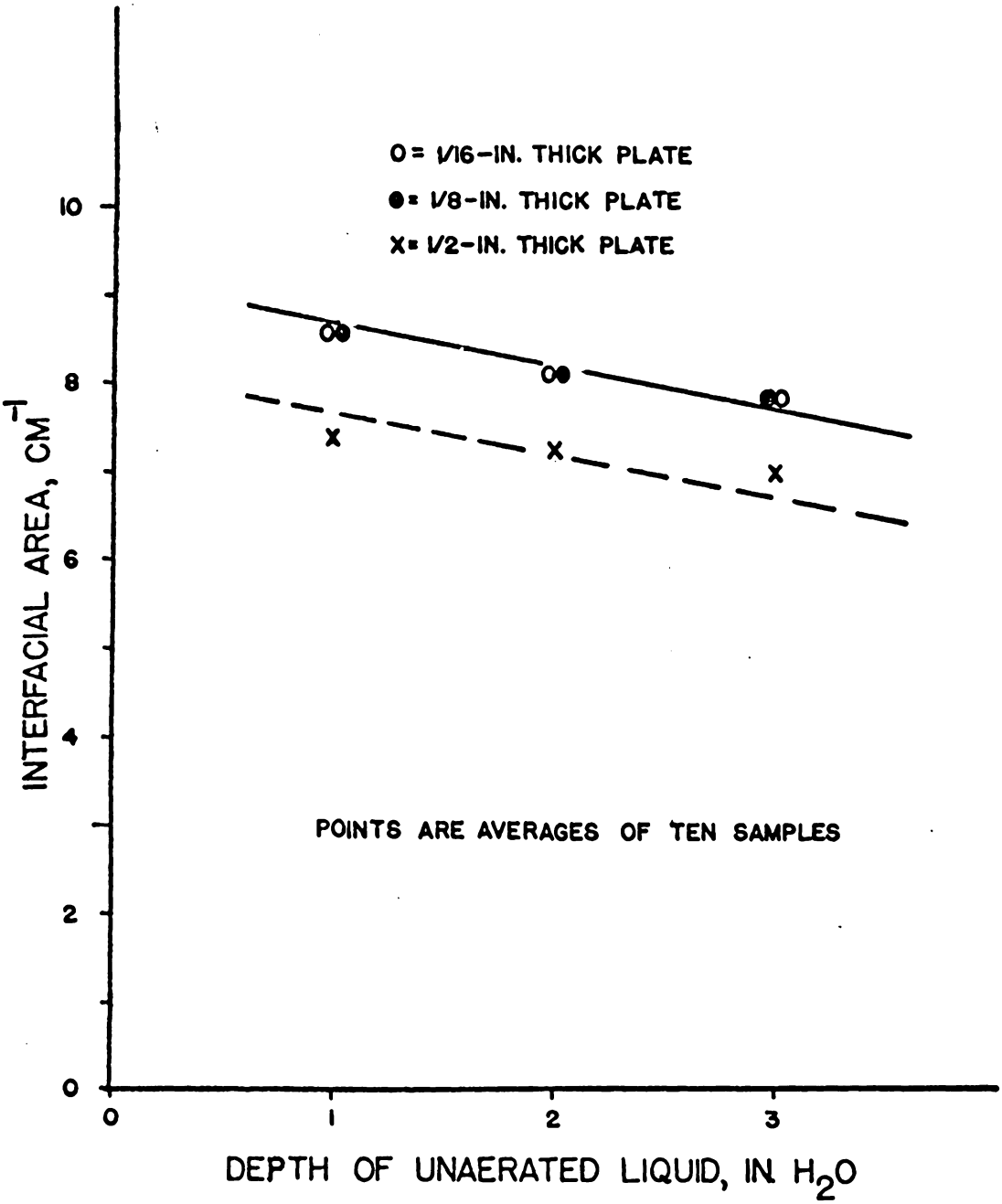

FIGURE 34. EFFECT OF PLATE THICKNESS AND DEPTH OF UNAERATED LIQUID ON TRAY ON THE INTERFACIAL AREA FOR THIRTY-SIX 1/8-IN. DIAMETER HOLES IN A PLATE WITH A SLOT VELOCITY OF 30 FEET PER SECOND

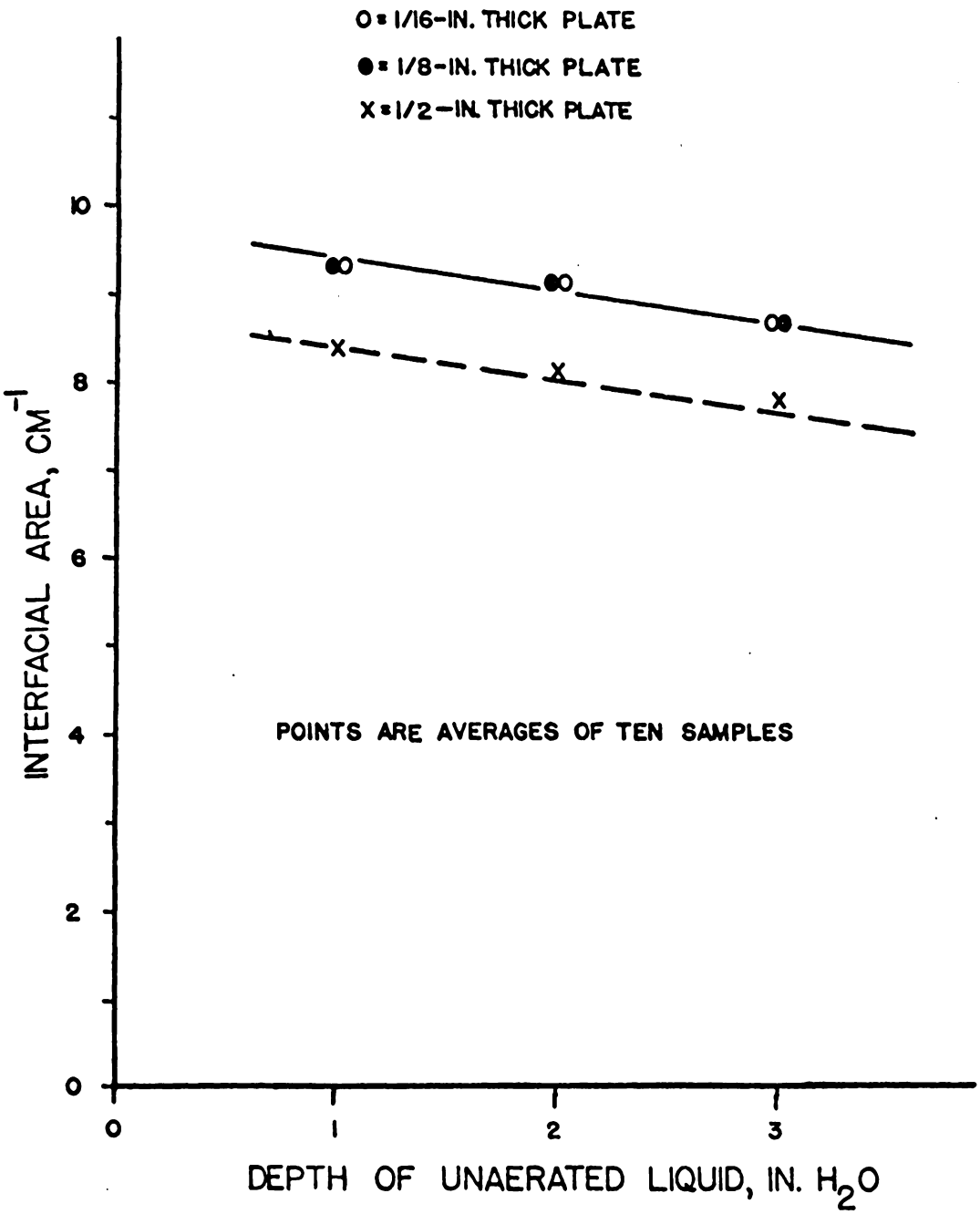

FIGURE 35. EFFECT OF PLATE THICKNESS AND DEPTH OF UNAERATED LIQUID ON TRAY ON INTERFACIAL AREA FOR THIRTY-SIX 1/8-IN. DIAMETER HOLES IN A PLATE WITH A SLOT VELOCITY OF 34 FEET PER SECOND

Sample Calculations

Examples of calculations which were performed during this investigation were presented in the following section.

Titre of Carbon Dioxide Absorbed. In applying equation 8 it was necessary to remember that this equation was applicable for liquids which had been exposed for only one contact time - for the case covered in this investigation the bulk concentration on the sieve-tray was adjusted to correspond to liquid which had been exposed for one contact time. Thus, the feed to the sieve-tray had additional caustic added to compensate for the mean residence time of the liquid on the tray being greater than the time of contact. The titre of the carbon dioxide absorbed was determined from the following formula:

$$M = k + j$$

where:

M = total titre of carbon dioxide absorbed, ml

k = titre of carbon dioxide absorbed for one contact time, ml

j = titre of carbon dioxide absorbed for difference between feed and fresh solution (pure water or 0.085 N sodium hydroxide solution), ml

For the case of test 1, Table V, page 50 this was:

$$M = 7.66 + 88.14$$

$$M = 95.80 \text{ ml}$$

Quantity of Carbon Dioxide Absorbed. The quantity of carbon dioxide absorbed was computed from the following relation:

$$Q = \frac{F}{L}\left(\frac{MN}{1000\ p}\right)$$

where:

Q = quantity of carbon dioxide absorbed, mols / sec

F = feed rate, ml / sec

L = sample size, ml

M = titre of sample, ml of sodium hydroxide solution

N = normality of titrating solution

p = equivelants of H_2CO_3 per equivelant of NaOH

Substituting data from Table V, test 1, page 50:

$$Q = \frac{20}{20} \left(\frac{95.80 \times 0.0340}{2 \times 1000} \right)$$

$$Q = 1.639 \times 10^{-3} \text{ mol / sec}$$

Determination of Time of Penetration (Contact). The time of penetration (contact) was determined from the following relation:

$$R = \frac{Q_{caus.}}{Q_{water}}$$

where:

R = ratio of quantities absorbed

$Q_{caus.}$ = quantity or titre of CO_2 absorbed in 0.085 N caustic for one contact time

Q_{water} = quantity or titre of CO_2 absorbed in water for one contact time

Substituting data from Table V, test 1, page 50:

$$R = \frac{138.15}{95.80}$$

$$R = 1.442$$

The quantity t_c is then evaluated by using R to evaluate t_c from Figure 16, page 45:

$$t_c = 0.080 \text{ sec}$$

Evaluation of Interfacial Carbon Dioxide Concentration. The interfacial CO_2 concentration was evaluated from the following formula:

$$c_i = \left(\frac{p_{CO_2}}{760} \right) c_s$$

where:

c_i = interfacial concentration of CO_2, mol / cc

p_{CO_2} = partial pressure of CO_2, mm Hg

c_s = solubility of CO_2, mol / cc-atm.

Evaluating for 25 °C at an atmospheric pressure of 721.50 mm Hg (p_{H_2O} = 23.76 mm Hg):

$$c_i = \left(\frac{721.50 - 23.76}{760.00} \right) (3.40 \times 10^{-5})$$

$$c_i = 3.10 \times 10^{-5} \text{ mol / cc}$$

Evaluation of Total Interfacial Area. The total interfacial area available for mass transfer was evaluated from equation 8 on page 45:

$$a = \frac{Q}{2(c_i - c_o)} \sqrt{\frac{\pi t_c}{D}}$$

where:

a = total interfacial area for mass transfer, cm^2

Q = quantity of CO_2 absorbed in water, mol / sec

c_i = interfacial CO_2 concentration, mol / sec

c_o = bulk concentration of CO_2, mol / sec

t_c = time of contact, sec

D = diffusivity of CO_2 in water, cm^2 / sec

Substituting data from Table V, test 1, page 50:

$$a = \frac{1.639 \times 10^{-3}}{2(3.10 - 0.00) \times 10^{-5}} \sqrt{\frac{3.1416(0.80)}{1.92 \times 10^{-5}}}$$

$$a = 3021 \text{ cm}^2$$

Evaluation of Column F-factor. The column F-factor was evaluated from the following formula:

$$F = U\sqrt{\rho}$$

where:

F = column F-factor, (lb mass / ft sec^2) $^{1/2}$

U = gas velocity through column, ft / sec

ρ = density of CO_2, lb mass / ft^3

Substituting data from Table V, test 1, page 50:

$$F = 0.625$$

$$F = 0.206$$

Evaluation of Total Volume of Liquid on Tray. The total volume of aerated liquid on the tray was evaluated from the following formula:

$$Z = \frac{\pi r^2 h}{V}$$

where:

Z = total volume of liquid on tray, cm^3

r = radius of sieve-tray, cm

h = depth of unaerated liquid on tray, cm

V = froth density (from Figure 6, page 21), gm / cc

= liquid density, gm / cc

Substituting data from Table V, test 1, page 50:

$$Z = \frac{3.1416(5.08)^2(2.54)}{0.50}$$

$$Z = 411 \text{ cm}^3$$

Evaluation of Interfacial Area per Unit Volume (Expt.) The interfacial area per unit volume was evaluated from the following formula:

$$a' = \frac{a}{Z}$$

where:

a' = interfacial area per unit volume, cm^{-1}

a = total area available for mass transfer, cm^2

Z = volume of liquid on tray, cm^3

Substituting data from Table V, test 1, page 50:

$$a' = \frac{3021}{411}$$

$$a' = 7.3 \text{ cm}^{-1}$$

Evaluation of Interfacial Area per Unit Volume (Calc.) The interfacial area per unit volume was evaluated from the following formula (equation 9, page 47):

$$a' = \frac{3(1-V)}{r}$$

where:

a' = interfacial area per unit volume, cm^{-1}

V = froth density (Figure 6, page 21), gm / cc

r = mean radius of froth bubble (Figure 7, page 22), cm

Substituting data from Table V, test 1, page 50:

$$a' = \frac{3(1-0.50)}{0.215}$$

$$a' = 7.0 \text{ cm}^{-1}$$

IV. DISCUSSION

The following section contains a discussion of the problems encountered and the results obtained from the investigation, recommendations for future work, and limitations imposed during the investigation.

Discussion of Experimental Work

This section contains a discussion of the experimental work.

Reproducibility of Data. Preliminary tests of the equipment were conducted to determine the reproducibility of the data and to eliminate possible sources of error. The preliminary results were so scattered that it was impossible to interpret the data. The source of this variation was found to be the reaction column feed pump, a centrifugal pump. Varying depth of liquid in the feed tank (hence a variance in the net-positive-suction-head) coupled with transients inherent in the operation of the pump were found to be the principal factors causing this variation. Through the use of a positive displacement pump, the maxium variation of contact times within a ten sample test was reduced to less than 1.0 percent about the test mean.

Restrictions on the Determination of Time of Penetration. Sience the data of Danckwerts[5] was based upon exposure of the fluid for a single contact time, it was necessary that the bulk concentration on the tray correspond ot liquid which had been exposed for one contact time. If this were not true, the concentration differences (see Equation 8, page 46) would be different for the water and 0.085 M caustic solution. In addition for contact times greater than about 0.090 seconds the evaluation of contact time from the curve of contact time versus the ratio of carbon dioxide absorbed, Figure 16, page 45, becomes somewhat indeterminate due to flattening of the curve.

Discussion of Results

The following section contains a discussion of the results obtained in this investigation.

Effect of Hole Size on Interfacial Area and Contact Time. The effect of hole sizes on interfacial area per unit volume and contact time was shown in Figures 19, 20, 21, and 22 on pages 63, 64, 65, and 66. These figures fail to show any significant differences or trends for the three hole sizes investigated, 1/8-inch, 1/4-inch and 3/8-inch diameter holes. This implied that there was no significant effect of orifice diameter on bubble diameter. Leibson[20] has shown that bubble diameter varied as the 0.05 power of the orifice diameter; this would imply a two percent variation about the mean for bubble diameter or time of penetration for the variation in orifice diameter used in this

investigation. Leibson's equation was for single orifices and hence no allowance was made for coalescence or interraction of bubbles from multiple orifices; these effects coupled with errors inherent in the analysi may have been sufficient to cancel this two percent variation.

Effect of Liquid Rate on Interfacial Area and Contact Time. The effect of liquid rate on contact time and interfacial area was shown in Figures 17 and 18 on pages 61 and 62. These figures showed that the liquid feed rate had no effect upon the interfacial area per unit volume or contact time for a sieve-tray with a constant depth of unaerated liquid on the tray. Preliminary calculations showed that the mean horizontal velocity of liquid across the tray was insufficient to change the rate of mass transfer from the bubbles rising in the liquid more than one percent. The results of this investigation were not accurate enough to detect variations of this magnitude. While the liquid flow rate did not have a direct effect upon the parameters under investigation a change in liquid flow rate resulted in a corresponding change in the depth of unaerated liquidon the tray. This effect was caused by the inadequate liquid handeling capacity of the downcomer; consequently the downcomer had to be adjusted for a change in liquid rate to keep the depth of unaerated liquid on the tray constant.

Effect of Free Area on Contact Time and Interfacial Area. The effect of free area on the interfacial area per unit volume and contact time was shown in Figures 23, 24, 25, 26, and 27 on pages 67, 68, 69, 70, and 71. These figures showed that there was no significant influence of free area on contact time; this would also imply that the interraction

of multiple orifices on a sieve-tray had a negligible effect upon the average bubble diameter and velocity. However, the free area of the plate was shown to have a definite effect upon interfacial area of the tray. Since the time of penetration was unaffected - implying that the bubble diameter was also unaffected, it would be expected that froth density would decrease for an increase in plate free area at constant slot velocity. An increase in free area at constant slot velocity corresponded to an increase in column F-factor and Figure 6, page 21 showed that froth density did indeed decrease with increasing F-factor, thus implying internal consistency of the data.

Effect of Plate Thickness on Interfacial Area and Contact Time. The effect of plate thickness on interfacial area and contact time was shown in Figures 28 through 35 on pages 72 through 79. From these figures it was easily seen that plate thickness had a significant influence upon the interfacial area and contact time. This interraction was quite small for 1/16-inch and 1/8-inch thick plates; however, for the 1/2-inch thick plate the effect was quite pronounced. This effect is most readily explained through the increase in kinetic energy required for the flow through the thicker plates. The increase in kinetic energy brought about a corresponding increase in the velocity of rise of bubbles in the liquid, hence a shorter contact time and a lower free area due to the decrease in hold-up time caused by the higher velocity.

Effect of Slot Velocity. The effect of slot velocity upon interfacial area and contact time was shown in Figures 17 through 35, pages 61 through 79. These figures clearly demonstrated that contact

time was a direct, linear, decreasing function of slot velocity. Figure 5, page 20 showed that an increase in slot velocity (this corresponded to an increase in frequency since bubble size was essentially constant) increased the velocity of rise of bubbles in liquid. For seal depths greater than 2.0 inches (approximately 1.0 inch of unaerated liquid) the velocity of rise increased as a linear function of the frequency. This inferred that the time of contact should also be a linear function of the slot velocity. Figures 17 through 35 confirmed this inference. Figures 17 through 35 also showed that the interfacial area increased with increasing slot velocity. Since bubble size was essentially constant and only frequency changed with velocity, it would be expected that the froth density would decrease with increasing slot velocity (a corresponding increase in column F-factor). Figure 6, page 21 showed that this occurred.

Effect of Depth of Unaerated Liquid on Tray on Contact Time and Interfacial Area. Figures 17 through 35, pages 61 through 79 demonstrated the effect of the depth of unaerated liquid on the tray on the contact time and interfacial area. These figures showed that contact time increased slightly with decreasing depth of liquid: this would correspond to a decrease in the velocity of rise of bubbles. Figure 5, page 20 showed that velocity does decrease as the depth of liquid decreases. These figures also showed that the interfacial area increased with decreasing depth of liquid; since bubble diameter is approximately constant this would infer that the froth density decreased with decreasing depth of liquid. Gerster[21] has shown that froth density does decrease with decreasing depth of liquid on the tray.

Discussion of Interfacial Areas Obtained. The interfacial areas obtained in this investigation were evaluated through the use of equation 8, page 46. These areas were compared to an independent determination of interfacial area through the use of equation 9, page 47 and Figures 6 and 7 on pages 21 and 22. The results of these evaluations were presented in Tables V through XV, pages 50 through 61. These tables showed that the areas predicted by equation 8 were, in general, slightly greater than those predicted by the independent results of equation 9. For the most part the difference between these two predictions was less than sixteen percent; however, in two cases this difference was twenty-three percent.

Part of the discrepancy between the interfacial areas predicted by equations 8 and 9 was reconciled in that the gas used to evaluate the parameters in Figures 6 and 7 was air; whereas, the gas used in this investigation was carbon dioxide. Leibson [20] has shown that the diameter of a gas bubble varied as the 0.05 power of the gas viscosity. Since the viscosity of air was about forty percent greater than carbon dioxide, it was expected that the interfacial areas for the carbon dioxide and water system used in this investigation would be about two percent greater than the values predicted using the independent air and water system on which Figures 6 and 7 were based. In addition data given in Figures 6 and 7 were for 1/8-inch thick plates with a depth of unaerated liquid of slightly more than two inches. Gerster[21] has shown that the depth of unaerated liquid on the tray affected the froth density and hence the interfacial area. In evaluating the interfacial area from equation 9 no allowance was

made for the variation of froth density with depth of unaerated liquid. This was because the data of Gerster was more qualitative than quantitative and could not be applied to the data from which equation 9 was evaluated. In addition this investigation demonstrated that plate thickness had a significant effect upon the interfacial area - this was also not taken into account in using equation 9 as an independent evaluation of the interfacial area per unit volume.

While most of these effects were rather small and only contributed slightly to the overall discrepency between the two predictions, the variation of interfacial area with depth of unaerated liquid was quite significant - the results of this investigation showed that the interfacial area increased about twelve percent for a decrease in depth of unaerated liquid from three inches to one inch. Thus the variation of interfacial area with depth of unaerated liquid contributed most significantly to inconsistency of the interfacial areas predicted by equation 8 and 9.

Discussion of Contact Times Obtained. The times of contact obtained in this investigation were evaluated by equation 8, page 46 and Figure 16, page 45. The results of these evaluations were presented in Tables V through XV on pages 50 through 61. These contact times varied between 0.043 and 0.080 seconds. Higbie[11] theorized and demonstrated that the contact time should be the time for a bubble to rise a height equivelant to the diameter of the bubble. The mean bubble diameter for the conditions used in this investigation was about 0.43 centimeters. Bowman[2] has shown that the velocity of rise of carbon

dioxide bubbles in water varied from twenty to forty centimeters per second for the conditions employed in this investigation. According to Higbie this would imply that the time of contact should vary between 0.010 and 0.021 seconds. However, the apparatus which Higbie used to develop his theory was a glass tube 0.30 centimeters in internal diameter; Higbie measured the rate of absorption of carbon dioxide bubbles rising in this tube. These bubbles were approximately the same diameter as the internal diameter of the tube and hence the walls exerted a significant drag on the liquid layer next to the bubble: this drag was sufficient to shorten the contact time significantly.

The results of this investigation show that bubbles rising in a liquid with no wall effects have a contact time approximately four times as great as those predicted by Higbie. A more realistic estimate of the contact time would be the time required for a bubble to rise a height equivelant to half of its circumferance - this would correspond to liquid flowing from the top of the bubble around to the bottom. In actuality the liquid probably leaves the bubble before reaching the bottom thus creating two zones of liquid contact in which there were different rates of surface renewal or times of contact. An equally important factor in reconciling the difference in contact times was that a heavy froth was formed on the tray with multiple orifices while the tube which Higbie used had no such froth. The gas hold up in this froth was up to fifty percent greater than for gas bubbles in deep liquids. These two effects caused the increase in contact times measured in this investigation.

Limitations

The limitations that existed during the experimental portion of this investigation were listed below.

Slot Velocity. Slot velocities of twenty-two, twenty-six, thirty, and thirty-four feet per second were used in this investigation.

Depth of Liquid. Depths of unaerated liquid on the sieve-tray of one, two, and three inches of unaerated liquid were used in this investigation.

Hole Diameter. Hole diameters of 1/8, 1/4, and 3/8 inches were used in the sieve-trays for this investigation.

Tray Thickness. Tray thicknesses of 1/16, 1/8, and 1/2 inches were used in this investigation.

Free Area. Sieve-tray free areas of 1.56, 3.52, and 7.04 percent were used in this investigation.

Temperature. The temperature of the reactants was maintained at 25.0 ^{o}C with an accuracy of 0.1 ^{o}C.

Liquid Rate. Liquid feed rates of 10, 20, and 30 cubic centimeters per second were used in this investigation.

Recommendations

Since viscosity has a significant effect on interfacial area, it is recommended that the variation of interfacial area with viscosity, as indicated by Figure 9, page 25, be verified. If the variation of interfacial area with viscosity is as significant as predicted by

Figure 9, then it is likely that the contact time will also be a function of liquid viscosity. The data necessary to verify these possible variations is presented in the article by Danckwerts and Kennedy[5].

V. CONCLUSIONS

The determination of interfacial areas and effective contact times for a sieve-tray at slot velocities of 22, 26, 30, and 34 feet per second; plate thicknesses of 1/16, 1/8, and 1/2 inches; hole diameters of 1/8, 1/4, and 1/2 inches; liquid feed rates of 10, 20, and 30 cubic centimeters per second; sieve-tray free areas of 1.56, 3.52, and 7.04 percent; and depth of unaerated liquid on tray of 1.00, 2.00 and 3.00 inches yielded the following conclusions.

1. Effective contact times for a sieve-tray are greater than would be predicted from first principles by the method of Higbie.

2. Interfacial areas which can be predicted from first principles were consistent with the effective area available for mass transfer.

3. The liquid feed rate did not affect the contact time or interfacial area available for mass transfer.

4. The hole diameter did not have a significant effect upon the contact time or the interfacial area available for mass transfer.

5. A decrease in depth of unaerated liquid on the tray brought about an increase in the interfacial area available for mass transfer and time of contact. These increases were approximately linear.

6. An increase in plate thickness brought about a corresponding decrease in the time of contact and interfacial area available for mass transfer.

7. An increase in free area of the sieve-tray increased the interfacial area available for mass transfer; however, an increase in free area did not significantly affect the contact time.

8. An increase in slot velocity decreased the contact time and increased the interfacial area available for mass transfer.

VI. SUMMARY

The purpose of this investigation was to determine meaningful values of interfacial area and contact time for mass transfer on a sieve-tray. These values were determined by measuring the rates of absorption of carbon dioxide and forcing the parameters to give answers consistent with the rates of absorption. These values were checked by comparing the interfacial area determinations with independent measurements.

The interfacial areas and contact times were determined for liquid feed rates of 10, 20, and 30 cubic centimeters per minute; slot velocities of 22, 26, 30, and 34 feet per second; hole diameters of 1/8, 1/4, and 3/8 inches; tray thicknesses of 1/16, 1/8 and 1/2 inches; free areas of 1.56, 3.52, and 7.04 percent; and depth of unaerated liquid on the tray of 1.00, 2.00, and 3.00 inches.

The values of the interfacial area determined in this investigation were consistent with independent, previously measured values. The values of the contact times determined were about four times greater than previous estimations; this discrepency was attributed to wall effects and differences in froth characteristics.

VII. BIBLIOGRAPHY

1. Bakowski, S. G.: Zhur. Priklad Zhim, 39, 29 (1956).

2. Bowman, C. W. and A. I. Johnson: Mass Transfer from Carbon Dioxide Bubbles Rising in Water, Can. Jour. Chem. Eng., 40 139 (1962).

3. Chu, J. C., et al: Study of Bubbling Performance in Relation to Distillation and Absorption, Am. Inst. Chem. Eng. Jour., 3, 16 (1957).

4. Danckwerts, P. V.: Transient Mass Transfer, Am. Inst. Chem. Eng. Jour., 1, 456 (1955).

5. Danckwerts, P. V. and A. M. Kennedy: The Kinetics of Absorption of Carbon Dioxide into Neutral and Alkaline Solutions, Chem. Eng. Sci., 4, 202 (1958).

6. Davidson, J. F. and E. J. Cullen: The Determination of Diffusion Coefficients for Sparingly Soluble Gases in Liquids, Trans. Inst. Chem. Eng., 35, 51 (1957).

7. Davidson, L.: Ph. D., Thesis, Columbia University, (1951).

8. Davies, J. T.: "Advances in Chemical Engineering," Vol., IV, pp. 1-35. John Wiley and Sons, New York, N. Y., 1964.

9. Gibbs, R. K. and D. M. Himmelblau: Effect of Concentration on the Gas - Liquid Mass Transfer Coefficient, Ind. Eng. Chem. Fund., 2, 55 (1963).

10. Harned, H. S. and R. Davis: Solubility of Carbon Dioxide in Water and Salt Solutions, Jour. Am. Chem. Soc., 65, 2030 (1943).

11. Higbie, R.: Mass Transfer from Rising Bubbles, Tran. Am. Inst. Chem. Eng., 31, 365 (1935).

12. Hughes, R. R.: "Publication of the Heat Transfer and Fluid Mechanics Institute," University of Los Angeles, (1953).

13. Kishinevshij, M. Kh.: Zhur. Priklad Zhim, 29, 29 (1956).

14. Rennie, J. and F. Evans: The Formation of Froths and Foams above Sieve Plates, British Chem. Eng., 7, 498 (1962).

15. Siemes, W.: Chem. Ing. Tech., 26, 479 (1954).

16. Toor, H. L. and J. M. Marchello: A Mixing Model for Mass Transfer near a Boundary, Ind. Eng. Chem. Fund., 2, 8 (1963).

17. Toor, H. L and P. Raimondi: Interfacial Resistance in Gas Absorption, Am. Inst. Chem. Eng. Jour., 5, 86 (1959).

18. Whitman, W. G.: Predicition of Mass Transfer Coefficients for Two Films, Chem. and Met. Eng., 29, 146 (1923).

Addenda

19. Robinson, D. G.: Tray Efficiencies in Distillation Columns, Final Report from the University of Delaware, Am. Ins. of Chem. Eng., New York, (1958).

20. Leibson, I., et al: Rate of Flow and Mechanics of Bubble Formation from Single Submerged Orifices, Am. Ins. of Chem. Eng. Jour., 2, 296 - 306 (1956).

21. Smith, B. D.: "Design of Equilibrium Stage Processes," Mc Graw Hill Book Co., New York (1963).

VIII. ACKNOWLEDGEMENTS

The author wishes to express his sincere appreciation for the advice and assistance given him by Dr. George B. Wills, Professor, Department of Chemical Engineering, Virginia Polytechnic Institute, Blacksburg, Virginia. The author is also indebted to Dr. Fred W. Bull, Director, Virginia Engineering Experimental Station, Virginia Polytechnic Institute Blacksburg, Virginia for his advice in the design and construction of the equipment.

Appreciation is also expressed to Mr. Cy Pyle, Engineering Research Laboratory, E.I. DuPont de Nemours and Company, Wilmington, Delaware for suggesting the area of research for this investigation.

The author wishes to express his sincere gratitude to the Union Carbide Corporation without whose financial help this investigation would not have been possible.

The author is deeply indebted to his wife Carole for typing the final manuscripts for this thesis.

The two page vita has been removed from the scanned document. Page 1 of 2

The two page vita has been removed from the scanned document. Page 2 of 2

ABSTRACT

The purpose of this investigation was to determine meaningful values of interfacial area and contact time for mass transfer on a sieve-tray. These values were determined by measuring the rates of absorption of carbon dioxide into aqueous solutions and forcing the parameters to give answers consistent with the rates of absorption. These values were checked by comparing the interfacial area determinations with independent measurements.

The interfacial areas and contact times were determined for liquid feed rates of 10, 20, and 30 cubic centimeters per minute; slot velocities of 22, 26, 30, and 34 feet per second; hole diameters of 1/8, 1/4, and 3/8 inches; tray thicknesses of 1/16, 1/8, and 1/2 inches; free areas of 1.56, 3.52, and 7.04 percent; and depth of unaerated liquid on the tray of 1.00, 2.00, and 3.00 inches.

The values of the interfacial area determined in this investigation were consistent with independent, previously measured values. The values of the contact times determined were about four times greater than previous estimations; this discrepancy was attributed to wall effects and differences in froth characteristics.